UNIVERSITÀ DEGLI STUDI DI MILANO

DOCTORAL SCHOOL IN "PHILOSPHY AND HUMAN SCIENCES" – XXXII Cycle – **A.A. 2019**

Department of Philosophy

Department of Oncology and Hemato-Oncology

MED/27

DIRECT ELECTRICAL STIMULATION OF PRIMARY MOTOR AND FRONTAL PREMOTOR REGIONS: MAPPING AND PRESERVING NETWORKS FOR HAND MOTOR CONTROL DURING BRAIN TUMOUR RESECTION

PhD Thesis of

LUCA VIGANO'

R11526

Tutors: Prof. Lorenzo Bello

Prof. Corrado Sinigaglia

Coordinator of the PhD school: Prof. Andrea Pinotti

SUMMARY

ABSTRACT

This PhD project was funded by EDEN2020 (Enhanced Delivery Ecosystem for Neurosurgery in 2020). Brain disease represent a cost about 800 billion euros per year in Europe and outcome of treatment is demonstrated to critically depend on the knowledge of functional anatomy and its preservation. By combining pre-operative MRI and diffusion-MRI imaging, intra-operative ultrasounds, robotic assisted catheter steering, brain diffusion modelling and a robotics assisted neurosurgical robot (the Neuromate), EDEN2020 aims at realizing an integrated technology platform for minimally invasive neurosurgery which will provide a significative step change in treatment of brain disease. To date, neurosurgical instruments for diagnostic and therapy (drugs infusion) are inserted via rigid cannulas. This represents a primary technological limitation of treatment with direct consequences in patient's post-operative outcome, since the insertion of rigid cannulas cannot be planned along procedure-optimised trajectories which take into account tissue microstructures and respect the bundles' topographical anatomo-functional organisation. To bridge this gap, main aim of EDEN2020 is to engineer a steerable catheter for chronic neuro-oncological disease than can be robotically guided and kept in situ for extended period, which insertion can be tailored on clinical conditions and individual anatomy.

The correct trajectory and final positioning of a catheter must be planned and guided through the brain structures by the knowledge of the anatomo-functional organization of the neural circuits subserving the essential motor and cognitive functions to avoid lesions resulting in permanent deficits impacting on the quality of life of patients. In addition, since the diffusivity is enhanced when it follows the white matter pathways belongings to the network in which an individual tumour has grown, as showed by data generated by EDEN consortium, these circuits became the target of the drug. In EDEN animal trials (ovine model), the circuit targeted for delivery was the corticospinal tract, due to the anatomical restriction imposed by the sheep brain. In humans, this descending system, which is essential for everyday life activities allowing the skilled use of the hand (i.e. the ability to manipulate objects and tools), has a much higher level of complexity and its functional organisation has not yet been described in detail as in other animal models. The complexity of the neural organization

underlying motor control of hand gestures in humans results in a dramatic degree of freedom, but at the same time in a poor ability to recover after lesions. When this connectivity is infiltrated by a tumour and thus became the possible target of drug delivery devices (EDEN), its complexity must be taken into consideration to avoid the onset of deficits.

The great majority of brain tumours occurs in the frontal lobe and, particularly Low Grade Gliomas (LGGs), develop close or within the cortical but mostly subcortical structures involved in motor control. Therefore, to track safely the entrance and the trajectory of catheters, a reference atlas of the neural circuitry controlling hand movement is mandatory to identify which cortical and subcortical areas must not be lesioned to avoid permanent inability.

Based on this premises, this PhD project investigated, with a multidisciplinary approach, the frontal networks subserving hand function to provide a frame for understanding the connectivity involved in hand skilled movements, which became a possible target for drug delivery in tumours developing in primary motor and/or pre-motor regions.

The skilled use of the hand is allowed by the high level of human sensorimotor control implemented by the corticospinal system, particularly developed in primates, connecting distant and functionally different areas via subcortical bundles and finally acting on the spinal cord with a huge bundle of descending fibres. This complex network computes the sensory information related to the goal of the action to shape the appropriate motor command for motoneurons, the final common path to muscles. Non-human primate studies have demonstrated that the main motor output of the corticospinal tract is the primary motor cortex (M1), which act on the spinal motoneurons, in producing voluntary hand and finger movements. The monkey M1 has recently been demonstrated to represent an anatomo-functional non-unitary sector, subdivided in a caudal region dense with cortico-motoneuronal cells and a rostral sector with few monosynaptic connections to alpha-motoneurons and/or with slower projections to the spinal cord. To control and execute skilled hand movements, M1 is highly interconnected with other frontal and parietal cortical pre-motor regions, with subcortical structures such as the basal ganglia and with the cerebellum. A precise

description of the human circuitry allowing for realization of dextrous hand movement is still missing in the human, as the electrophysiological and anatomical experimental approaches developed in animal models cannot be performed (i.e. intracortical microstimulation, neuronal tracing, lesion studies etc.). The unique setting of brain tumour resection with the brain mapping technique gives a great opportunity to use clinical data to evaluate neural networks in humans. In this setting, during surgical resection, Direct Electrical Stimulation (DES) is applied onto the exposed cortical and subcortical areas in order to identify the eloquent sites, i.e. where DES elicits motor responses, thus individuating the structures directly acting on the motor descending pathways, or induces transient impairment of the execution of a task, due to its interference with the physiological activity of the stimulated area. This approach allows for the extension of the resection of the tumour beyond its boundaries, increasing the patients' survival while preserving their functional integrity. As has emerged by recent publications of our group, among the different stimulation paradigms available for intraoperative monitoring, the high frequency stimulation ('the pulse technique'), which elicits motor evoked potentials (MEPs), is the most reliable paradigm for mapping the descending fibres originating form primary and non-primary motor areas, also in lesions infiltrating M1, while long and short-range fronto-parietal premotor pathways are well identified when low frequency stimulation ('the Penfield technique') is applied while the patient is performing a dedicated object manipulation task, clearly interfering with its performance. With a multidisciplinary approach, by combining electrophysiological data with virtual anatomical dissections by means of high angular resolution diffusion imaging (HARDI) tractography we correlated the functional properties of the stimulated sites with specific anatomical structures.

In this PhD project, we focused on: the anatomo-functional properties of the human hand representation in M1 (study 1); the oncological and functional efficiency of high-frequency mapping in tumours harbouring within M1 (study 2); the frontal premotor pathways involved in controlling fine hand movements (study 3).

Study 1, conducted on 17 patients who underwent an awake procedure, reported a possible subdivision, based on anatomo-functional analysis, of the human hand-knob in two sectors (a posterior one, close to the central sulcus, and an anterior one, close

to the precentral sulcus) with different cortical excitability, different hand-muscle electromyographic (EMG) pattern when stimulations were delivered during the object manipulation task and, finally, with different local cortico-cortical connectivity. Overall data suggests that the two sectors may exert different roles in motor control.

Study 2 consisted of a retrospective analysis of 102 patients who underwent an asleep procedure for the removal of tumours harbouring with M1 and its descending fibres. The neurophysiological protocols adopted for the intraoperative brain mapping were correlated with the clinical condition, the tumour imaging features, the extent of the resection and the post-operative functional outcome. First, results indicated that M1 tumour removal is feasible and safe and the high frequency stimulation was revealed as the most efficient and versatile paradigm in guiding resection of M1, affording 85.3% complete resection and only 2% permanent morbidity. The study confirmed the possible subdivision of M1 in a rostral less excitable region and a caudal more excitable region reported in Study1 with its clinical impact: the rostral sector can be indeed considered a safe point of entry for surgery and thus for catheters.

Study 3 aimed at characterizing the effect of DES on the electrical activity (EMG) of hand movers during a dedicated object-manipulation task during subcortical stimulation of the frontal white matter anterior to M1 (precentral gyrus) and the anatomical evaluation of the stimulated sites by means of diffusion tractography, in 36 patients who underwent an awake surgery. Results indicated that stimulations of dorsal premotor connections with the spinal cord, dorsal striatum, local U-shaped connections and the superior longitudinal fasciculus I and II resulted in abrupt arrest of the hand, while more ventral stimulation, mainly targeting the third branch of the superior longitudinal fasciculus (SLF III) resulted in clumsy hand movements. Resection cavities analysis showed that transient post-operative upper-limb motor deficit occurred only disconnecting the supplementary motor area corticofugal fibres and the frontal U-shaped connections. Overall data suggests that DES on dorsal premotor white matter could interfere with areas involved in the very final stages of the motor program, while DES on ventral premotor white matter could halt the sensorimotor transformations necessary for correct hand shaping.

INTRODUCTION

1 Primary motor cortex and descending pathways for hand voluntary movement

Skilled use of the hand and the finger and object manipulation are unique features of dexterous human and non-human primates. Such highly refined digit movement is correlated with the development of a corticospinal system, which originates mainly from the primary motor cortex (M1), but also from premotor and parietal regions, and terminates on alpha motoneurons (Porter & Lemon, 1995). This chapter is focused on the anatomo-functional organisation of M1 and its descending pathways, i.e. the main structures which allows voluntary control of the hand.

1.1 *Functional organization of the primary motor cortex*

Almost 150 years ago, pioneering works of Fritsch and Hitzig (1870) in Germany and Ferrier in England (1874; 1875) showed for the first time that stimulation of the rostral bank of the central sulcus of different mammals evokes movement in the contralateral musculature and that lesions of the motor map directly cause impairment in movement performance. Later, direct electrical stimulation experiments in monkeys (Woolsey et al., 1952) and in humans in the neurosurgical epilepsy setting (Penfield & Boldrey, 1937) confirmed the existence of somatotopic organization of the motor cortex which is shared across different mammals: extending from medial to lateral, the foot, leg, hand and mouth are represented respectively. Body parts that are able to perform finer movements are represented with greater areas on the cortical surface. This proportional topographical organization is represented by the famous *motor homunculus* (Fig. 1). Nowadays, both imaging and stimulation data revealed a much more complex organization of the motor cortex, with overlapping representations and faded borders (Fornia et al., 2018; Meier et al. 2008; Park et al. 2001). Park and colleagues used stimulus-triggered averaging (StTA or single-pulse ICMS) of electromyographic (EMG) activity from 24 simultaneously recorded forelimb muscles (Hudson et al. 2017; Park et al. 2004; Park et al., 2001) to characterize the motor output of the intra-areal organization of the forelimb sector of monkeys' M1. They reported a muscle-based map with a concentric organization: a central core of distal muscles (i.e. wrist, digit, intrinsic hand), which is buried in the central sulcus and is bracketed by an intermediate zone with a distal and proximal intermingled representation, which is in

turn surrounded by a *horseshoe-shaped* proximal muscle zone (shoulder and elbow) (Fig. 2).

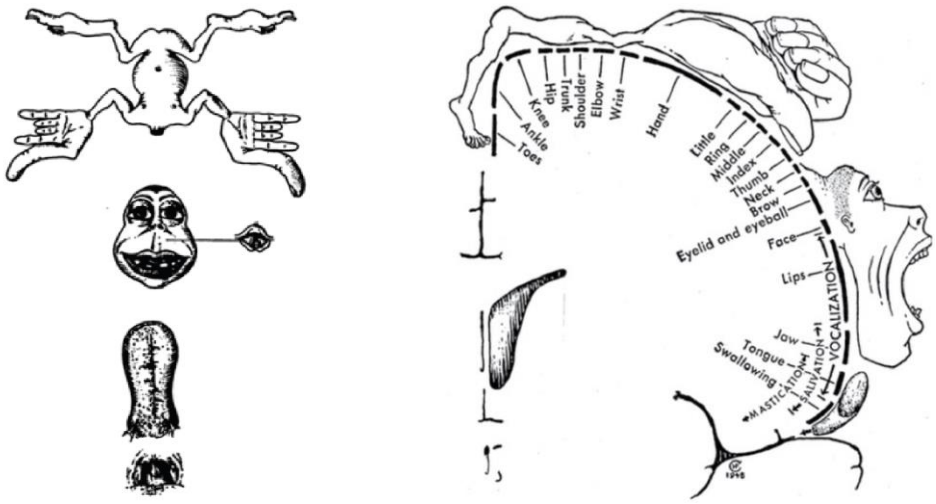

Fig. 1: Original drawing (left) of the sensorimotor homunculus presented in Penfield and Boldrey (1937). 2-D model on the homunculus represented on the Rolandic cortex (right), appeared for the first time in Penfield and Rasmussen (1954).

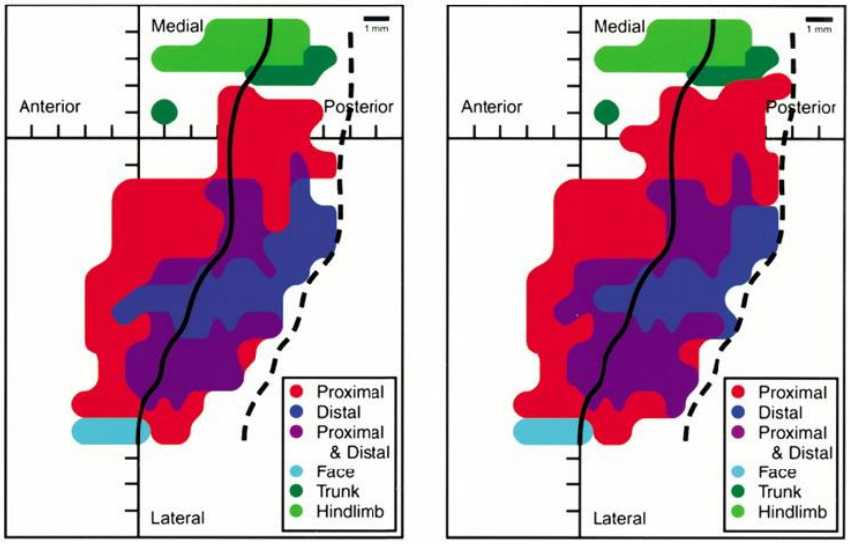

Fig. 2: Modified by Park et al. 2001. Muscle-based maps of two macaque monkeys plotting in 2-D the post-stimulus facilitation effects (obtained using repetitive intracortical microstimulation). The distal hand muscles (blue) in the central sulcus (in dashed line the fundus) are separated from the proximal muscles (red, on the convexity) by a region representing both distal and proximal (purple).

The main two features of this cortical structure showed by Park and Cheney (Hudson, et al. 2017; Park et al. 2004; Park et al. 2001), i.e. the overlapping representations and core-to-surround topography, could facilitate the computation of complex movement of the motor repertoire requiring the coordination of distal and proximal muscles. This two-level complexity has been confirmed with high-resolution fMRI also in humans by Graziano and colleagues (Meier et al. 2008), who showed a core of digit representation in the precentral gyrus bracketed by a wrist and forearm area.

Another set of data which highly contributed in the understanding of the functional organization of M1 is represented by micro-electrodes recording of behaving monkeys. Georgopoulos et al. (1982), recording M1 neurons during a reaching task in different directions, showed that single neurons population discharged was correlated to "*preferred directions*". Cells tuned for the same directions are not clustered within the cortical representation; each movement is indeed coded at a population level by all the neurons of the motor map, with patterns of activation shaped by the direction of the reaching movement, and not only by the cells with that specific preferred direction. Kalaska et al. (1989) modified the same experimental setting adding an external inertial load pulling the arm in eight directions during reaching movement, thus requiring the monkey to increase the force applied to compensate. They showed the existence of "*load-dependent discharges*", that covaried according to application of load (increased activity with opposite load, decreased activity with assisted load) for specific cells recorded. This study is a key indicator that M1 neurons code both kinematic (spatiotemporal aspect of movement, i.e. direction, amplitude, speed, path) and kinetic (causal forces and muscle activity) features of the movement (Evarts, 1968; Fetz & Cheney, 1980; Griffin et al. 2015; Kalaska et al., 1989). A more detailed description of movement-related information coded by M1 corticomotoneuronal cells is present below in paragraph 1.5 (*The corticospinal and cortico-motoneuronal systems*).

1.2 *The anatomy of M1*

Among the cortical areas, the primary motor cortex (M1), i.e. the functional definition of the grey matter located on the rostral bank of the central sulcus and on the convexity of the precentral gyrus, corresponds with cytoarchitectonic Brodmann Area 4 (BA4) and myeloarchitectonic area V42 (Vogt and Vogt, 1919) (Fig. 3). It is characterised by

the presence of giant pyramidal neurons, Betz cells, and heavy myelinization. Betz cells have a diameter about 60 μm, and transmit signals to the spinal cord at a velocity of about 70 m (Hall 2016). Pyramidal cells are more represented than non-pyramidal ones (Cajal 1909-1910). In the motor cortex (also called agranular cortex), it is in fact not possible to distinguish a clear layer IV with spiny stellate cells (the main target for afferent thalamic fibres). However, Yamawaki et al. (2014), using optogenetic stimulation of the ventrolateral motor nucleus in the mouse, recently demonstrated the existence of a population of neurons, located between layer III and V, with features typically associated with layer IV neurons: they receive inputs from the thalamus, and send cortico-cortical outputs to layers II and III. Nowadays M1 in not considered to be a single region, rather two sectors exist with different cytoarchitectural and receptor density characteristics, area 4posterior and area 4anterior, also supposed to play distinct roles in motor control (Geyer et al. 1996; Fig. 3). Jones (1983) showed the presence, in layers III, IV and V, of so-called basket cells, responsible for inhibitory effects on axon collaterals of corticofugal fibres in the motor cortex via GABAergic synapses. The pyramidal cells, which are responsible for motor output, are distributed from lamina II to lamina VI, however they are most highly concentrated in lamina III and lamina V. Ghosh and Porter (Ghosh & Porter, 1988) showed that in the monkey, the morphology and intracortical axon collaterals of pyramidal tract neurons (PTNs) are subdivided into fast and slow conducting, according to their axonal conduction velocity and membrane properties (Lance & Manning, 1954; Takahashi, 1965) . The morphology of these neurons differs in the different laminae: intracortical axon collaterals from lamina III (mainly cortico-cortical cells) may spread to all other laminae while the ones originating from cells in lamina V (mainly corticofugal cells) terminate in lamina V itself and in lamina VI. Recording of antidromic volleys from the pyramidal tract (medullary pyramids) primarily result in monosynaptic excitatory postsynaptic potentials in fast PTNs, in inhibitory potentials in slow PTNs and in both excitatory and inhibitory in other types of pyramidal cells, while antidromic volleys from the peduncle result in excitatory responses in all three classes.

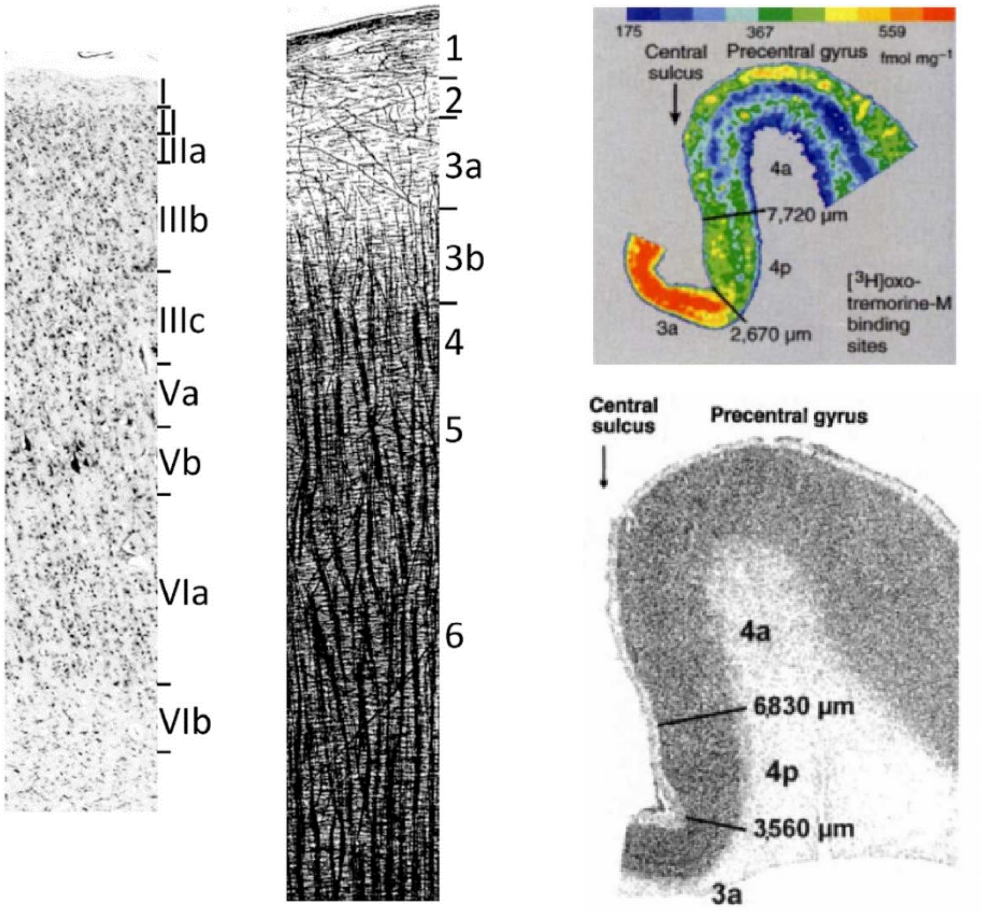

Fig. 3: Left panel: laminar pattern of cyto-architecture (left) and myelo-architecture (right) of the primary motor cortex (BA4). Reproduced from Palomero-Gallagher & Zilles, 2019. Right panel: Sections of the precentral gyrus showing the division between areas 4a and 4p by means of [^{3}H]oxotremorine-M binding sites on muscarin M_2 and M_4 receptors distribution (on top) and on Nissl-stain (below). Reproduce from (Geyer et al. 1996).

To exert control over complex hand behaviour, the pyramidal neurons of BA4 are involved in different loops connected with the basal ganglia, cerebellum and other cortical areas. Frontal white matter connectivity involved in motor programming and executing is described in more detail and discussed in Study 3.

1.3 *Afferent fibres to M1*

The main afferent fibres to reach the cortex of M1 are:

- *Thalamocortical fibres*, terminating in the dendritic spines of the pyramidal neurons with excitatory effect (Amassian and Weiner 1966). These thalamocortical

terminations are found mainly in lamina III and at the border between lamina III and IV (Sloper & Powell, 1979; Strick & Sterling, 1974).

- *Cortico-cortical fibres*: efferent fibres originate from M1 in layer III and reach the granular cortex (Jones et al. 1975); afferent fibres make contact with pyramidal (on the dendritic spines) and non-pyramidal (on the dendritic shaft) cells. Most of these fibres make local connections within M1, while commonly the afferent fibres from other granular cortical areas originate in the SMA, premotor cortex, BA1, 2 and 5 (Jones et al. 1975).

- *Callosal fibres*: originate from the contralateral BA4 lamina III and reach the dendritic spines of layers I through III (Sloper & Powell, 1979).

1.4 *M1 collaterals and spinal pathways*

Efferent projections from M1 are organised in specific patterns depending on the laminar structure of the cortex. All subcortical projections arise from pyramidal cells in layer V, except for cortico-thalamic fibres which arise from lamina VI and the corticostriate fibres which project from lamina III (Goldman-Rakic & Selemon, 1986). Small size pyramidal cells in the upper component of layer V project to the striatum (putamen) and claustrum. Small and medium size pyramidal cells in the middle and deeper part of lamina V give rise to connections to the red nucleus (corticorubral system) in the mesencephalon and to corticopontine, corticobulbar and corticonuclear connections (brainstem). Medium and large size neurons in the deeper part of lamina V give rise to the corticospinal system. The latter one and the rubrospinal systems are the only corticofugal connections originating solely from the motor cortex. These organisation of efferent fibres from M1 is summed up in the following illustration reproduced from Jones (1984) (Fig. 4).

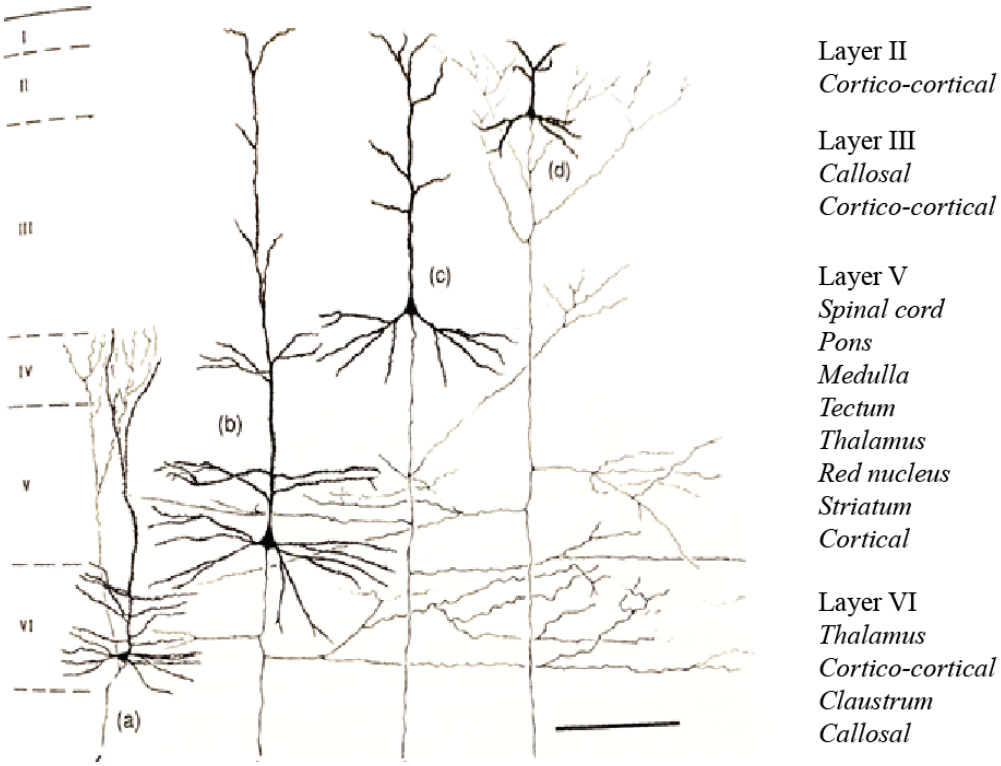

Fig. 4: Laminar origins of efferent projections (listed on the right) of cortical neurons. Reproduced from Jones (1984).

The existence of collateral corticospinal fibres reaching different subcortical structures is a main feature of the cortical output, especially when considering fast PTNs, mainly studied using fluorescent retrograde double labelling (Kuypers & Huisman, 1984). The functional role of the main corticospinal collateral bundles, i.e. the *corticorubral* (target = red nucleus), the *corticopontine* (target: ventrolateral pontine tegmentum), the *corticoreticular* (target = medullary reticular formation) and the *corticonuclear* (target = gracile and cuneate nucleus in the dorsal medulla) collaterals is theorised to be to send copies of cortical information to subcortical structures (Porter and Lemon, 1993). The corticonuclear collaterals have been hypothesized to mediate, with the production of efference copies, afferent sensory information generated by voluntary commands.

The knowledge regarding the functional role of all the other descending pathways, with respect to the corticospinal tract, is still not exhaustive especially in the human

primate, although is it possible to distinguish and characterize them according to their termination within the spinal grey matter. Kuypers (Kuypers & Brinkman, 1970), following this principle, organised the descending pathways in a dorsolateral and a ventromedial group:

1) **Dorsolateral brainstem pathways**: composed by the ***rubrospinal tract*** and the ***pontospinal tract***. While the first one originates from the neurons in the caudal magnocellular portion of the red nucleus (which receives cortical signals), the latter origins in the ventrolateral pontine tegmentum. They both descend contralaterally in the dorsolateral funiculus. Their target is the dorsolateral portion of the intermediate zone in the spinal cord and they have also some terminations in the lateral zone, where the motor nuclei are located that innervate the arm and the hand. Kuypers (1981) claimed that these pathways could be useful for flexion movements of proximal effectors, such as the wrist and the elbow. The rubrospinal fibres are less prevalent in humans, however we cannot rule out their involvement control of upper limb movement (Nathan & Smith, 1982).
2) **Ventromedial brainstem pathways**: composed of the ***reticulospinal, tectospinal*** and ***vestibulospinal tracts.*** These tracts originate respectively from the medial medullary reticular formation, the superior colliculus in the midbrain and the vestibular complex. They terminate bilaterally in the ventromedial portion of the intermediate zone and they also have access to the motoneurons innervating the trunk and the girdle. The most accredited theory about the functional role of these tracts interpret them as a system for controlling bilaterally the neck, head, trunk and proximal limb posture (Lawrence & Kuypers, 1968) as well as the control of respiration (de Troyer et al. 2005). More recent data showed that the corticoreticulospinal system is associated with the tone and the position of the proximal musculature (Buford & Davidson, 2004), as well as with the control of distal muscles bilaterally (Baker, 2011).

The following picture (Fig. 5) reproduced by Lemon (Lemon, 2008), shows the descending pathways (dorsolateral, ventromedial brainstem projections and corticospinal tract) with their spinal terminations.

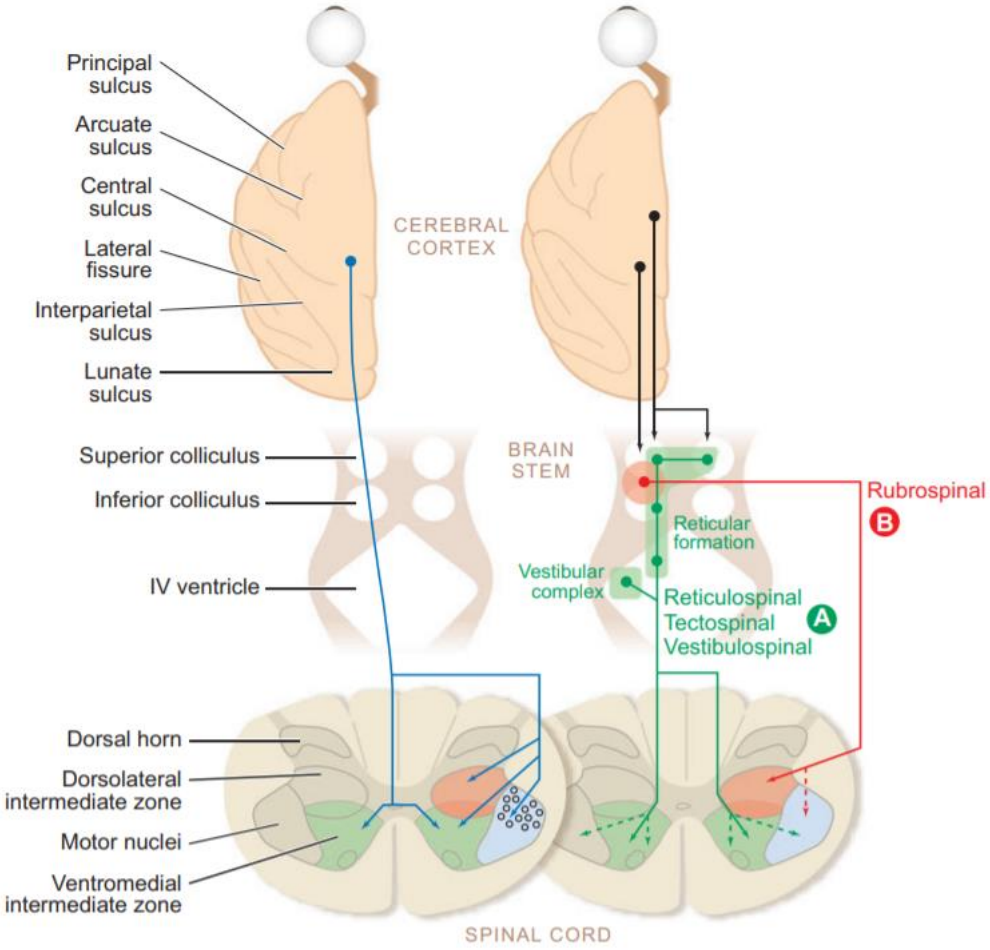

Fig. 5: Schematic representation of the descending fibres originating from the motor cortex. In blue the corticospinal tract, terminating in the lateral part of the intermediate zone (IZ) of the spinal cord; in red the rubrospinal tract, originating from the red nucleus and terminating in the dorsolateral portion of the IZ; in green the reticulospinal, tectospinal and vestibulospinal tracts projecting bilaterally to the ventrolateral portion of the IZ. Reproduced from Lemon (2008).

1.5 *The corticospinal and cortico-motoneuronal systems*

In higher order primates, corticospinal connections reach the ventromedial intermediate zone of the spinal cord bilaterally and the lateral intermediate zone of the spinal cord contralaterally, acting directly on the motor neurons innervating the hand muscles. The axons of the corticospinal tract descend from layer V pyramidal neurons through the corona radiata, the internal capsule, the cerebral peduncle (midbrain) and finally to the medulla where, on the ventral surface, they form the so-called medullary pyramids. Most of the fibres (90%), before reaching the spinal cord, cross the midline forming the lateral corticospinal tract (pyramidal medullary decussation). Each

corticospinal tract counts around 1 million of myelinated fibres: 97% of them are smaller than 4 μm of diameter, while only 3% have a bigger diameter (mean of 16 μm). According to (Dum & Strick, 1991), around 49% of corticospinal neurons are located, in monkey, in M1, while the remaining component of the fibres are arising from the superior precentral sulcus (7-10%), the arcuate premotor area (4-9.6%), the SMA (12.2-18%) and the cingulate motor areas (dorsal 8-10.5%, ventral 6.1-6.8%, rostral 2.9-4%). However, the fibres originating from the rostral sector of the precentral gyrus (area BA6) terminate mainly in the ventromedial component of the intermediate zone of the spinal cord (Kuypers & Brinkman, 1970), an area devoted to the bilateral control of the trunk and girdles via propriospinal connections. Corticospinal axons originating from M1 are not only highest in proportion (Maier, 2002), but they are also the thickest and fastest, probably having the most powerful synaptic connection in the spinal cord (Innocenti & Caminiti, 2017). A direct connection with motoneurons in the dorsolateral segment of the intermediate zone seems a unique feature of bundles arising from the caudal-most sector of the primary motor cortex (Morecraft et al., 2013; Rathelot & Strick, 2009; Witham et al. 2016). Precisely, the caudal sector of M1 (the so-called "new-M1"), incorporating the bank of the central sulcus, shows dense cortico-motoneuronal (CM) projections to the ventral horn of the spinal cord, whereas the rostral sector (the so-called "old-M1") shows very few CM projections (Rathelot & Strick, 2009; Witham et al., 2016). Intracortical Microstimulation (ICMS) of the two sectors showed that both elicits long latency monosynaptic Excitatory Post-Synaptic Potentials (EPSPs), but only the new-M1 evokes fast monosynaptic responses (Witham et al., 2016). Based on these observations it had been hypothesised that the two regions may exert different roles in motor control through different corticospinal connections: the new-M1 would act directly on the motor output, while the old-M1 would shape the motor output via indirect pathways, by acting on spinal interneurons. In the first study (Study 1) reported in the present thesis, we analysed the quantitative motor output (MEPs) when stimulating the human hand-knob region in a rostro-caudal fashion, from the central sulcus to the precentral one, with the aim of investigating the possible existence, similarly to the monkey's M1, of different sectors within the human M1 hand representation. Results are discussed in light of functional data coming from the

monkey literature, where the posterior-to-anterior transition between the new-M1, old-M1 and caudal dPM (F2) has been architectonically validated.

Morecraft and colleagues (Morecraft et al., 2013) analysed the terminal distribution (from C5 to T1 spinal segments) of cortico-motoneuronal output from the hand representation of M1 in the macaque using high-resolution anterograde tracing and stereology. 98% of labelled neurons reached the cord contralaterally, mainly terminating in the intermediate zone, lamina VII (59%) with a highest concentration at level of C5-C7, therefore acting indirectly on hand-arm motoneurons, while 18% of boutons were labelled in lamina IX, making synapses directly with motoneurons innervating flexors acting on the shoulder and elbow rostrally (C5-C7) and flexors, abductors and adductors innervating the hand and wrist caudally (C8-T1). Although some of these cortico-motoneuronal (CM) cells projects to motoneurons of single muscles, most of them make monosynaptic connections with motoneurons of multiple synergist muscles (Buys et al. 1986; Fetz & Cheney, 1980; Porter & Lemon, 1995; Schieber & Rivlis, 2007). CM neurons can give rise to different combinations of spinal interneuron networks and spinal motor neuron pools (in addition to the other corticospinal axons terminating only on spinal interneurons): a single CM axon usually branches to different agonist motoneurons and could indirectly suppress the respective antagonist motoneurons via local inhibitory interneurons (Cheney et al. 1985; Kasser & Cheney, 1985) (Fig. 6). This mechanism allows for coordination within a muscle field of agonist and antagonist muscles.

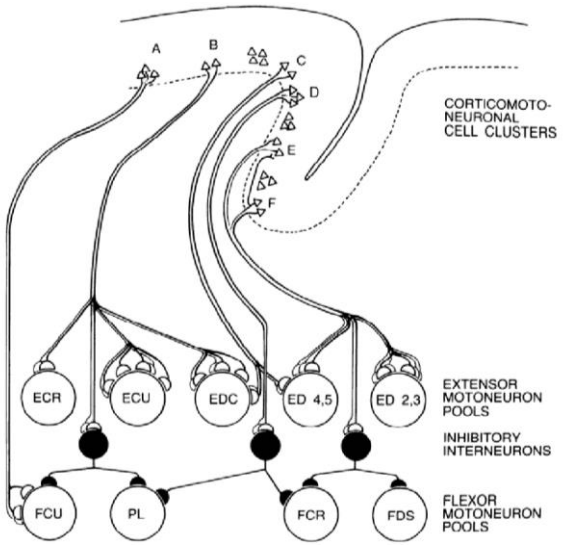

Fig. 6: In this example, reproduced from Cheney, Fetz and Palmer (1985), CM cells projects to a set of extensors motoneurons and inhibitory interneurons that could act on the antagonist muscles (flexors in this case).

The functional correlation between the activity of cortical CM cells and their target muscles is not clear, however we know certainly that independent finger movements and thus the index of dexterity is highly correlated with the development of dense cortico-motoneuronal connections (Heffner & Masterton, 1983; Lemon & Griffiths, 2005). From rodents to New World monkeys, Old World monkeys and finally humans, the increase in manual abilities is correlated with an increase both in the number of corticospinal fibres and in the amplitude of cortico-motoneuronal EPSPs (Courtine et al., 2007). Comparing the firing of M1 CM-cells during a 'precision grip' and a 'power grip', Muir and Lemon (Muir & Lemon, 1983) showed a specific role for this neural population in the control of independent finger movements in a task-specific situation ('precision grip') rather than in an a-specific activation of the muscles innervated. In line with this finding, evidence from studies using post-spike facilitation suggested that CM cells of M1 facilitate complex functional muscle synergies rather than single muscle recruitment (Buys et al. 1986; Fetz & Cheney, 1980). Individual CM cells seem to be functionally tuned: different CM neuron populations fire selectively to different functions of the same target muscle, used for example as an agonist, synergist, fixator or antagonist (Griffin et al., 2015). The authors claim that this functional tuning could be an emergent property of the evolutionary process which associates the development of direct access to motoneurons, and the consequent bypassing of spinal interneurons, with the acquisition of highly skilled movement (Griffin et al., 2015; Rathelot & Strick, 2009). This system provides a higher number of degrees of freedom in terms of possible synergies to control, compared to the fixed number of synergies represented in spinal machinery. Moreover, it was shown that CM cells code not only a precision grip realized with the finger, but also the same motor act realized with a rake (Quallo et al. 2012). This suggests that the same CM population is involved in the computation of tool use movements. In addition to the control of fine independent digit movement, CM cells have been shown to discharge in the stabilisation period of a given movement (Bennett & Lemon, 1994; Quallo et al., 2012).

1.6 *Lesions of the primary motor cortex*

Damage to cortical motor areas and the pyramidal tract, both naturally occurring or experimentally induced, have helped in understanding the different roles in motor control of specific structures. However, ascribing a 1:1 correlation between symptoms

and damaged tissue should be treated with caution: in a post-lesional behavioural scenario, compensatory effects of other areas in the same network and fast plastic changes of the lesioned structure may occur (Rouiller et al., 1998; Schmidlin et al. 2008; Vavrek et al. 2006). Cortical primary motor cortex lesions usually result in muscle weakness, loss of precision, speed and coordination between joints. Unilateral lesions of the hand representation of M1 (Danny-Brown & Botterel, 1947; Fulton, 1949; Travis, 1955), as well as reversible inactivation of the same area (Rouiller 1998), cause a dramatic loss of skill in prehension grip and wrist orientation allowing for a precision grip. Hoffman and Strick (Hoffman & Strick, 1995) lesioned the M1 arm representation of a monkey trained in performing step-tracking movements of the wrist in different directions. After surgery the correct pattern of contraction between agonist, synergist and antagonist was lost and the movements were misdirected and slower. The co-contraction of the wrist flexor and extensor was the most impaired pattern. Besides confirming the crucial role of M1 in computing the direction of the hand trajectory (Georgopoulos et al., 1982), the authors showed its relevance in generating functional spatiotemporal patterning of agonist and antagonist muscle activations. In paragraph 1.2, *"The anatomy of M1"*, we reported the existence of a gradient in laminar structure between area 4p in humans, buried in the central sulcus and supposed to host the highest concentration of CM projections, and the anterior area 4a (Geyer et al. 1996), while in paragraph 1.5, *The corticospinal and corticomotoneuronal systems*, we discussed the anatomo-functional distinction between the caudal new-M1, dense of CM cells, and the rostral old-M1 (Rathelot & Strick 2009; Witham et al. 2016). Unfortunately, lesion studies in the Old-World monkey aimed at discriminating between the post-operative outcome of lesions induced in the posterior or anterior sector of the hand representation of M1, are still missing. In Roullier et al. (1998) reversible partial inactivation of M1 was administered to seven monkeys. Monkeys with lesions limited to the convexity of the central sulcus had post-operative milder deficits in the precision grip task compared to monkeys whose lesions extended from the convexity to the depth of the central sulcus (Fig. 7). Schieber & Poliakov (1998) made intra-cortical injections of muscimol in the hand area of M1 and evaluated the behavioural outcome in flexions and extensions of the fingers and the wrist. As explicitly stated by the authors, it was beyond the aim of the study to discriminate

between deficits produced by transient lesions of the caudal or rostral portion of area 4, however the existence of a double representation of the hand and fingers was at the time already suggested (Preuss et al. 1997; Strick & Preston, 1982). Nevertheless, the authors declared to have performed the injections in the anterior bank and lip of the central sulcus, likely inactivating what in 2009 Rathelot and Strick named as new-M1. Without an electrophysiological and histological verification of the site, we can perhaps ascribe the main result of that work to the caudal-most part of M1. Monkey movements were characterized by weakness, slowness and a clear deficit in finger individuation and these three symptoms were dissociable. The loss of independent finger movement was configurated as an impossibility for all the other fingers to move autonomously from the finger in the pre-shaping phase.

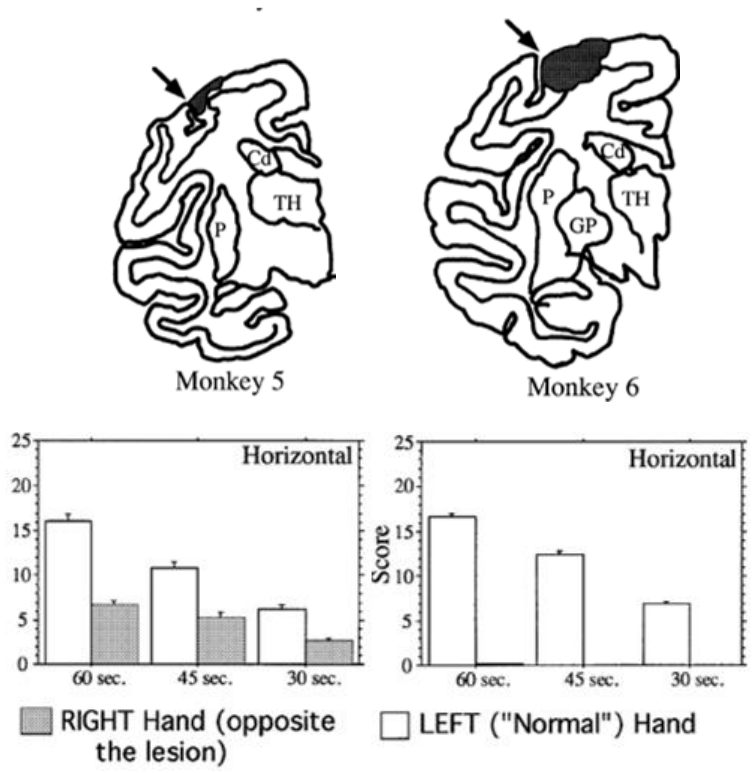

Fig. 7: Modified from Roullier et al. (1998). On the top the anatomical extension of partial inactivation of M1 hand-region in two macaque monkeys. In monkey 5 the lesion had a lesser volume, sparing the central sulcus. In the lower panel is showed the post-lesion functional outcome measured with a precision grip task. Scores correspond to the number of slots successfully retrieved during the three test periods considered (60, 45 and 30 s). The larger lesion of Monkey 6 correlated with a poorer outcome.

Darling et al. (2014) surgically removed the grey matter of the rostral M1 in one macaca mulatta and the rostral M1 plus 1/3 of the caudal M1 in a second monkey

(according to Rathelot and Strick new and old M1 separation) and evaluated the post-operative motor function using a foraging board task in which the monkey can freely choose the hand to retrieve the food. Immediately post-op, a clear contralesional hand paresis occurred and the monkeys explored the board only with the ipsilesional one. However, after 3 weeks, both monkeys spontaneously recovered without any forced use, showing a precision grip and a food manipulation comparable to the pre-operative behaviour. This recovery occurred even in the monkey with 1/3 of the new-M1 ablated, however with the tendency to use less the contralesional versus the ipsilesional hand. Savidan and colleagues (2017) injected ibotenic acid in the rostral bank of the central sulcus (new-M1) of a macaque, producing an irreversible impairment in the grasping skill of the contralateral hand. The ability that was most compromised by the lesion was the complex precision grip which required both the pro-supination and the wrist deviations (measured with a modified Brinkman board task). This suggests that lesioning the caudal grey matter of M1 could result in more dramatic fine finger movement deficit, although a study which compare the post-lesion outcome between the two sectors in the same animal is still missing.

In the New-World monkey, where M1 neurons are unfolded on the convexity, it is possible to lesion selectively the posterior or the anterior sector of the hand representation. Friel et al. (2015) made small ischemic lesions in the two sectors and were able to dissociate between different sensorimotor deficits. Monkeys were trained to retrieve food from wells positioned on a board. After lesioning the rostral portion, they made aiming errors and needed to contact the surface of the board before entering with the fingers in the wells. After lesions in the caudal sector, monkeys frequently visually inspected their finger to detect the effective presence of food after the retrievals. The aiming errors caused by anterior lesions indicate a deficit in the processing/integration of proprioceptive inputs and are coherent with the proximal representation of the sector, while the deficit in the integration between the tactile information and the motor output determined by posterior lesions is instead coherent with the more distal representation of the central sulcus area and its cutaneous afferences.

In humans, ischemic cortical stroke of the hand representation in M1, the hand-knob region, (which represents less than 1% of all the ischemic strokes) determines an

immediate hand paresis followed by a good extent of recovery in the months after the event (Orosz et al., 2018; Peters et al., 2009).

1.7 *Lesions of the corticospinal tract*

Lawrence and Kuypers (1968) showed that after a complete pyramidotomy a permanent deficit in independent finger movements enabling a precision grip occurs. However, to quantify the amount of effective CM fibres injured, dedicated paradigms are required. Sasaki et al. (Sasaki et al., 2004) selectively damaged the lateral funicle at the border between C4 and C5, just rostral to the forelimb CM neurons. After an initial complete inability to move the fingers independently (a similar outcome to the pyramidotomy performed by Lawrence and Kuypers), after 1-28 days the monkeys were again able to retrieve the food with a grasping movement (although they were slower, and they showed a deficit in pre-shaping and in force between the index and the thumb finger). Given that the lesion damaged both the CM projections from C5 and the corticospinal projection to segmental interneurons below the lesion, the authors concluded that these two pathways are not the only responsible for the control of fingers movement. In the takeover of the lost function, the authors proposed different structures such as the rubrospinal system and the propriospinal neurons in C3-C4 (and obviously the possible spared CM fibres), based on the electrophysiological result of their work: EPSPs recorded after the lesion had longer latencies compared to pre-operative volleys of CM cells. These responses could be generated both from spared slower CM projections in C4-C5 or from propriospinal projections in C3-C4, which can mediate CM EPSPs. Other studies in monkey (Freund et al., 2006; Galea & Darian-Smith, 1997) confirmed the same reversible behavioural outcome after a unilateral lesion of the lateral CST at cervical level: after an initial deficit in force, speed and accuracy, a progressive recovery occurred however the monkey never regained completely the independent finger movement, especially the thumb (this deficit probably reflects the lack of CM fast projections to the hand motoneurons).

Evaluating the motor outcome of the hand/finger movement after selective lesions (ischemic strokes) of the human primary motor cortex or the corticospinal tract is challenging, considering that lesions may occur for instance in the cortical grey matter, in the corona radiata, in the internal capsule or in the pons, and thus damaging the CST

obviously in an uncontrolled way. Stroke literature usually groups and evaluate the functional outcome without precise anatomical discriminations. Furthermore, there may also be insults to tissue surrounding the lesion. Finally, correlation between the functional outcome and the damaged structure should always take into account the spared connectivity. However, ischemic episodes in basis pontis or in the posterior limb of the internal capsule usually cause a contralesional hemiparesis. Lang and Schieber (2004) evaluated the long-term impairment in independent finger movements after stroke in M1 and the CST, highlighting their crucial role in skilled hand motor control. An examination of the mechanism of recovery and plasticity after damages of M1 and its connections to the spinal cord goes beyond the scope of this dissertation and will not be discussed here.

In the neurosurgical setting for brain tumour removal, the resection of lesions harbouring in M1 and its descending pathways has historically been considered unfeasible, since damages of these structures is usually correlated with permanent motor deficits with a poor possibility of recovery (Ius et al. 2011). The second study of this PhD project (Study 2) directly challenges this idea, reporting a series of 102 asleep procedures guided by high frequency stimulation, reaching an optimal balance between the oncological and the functional outcome.

2 Brain tumours and surgical removal: *the functional approach*

A primary brain tumour is an expansive, infiltrating and chronic process of uncontrolled cells proliferation originating from brain tissues, cranial nerves, meninges, pineal, pituitary, vascular and osseous elements. Tumours harbouring in the central nervous system (CNS) are considered a rare disease, with a rate of incidence around 6 cases per 100'000 people/year in Europe (according to *Surveillance of Rare Cancers in Europe*, RARECARE-2012). They usually do not spread outside the CNS, showing a high tropism to the subarachnoid space. Malignancy is determined on histology and molecular parameters. The World Health Organization (WHO) classifies the CNS tumours basing on nuclear atypia, cellularity, mitotic activity, vascular proliferation and necrosis, in three main groups (grade I, II, III) with increasing malignancy. **Grade I** tumours are *low grade glioma, LGG*, characterized by a low

proliferative potential. This group contains mainly low-grade astrocytoma. **Grade II** are also tumours with low proliferative potential, *LGG*, but they tend to recur after surgical removal and degenerate in higher grades. Protoplasmic astrocytoma and oligoastrocytoma and oligodendroglioma represent this category. **Grade III** group includes faster growing neoplasms, *high-grade-gliomas*, *HGG*, such as anaplastic oligodendroglioma and anaplastic astrocytoma. Finally, **grade IV** tumours are the fastest growing cytologically malignant lesions (glioblastoma, gliosarcoma and giant cell glioblastoma). CNS tumours often cause oedema, reduced blood flow, displacement and/or degeneration of cortical and subcortical structures. Behavioural deficits can occur due to the disruption of neural networks belongings to eloquent areas, i.e. the areas involved in computations of complex functions such as sensory-motor integration, language, executive functions and visuospatial activities. The occurrence of pre-operative deficits is determined by the localisation of the mass and by the WHO grade. Low grade glioma patients tend to show minimal acute symptoms, however lesion infiltration could be extended, while high grade glioma patients may be affected by acute deficits, considering the vascular lesions and the increase of intracranial pressure caused by fast growing neoplasms.

Neurosurgical removal of brain tumours is the most impacting treatment, allowing for relieving symptoms, determining the histological and molecular features of the lesion and prolonging the patient's survival. Based on the histological and molecular parameters, the surgical resection of the tumours could be followed by different adjuvant treatments: radiotherapy (RT) or chemotherapy (CHT). The main factor affecting the prognosis is the extent of resection (estimated by the extent of tumour residual after the surgical treatment) (Rossi et al., 2019; Smith et al., 2008). It follows that the main oncological goal of surgery is to achieve maximal tumour removal. However, tumour localisation or infiltration of eloquent areas is the main factor limiting the extent of resection, their preservation is crucial for maintaining patient's functional integrity. Reaching the maximum of the resection while maintaining patient's integrity, directly impacting both on survival and quality of life, is the actual endpoint of the surgery (Bello et al., 2014; Duffau, 2010; Rossi et al., 2019; Sanai & Berger, 2008), accomplished nowadays with the so-called functional approach, i.e. lesion resection performed until functional boundaries are encountered with the aid of

the brain mapping technique. In modern neurosurgery, the individuation of eloquent structures is performed with a multimodal approach combining pre-operative neurological examinations and intraoperative brain mapping.

The use of intraoperative neurophysiology is crucial, especially in individuating and preserving the motor pathways and particularly the corticospinal system, which is known for its low degree of postoperative plasticity (Robles et al. 2008). It enables intraoperative monitoring to be performed (which comprehends the recording of free-running EMG, electroencephalography, EEG, electrocorticography, EcoG, and the constant monitoring of motor evoked potentials, MEPs) and the intraoperative brain mapping technique delivers direct electrical stimulation (DES) on the cortex and on subcortical white matter with two stimulation paradigm: the 'pulse technique' (High Frequency stimulation, 250-500 Hz, HF-DES) and the 'Penfield' technique (Low Frequency stimulation, 60 Hz, LF-DES) (see General Material and Methods for a detailed description of the routine). During surgery, the choice of HF or LF-DES paradigm to be used to perform brain mapping depends on the clinical context (critically the specific neurological function to be preserved and the clinical conditions that may affect excitability of the patient's brain tissue). By inducing a clear motor output, Motor Evoked Potentials (MEPs), HF-DES is effective in mapping primary and non-primary motor areas/pathways (Bello et al., 2014; Fornia et al., 2018; Viganò et al., 2019). LF-DES, on the other hand, may elicit a motor output when applied to motor areas, although with differences with respect to HF-DES (Bello et al. 2014). Additionally, LF-DES, by transiently interfering with the neuronal activity of a small amount of tissue below the probe, affects the execution of specific tasks (Bello et al., 2014; Rossi et al., 2018) when applied on neural networks underlying their execution during awake neurosurgery. In the following paragraphs the use of the two paradigms both for preserving motor pathways and in the awake setting for preserving higher sensory-motor and cognitive functions is presented.

2.1 *Direct electrical stimulation to map the corticofugal system*

When applied on an eloquent motor area, the direct electrical stimulation produces positive responses, e.g. a contralateral hand activation after the stimulation of the upper-limb representation in the primary motor cortex. Two paradigms of stimulations for intraoperative mapping are, at present, available:

- **Low frequency stimulation** (LF-DES) consists in trains lasting from 1 to 4 seconds of biphasic square wave pulses (0.5 milliseconds each phase) at 60 Hz (Inter stimulus interval, ISI, 16.6 milliseconds). LF-DES is delivered through a bipolar probe (2 ball tips, 2 mm diameter, spaced by 5 mm) (Fig. 8).
- **High frequency stimulation** (HF-DES) is delivered by a monopolar probe (straight tip, 1.5 mm diameter frontal reference) with the following parameters: 1–9 pulses (usually 5, "To5" technique), pulse duration 0.5–0.8 milliseconds, ISI 2–4 milliseconds) with anodal polarity for cortical stimulation and cathodal polarity for subcortical stimulation. Fig. 8 shows the difference between the electrical field induced by the bipolar vs the monopolar probe (the latter one being less focal).

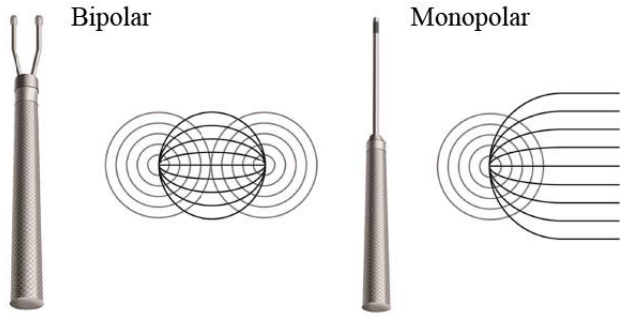

Fig. 8: Scheme of the electric field of the bipolar (left) and monopolar (right) probe.

The localization of positive sites at cortical level and the evaluation of the cortical excitability (performed by identifying the stimulation sites with the lowest cortical motor threshold, cMT) is crucial for the choice of the safe entry point for the resection and for the placement of the strip electrode (4-contact strip, HF-DES, 5stim, 250-500Hz) used to monitor the integrity of the corticofugal pathways through the whole procedure (Fig. 9).

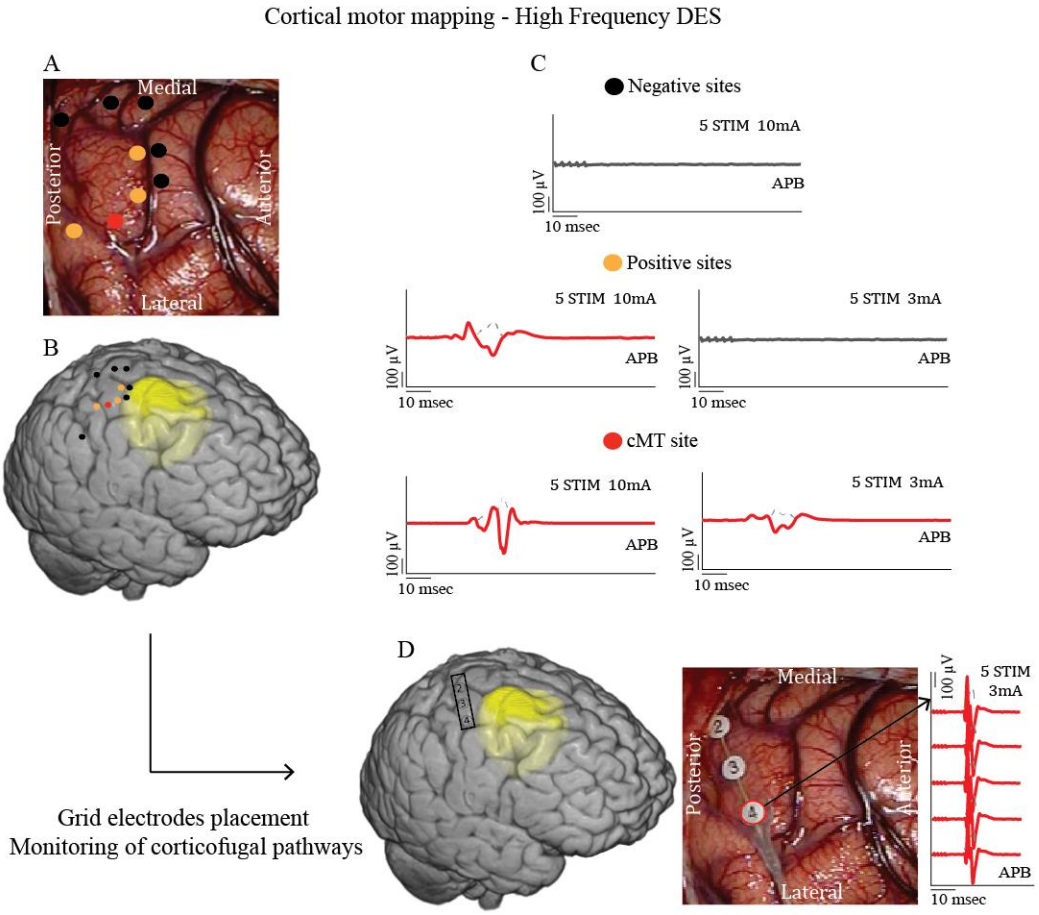

Fig. 9: Cortical motor mapping in the hand-knob region with the 'To5' approach (HF-DES, train of 5 pulses). A motor-map is identified (A-B), and different sites are compared basing on MEPs occurrence and amplitude (C). The site with the lowest cortical motor threshold (cMT, in this case 3mA; showed in red) is useful for the grid electrodes placement which monitors the corticofugal pathways for the whole procedure eliciting MEPs (D). The discrimination between positive (red/orange) and negative (black) sites is crucial in the individuation of the safe entry point and to establish the cortical boundaries of the resection.

The identification of the subcortical motor threshold (sMT) is useful to estimate the distance between the stimulator and the descending motor projections, allowing the surgeon to trace the subcortical boundaries of the resection. For HF-DES, a relationship between the amount of current and the distance from the corticospinal tract (1mA corresponds to 1mm) is reported (Raabe et al. 2014). When the sMT corresponds to 3mA, usually the extension of the resection is stopped to guarantee the preservation of the corticospinal descending fibres (Fig. 10).

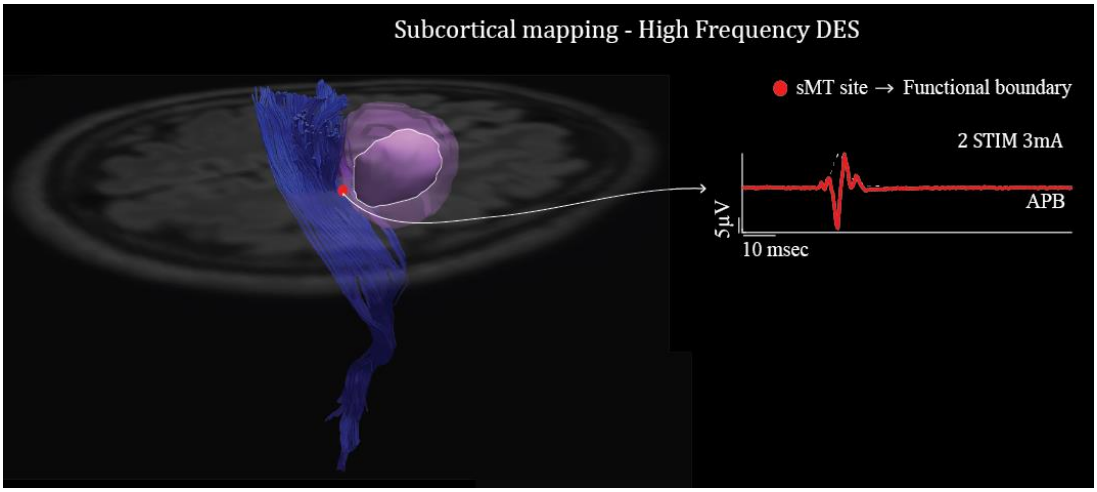

Fig. 10: Subcortical mapping with HF-DES. When the site with the lowest subcortical motor threshold (sMT, in this case 3mA with trains of 2 pulses) is found, the progression of the resection is stopped to avoid damages to the descending motor pathways.

High frequency stimulation was demonstrated to target preferentially the axons of the corticospinal fast-conducting myelinated fibres (Deletis et al. 2001). The multipulse high frequency technique delivered by the monopolar probe was also indicated as the most efficient in the identification of the corticospinal fibres during subcortical mapping (Szelényi et al., 2011). Moreover, a recent paper published by our group reported the experience on 591 surgeries involving the corticofugal tract in which the combined use of HF and LF-DES was tailored by patient clinical history and neuroradiological tumour features (Bello et al. 2014). HF-DES resulted as the most versatile neurophysiological paradigm, allowing a high percentage of resection and a low rate of deficits. It was demonstrated that is applicable and effective even when the lesion is highly infiltrating and/or compressing the motor pathways, when there is a history of uncontrolled seizures or previous treatments. What is still missing in the neurosurgical literature is the identification of the best intraoperative neurophysiological strategy that allows the maximum extent of resection with the simultaneous preservation of the cortico-motoneuronal system in lesions harbouring within M1 and the corticospinal tract. To this aim, Study 2 of this thesis reviewed the HF cortical and subcortical mapping in a series of 102 patients with M1 tumours, in correlation with the functional and oncological outcome.

2.2 *Direct electrical stimulation: the awake setting*

When applied to the primary cortex and its descending fibres, HF and LF-DES, evoking a motor output with quantitative features (amplitude and latency of responses; stimulation threshold) are applicable in the asleep-asleep setting. Differently, the identification of structures subserving higher sensory-motor and cognitive functions (attention, memory, language, visuo-spatial and constructional abilities, executive functions etc.) requires the collaboration of the patient performing, intraoperatively, specific tests, tailored for specific functions, simultaneously to the progressing of the resection. During the intraoperative mapping, both HF and LF-DES at cortical and subcortical level are expected to interfere with the performance of a given task only when applied on areas and/or tracts directly involved in the neural substrate implementing the tested function. However it is not clear if the application of DES causes a transient interference on the ongoing task-related computations needed for its execution or acts on inhibitory circuits preventing or suppressing task realization (Borchers et al. 2012; Filevich et al. 2012; Lüders et al. 1995), it is still considered the goal standard in neuro-oncology (de Witt et al. 2012), being the most reliable technique in functional brain structures individuation. The tissue surrounding the tumour can be recognized as eloquent if, during DES application, a clear error or disruption occurs, and thus preserved, or, conversely, be resected if not responsive to DES. This brain mapping strategy allows at cortical level to define the safe entry point and to extend subcortically the resection until functional boundaries are encountered (Fig. 11). To this aim, the collaboration between neurosurgery and neuropsychology is crucial to guarantee to each patient a tailored awake surgery comprehensive of an extensive pre-op neuropsychological assessment, a proper pre-op training and a correct real-time evaluation of the specific type of symptoms/error elicited by DES to be reported to the surgeon.

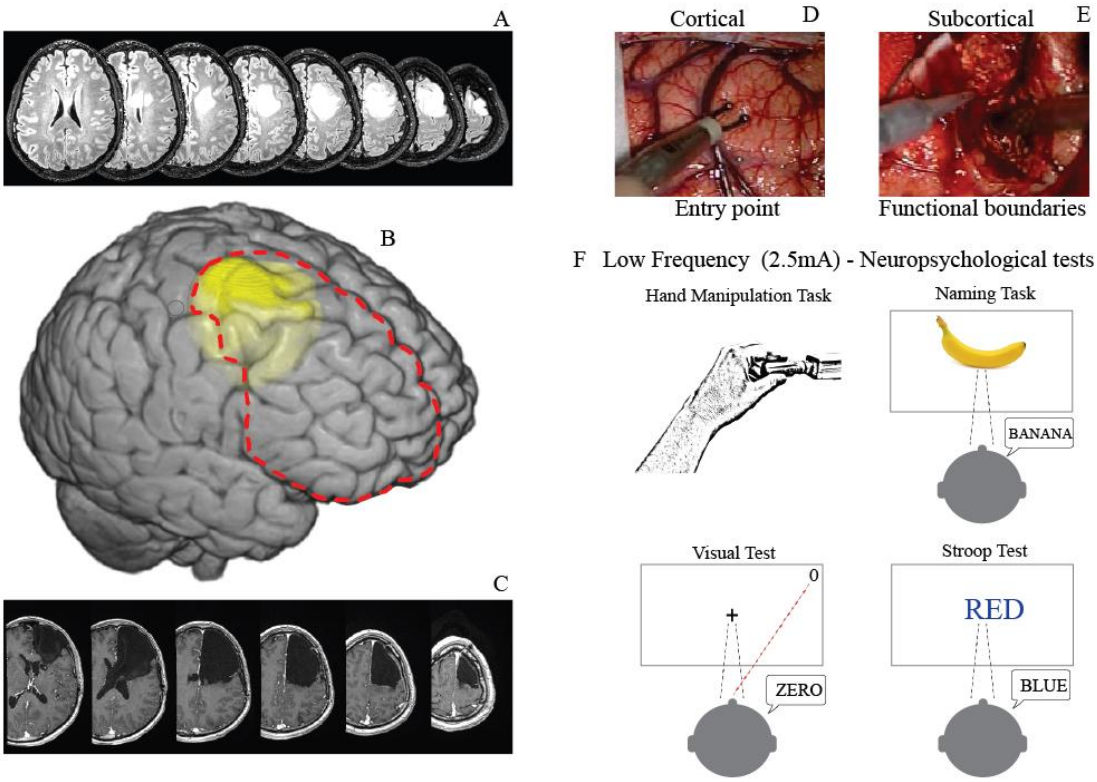

Fig. 11: Rationale underlying the awake brain mapping technique. Left panel: the localisation of the tumour (right frontal lobe) is showed on the pre-operative Flair (A) and on the 3D reconstruction of patient's brain (yellow, B). In C is showed the resection cavity on the post-operative T1 (also represented on the 3D reconstruction by the red dashed line, B). Right panel: Direct electrical stimulation (DES) concomitant to specific intraoperative tools: Hand manipulation task; Naming task; Visual test; Stroop test (F). This procedure allows the identification of the safe entry point at cortical level (D) and to extend the resection until the functional boundaries at subcortical level are found (E).

2.3 *Direct electrical stimulation to map the non-primary areas involved in motor control*

To map the other areas crucially involved in motor control but unlikely to respond to current stimulaiton with motor response, our group recently introduced a hand-object manipulation task (HMt) (Fig. 11-F, Rossi et al. 2018). During the test, the patient has to perform a rotational movement of a tool that resembles a screwdriver. The task, requiring a shaping, holding and releasing of the tool phase, thus resembling a precision grip, involves the integration of proprioceptive and tactile information to compute the muscle synergies needed to shape the complex finger movements. The HMt is realised with a self-generated progamming and rhythm, in absence of visual guidance and any extenal cue. The test, administered in awake procedures which

required the preservation of non-prymary motor pathways, was shown to be feasible and effective in preserving post-operative ideomotor apraxia symptoms (Rossi et al. 2018).

Neurophysiological, behavioural, imaging and clinical data provided by strict adherence to the clinical routine (See General Materials and Methods) were stored, anonymized, evaluated for research purposes and allowed the three studies presented in the thesis.

REFERENCES

Amassian V, Weiner H. (1966). Monosynaptic and polysynaptic activation of pyramidal tract neurons by thalamic stimulation. The thalamus. New York: Columbia University Press; pp. 255–282.

Baker, S. N. (2011, December). The primate reticulospinal tract, hand function and functional recovery. Journal of Physiology, Vol. 589, pp. 5603–5612.

Bello, L., Riva, M., Fava, E., Ferpozzi, V., Castellano, A., Raneri, F., Pessina F, Bizzi A, Falini A, Cerri, G. (2014). Tailoring neurophysiological strategies with clinical context enhances resection and safety and expands indications in gliomas involving motor pathways. Neuro-Oncology, 16(8), 1110–1128.

Bennett, K. M., & Lemon, R. N. (1994). The influence of single monkey cortico-motoneuronal cells at different levels of activity in target muscles. The Journal of Physiology, 477(Pt 2), 291–307.

Borchers, S., Himmelbach, M., Logothetis, N., & Karnath, H. O. (2012, January). Direct electrical stimulation of human cortex-the gold standard for mapping brain functions? Nature Reviews Neuroscience, Vol. 13, pp. 63–70.

Buford, J. A., & Davidson, A. G. (2004). Movement-related and preparatory activity in the reticulospinal system of the monkey. Experimental Brain Research, 159(3), 284–300.

Buys, E. J., Lemon, R. N., Mantel, G. W., & Muir, R. B. (1986). Selective facilitation of different hand muscles by single corticospinal neurones in the conscious monkey. The Journal of Physiology, 381, 529–549.

Cajal, S.R., 1909, 1910, Histologie du système nerveux de l'homme et des vertébrés. (Translated by L. Azoulay). Paris: Maloine. There is an English translation: Histology of the nervous system of man and vertebrates (translated by N. Swanson and L.W. Swanson), New York: Oxford University Press, 1995).

Cheney, P. D., Fetz, E. E., & Palmer, S. S. (1985). Patterns of facilitation and suppression of antagonist forelimb muscles from motor cortex sites in the awake monkey. Journal of Neurophysiology, 53(3), 805–820.

Courtine, G., Bunge, M. B., Fawcett, J. W., Grossman, R. G., Kaas, J. H., Lemon, R., … Edgerton, V. R. (2007). 1. Courtine G, Bunge MB, Fawcett JW, et al. Can experiments in nonhuman primates expedite the translation of treatments for spinal cord injury in humans? Nature medicine. 2007;13(5):561-6. Available at: http://www.ncbi.nlm.nih.gov/pubmed/17479102.Can expe. Nature Medicine, 13(5), 561–566.

Darling, W. G., Morecraft, R. J., Rotella, D. L., Pizzimenti, M. A., Ge, J., Stilwell-Morecraft, K. S., … Cheney, P. (2014). Recovery of precision grasping after motor cortex lesion does not require forced use of the impaired hand in macaca mulatta. Experimental Brain Research, 232(12), 3929–3938.

Deletis, V., Isgum, V., & Amassian, V. E. (2001). Neurophysiological mechanisms underlying motor evoked potentials in anesthetized humans. Part 1. Recovery time of corticospinal tract direct waves elicited by pairs of transcranial electrical stimuli. Clinical Neurophysiology, 112(3), 438–444.

Denny-Brown, D. & Botterell, E.H. (1947) The motor function of the agranular frontal cortex. Res. Publ. Ass. Nerv. Ment. Dis., 27, 235–345.

de Troyer, A., Kirkwood, P. A., & Wilson, T. A. (2005). Respiratory action of the intercostal muscles. Physiological Reviews, 85(2), 717–756.

de Witt Hamer, P. C., Robles SG, Zwinderman AH, Duffau H, Berger MS. (2012). Impact of Intraoperative Stimulation Brain Mapping on Glioma Surgery Outcome: A Meta-Analysis Diffuse low-grade gliomas. Journal of Clinical Oncology, 30(20), 2559–2565.

Duffau, H. (2010). Introduction. Surgery of gliomas in eloquent areas: from brain hodotopy and plasticity to functional neurooncology. Neurosurgical Focus, 28(2)

Dum, R. P., & Strick, P. L. (1991). The origin of corticospinal projections from the premotor areas in the frontal lobe. The Journal of Neuroscience : The Official Journal of the Society for Neuroscience, 11(3), 667–689.

Evarts, E. v. (1968). Relation of pyramidal tract activity to force exerted during voluntary movement. Journal of Neurophysiology, 31(1), 14–27.

Ferrier, D. (1874). Experiments on the brain of monkeys. No. I. Proc. R. Soc. Lond. 23, 409–430.

Ferrier, D. (1875). The Croonian Lecture: experiments on the brain of monkeys. Philos. Trans. R. Soc. Lond. 165, 433–488.

Fetz, E. E., & Cheney, P. D. (1980). Postspike facilitation of forelimb muscle activity by primate corticomotoneuronal cells. Journal of Neurophysiology, 44(4), 751–772.

Filevich, E., Kühn, S., & Haggard, P. (2012, November). Negative motor phenomena in cortical stimulation: Implications for inhibitory control of human action. Cortex, Vol. 48, pp. 1251–1261.

Fornia, L., Ferpozzi, V., Montagna, M., Rossi, M., Riva, M., Pessina, F., Martinelli Boneschi F, Borroni P, Lemon RN, Bello L, Cerri, G. (2018). Functional Characterization of the Left Ventrolateral Premotor Cortex in Humans: A Direct Electrophysiological Approach. Cerebral Cortex (New York, N.Y. : 1991), 28(1), 167–183.

Freund, P., Schmidlin, E., Wannier, T., Bloch, J., Mir, A., Schwab, M. E., & Rouiller, E. M. (2006). Nogo-A-specific antibody treatment enhances sprouting and functional recovery after cervical lesion in adult primates. Nature Medicine, 12(7), 790–792.

Friel, K. M., Barbay, S., Frost, S. B., Plautz, E. J., Hutchinson, D. M., Stowe, A. M., Dancause N, Zoubina EV, Quaney BM, Nudo, R. J. (2005). Dissociation of sensorimotor deficits after rostral versus caudal lesions in the primary motor cortex hand representation. Journal of Neurophysiology, 94(2), 1312–1324.

Fritsch G, Hitzig E. Über die elektrische Erregbarkeit des Grosshirns. Arch Anat. Physiol Wissen 1870;37:300–32.

Fulton, J.F. (1949) Physiology of the Nervous System, 3rd edn. Oxford University Press, New York, p. 667.

Galea, M. P., & Darian-Smith, I. (1997). Corticospinal projection patterns following unilateral section of the cervical spinal cord in the newborn and juvenile macaque monkey. The Journal of Comparative Neurology, 381(3), 282–306.

Georgopoulos, A., Kalaska, J., Caminiti, R., & Massey, J. (1982). On the relations between the direction of two-dimensional arm movements and cell discharge in primate motor cortex. The Journal of Neuroscience, 2(11), 1527–1537.

Geyer, S., Ledberg, A., Schleicher, A., Kinomura, S., Schormann, T., Bürgel, U., Klingberg T, Larsson J, Zilles K, Roland, P. E. (1996). Two different areas within the primary motor cortex of man. Nature, 382(6594), 805–807.

Ghosh, S., & Porter, R. (1988). Morphology of pyramidal neurones in monkey motor cortex and the synaptic actions of their intracortical axon collaterals. The Journal of Physiology, 400, 593–615.

Goldman-Rakic, P. S., & Selemon, L. D. (1986). Topography of Corticostriatal Projections in Nonhuman Primates and Implications for Functional Parcellation of the Neostriatum.

Griffin, D. M., Hoffman, D. S., & Strick, P. L. (2015). Corticomotoneuronal cells are "functionally tuned". Science (New York, N.Y.), 350(6261), 667–670.

Hall JE. (2016). Guyton and Hall: Textbook of Medical Physiology. Thirteenth edition. 2016. John E. Hall Elsevier, Hardcover.

Heffner, R. S., & Masterton, R. B. (1983). The role of the corticospinal tract in the evolution of human digital dexterity. Brain, Behavior and Evolution, 23(3–4), 165–183.

Hoffman, D. S., & Strick, P. L. (1995). Effects of a primary motor cortex lesion on step-tracking movements of the wrist. Journal of Neurophysiology, 73(2), 891–895.

Hudson, H. M., Park, M. C., Belhaj-Saïf, A., & Cheney, P. D. (2017). Representation of individual forelimb muscles in primary motor cortex. Journal of Neurophysiology, 118(1), 47–63.

Innocenti, G. M., & Caminiti, R. (2017). Axon diameter relates to synaptic bouton size: structural properties define computationally different types of cortical connections in primates. Brain Structure and Function, 222(3), 1169–1177.

Ius, T., Angelini, E., Thiebaut de Schotten, M., Mandonnet, E., & Duffau, H. (2011). Evidence for potentials and limitations of brain plasticity using an atlas of functional resectability of WHO grade II gliomas: Towards a "minimal common brain." NeuroImage, 56(3), 992–1000.

Jones, E. G., Burton, H., & Porter, R. (1975). Commissural and Cortico-cortical "Columns" in the Somatic Sensory Cortex of Primates. Science, Vol. 190, pp. 572–574.

Jones EG. 1984. Laminar distribution of cortical efferent cells. In: Peters A, Jones EG., editors. Cerebral Cortex. Vol. 1 Cellular Components of the Cerebral Cortex. New York: Plenum Press; p. 521–553.

Kalaska, J., Cohen, D., Hyde, M., & Prud'homme, M. (1989). A comparison of movement direction-related versus load direction- related activity in primate motor cortex, using a two-dimensional reaching task. The Journal of Neuroscience, 9(6), 2080–2102.

Kasser, R. J., & Cheney, P. D. (1985). Characteristics of corticomotoneuronal postspike facilitation and reciprocal suppression of EMG activity in the monkey. Journal of Neurophysiology, 53(4), 959–978.

Kuypers, H. G. J. M., & Brinkman, J. (1970). Precentral projections to different parts of the spinal intermediate zone in the rhesus monkey. Brain Research, 24(1), 29–48.

Kuypers, H. (1981) Anatomy of the descending pathways. In: Brooks, V., Ed., The Nervous System, Handbook of Physiology, Vol. 2, Williams and Wilkins, Baltimore, 597-666.

Kuypers HGJM, Huisman AM (1984) Fluorescent neuronal tracers. In: Ferdoroff S (ed) Advances in cellular neurobiology, Vol 5. Academic Press, London, pp 307–340

Lance, J. W., & Manning, R. L. (1954). Origin of the pyramidal tract in the cat. The Journal of Physiology, 124(2), 385–399.

Lang, C. E., & Schieber, M. H. (2004). Reduced muscle selectivity during individuated finger movements in humans after damage to the motor cortex or corticospinal tract. Journal of Neurophysiology, 91(4), 1722–1733.

Lawrence, D. G., & Kuypers, H. G. (1968). The functional organization of the motor system in the monkey. I. The effects of bilateral pyramidal lesions. Brain : A Journal of Neurology, 91(1), 1–14.

Lemon, R. N. (2008). Descending Pathways in Motor Control. Annu Rev Neurosci. 31:195-218.

Lemon, R. N., & Griffiths, J. (2005). Comparing the function of the corticospinal system in different species: organizational differences for motor specialization? Muscle & Nerve, 32(3), 261–279.

Lüders, H. O., Dinner, D. S., Morris, H. H., Wyllie, E., & Comair, Y. G. (1995). Cortical electrical stimulation in humans. The negative motor areas. Adv Neurol.

Maier, M. A. (2002). Differences in the Corticospinal Projection from Primary Motor Cortex and Supplementary Motor Area to Macaque Upper Limb Motoneurons: An Anatomical and Electrophysiological Study. Cerebral Cortex, 12(3), 281–296.

Meier, J. D., Aflalo, T. N., Kastner, S., & Graziano, M. S. A. (2008). Complex organization of human primary motor cortex: a high-resolution fMRI study. Journal of Neurophysiology, 100(4), 1800–1812.

Morecraft, R. J., Ge, J., Stilwell-Morecraft, K. S., Mcneal, D. W., Pizzimenti, M. A., & Darling, W. G. (2013). Terminal distribution of the corticospinal projection from the hand/arm region of the primary motor cortex to the cervical enlargement in rhesus monkey. Journal of Comparative Neurology, 521(18), 4205–4235.

Muir, R. B., & Lemon, R. N. (1983). Corticospinal neurons with a special role in precision grip. Brain Research, 261(2), 312–316.

Nathan, P. W., & Smith, M. C. (1982). The rubrospinal and central tegmental tracts in man. Brain : A Journal of Neurology, 105(Pt 2), 223–269.

Orosz, P., Szőcs, I., Rudas, G., Folyovich, A., Bereczki, D., & Vastagh, I. (2018). Cortical Hand Knob Stroke: Report of 25 Cases. Journal of Stroke and Cerebrovascular Diseases : The Official Journal of National Stroke Association, 27(7), 1949–1955.

Palomero-Gallagher, N., & Zilles, K. (2019, August 15). Cortical layers: Cyto-, myelo-, receptor- and synaptic architecture in human cortical areas. NeuroImage, Vol. 197, pp. 716–741.

Park, M. C., Belhaj-Saı, A., & Cheney, P. D. (2004). Properties of Primary Motor Cortex Output to Forelimb Muscles in Rhesus Macaques. J Neurophysiol, 92, 2968–2984.

Park, M. C., Belhaj-Saı, A., Gordon, M., & Cheney, P. D. (2001). Consistent Features in the Forelimb Representation of Primary Motor Cortex in Rhesus Macaques.

Penfield, W., & Boldrey, E. (1937). Somatic motor and sensory representation in the cerebral cortex of man as studied by electrical stimulation. Brain, 60(4), 389–443.

Peters, N., Müller-Schunk, S., Freilinger, T., Düring, M., Pfefferkorn, T., & Dichgans, M. (2009). Ischemic stroke of the cortical "hand knob" area: stroke mechanisms and prognosis. Journal of Neurology, 256(7), 1146–1151.

Porter R, Lemon R. 1993. Corticospinal function and voluntary movement. Oxford, UK: Oxford Science.

Preuss, T. M., Stepniewska, I., Jain, N., & Kaas, J. H. (1997). Multiple divisions of macaque precentral motor cortex identified with neurofilament antibody SMI-32. Brain Research, 767(1), 148–153.

Quallo, M. M., Kraskov, A., & Lemon, R. N. (2012). The activity of primary motor cortex corticospinal neurons during tool use by macaque monkeys. Journal of Neuroscience, 32(48), 17351–17364.

Raabe, A., Beck, J., Schucht, P., & Seidel, K. (2014). Continuous dynamic mapping of the corticospinal tract during surgery of motor eloquent brain tumors: evaluation of a new method. Journal of Neurosurgery, 120(5), 1015–1024.

Rathelot, J.-A., & Strick, P. L. (2009). Subdivisions of primary motor cortex based on cortico-motoneuronal cells. Proceedings of the National Academy of Sciences of the United States of America, 106(3), 918–923.

Robles, S. G., Gatignol, P., Lehéricy, S., & Duffau, H. (2008). Long-term brain plasticity allowing a multistage surgical approach to World Health Organization Grade II gliomas in eloquent areas. Journal of Neurosurgery, 109(4), 615–624.

Rossi, M., Ambrogi, F., Gay, L., Gallucci, M., Conti Nibali, M., Leonetti, A., … Bello, L. (2019). Is supratotal resection achievable in low-grade gliomas? Feasibility, putative factors, safety, and functional outcome. Journal of Neurosurgery, 1–14.

Rossi M, Fornia L, Puglisi G, Leonetti A, Zuccon G, Fava E, Milani D, Casarotti A, Riva M, Pessina F, Cerri G, Bello L. 2018. Assessment of the praxis circuit in glioma surgery to reduce the incidence of postoperative and long-term apraxia: a new intraoperative test. J Neurosurg. 23:1-11

Rouiller, E. M., Yu, X. H., Moret, V., Tempini, A., Wiesendanger, M., & Liang, F. (1998). Dexterity in adult monkeys following early lesion of the motor cortical hand area: the role of cortex adjacent to the lesion. The European Journal of Neuroscience, 10(2), 729–740.

Sanai, N., & Berger, M. S. (2008). Glioma extent of resection and its impact on patient outcome. Neurosurgery, 62(4), 753–764; discussion 264-6.

Sasaki, S., Isa, T., Pettersson, L. G., Alstermark, B., Naito, K., Yoshimura, K., Seki K., Ohki, Y. (2004). Dexterous finger movements in primate without monosynaptic corticomotoneuronal excitation. Journal of Neurophysiology, 92(5), 3142–3147.

Savidan, J., Kaeser, M., Belhaj-Saïf, A., Schmidlin, E., & Rouiller, E. M. (2017). Role of primary motor cortex in the control of manual dexterity assessed via sequential bilateral lesion in the adult macaque monkey: A case study. Neuroscience, 357, 303–324.

Schieber, Marc H., & Rivlis, G. (2007). Partial reconstruction of muscle activity from a pruned network of diverse motor cortex neurons. Journal of Neurophysiology, 97(1), 70–82.

Schieber, M H, & Poliakov, A. v. (1998). Partial inactivation of the primary motor cortex hand area: effects on individuated finger movements. The Journal of Neuroscience : The Official Journal of the Society for Neuroscience, 18(21), 9038–9054.

Schmidlin, E., Brochier, T., Maier, M. A., Kirkwood, P. A., & Lemon, R. N. (2008). Pronounced reduction of digit motor responses evoked from macaque ventral premotor cortex after reversible inactivation of the primary motor cortex hand area. The Journal of Neuroscience : The Official Journal of the Society for Neuroscience, 28(22), 5772–5783.

Sloper, J. J., & Powell, T. P. (1979). An experimental electron microscopic study of afferent connections to the primate motor and somatic sensory cortices. Philosophical Transactions of the Royal Society of London. Series B, Biological Sciences, 285(1006), 199–226.

Smith, J. S., Chang, E. F., Lamborn, K. R., Chang, S. M., Prados, M. D., Cha, S., Tihan T, Vandenberg S, McDermott MW, Berger, M. S. (2008). Role of extent of resection in the long-term outcome of low-grade hemispheric gliomas. Journal of Clinical Oncology : Official Journal of the American Society of Clinical Oncology, 26(8), 1338–1345.

Strick, Peter L., & Sterling, P. (1974). Synaptic termination of afferents from the ventrolateral nucleus of the thalamus in the cat motor cortex. A light and electron microscope study. Journal of Comparative Neurology, 153(1), 77–105.

Strick, P L, & Preston, J. B. (1982). Two representations of the hand in area 4 of a primate. I. Motor output organization. Journal of Neurophysiology, 48(1), 139–149.

Szelényi, A., Senft, C., Jardan, M., Forster, M. T., Franz, K., Seifert, V., & Vatter, H. (2011). Intra-operative subcortical electrical stimulation: A comparison of two methods. Clinical Neurophysiology, 122(7), 1470–1475.

Takahashi, K. (1965). Slow and fast groups of pyramidal tract cells and their respective membrane properties. Journal of Neurophysiology, 28(5), 908–924.

Travis, A.M. (1955) Neurological deficiencies after ablation of the precentral motor area in Macaca mulatta. Brain, 78, 155–73.

Vavrek, R., Girgis, J., Tetzlaff, W., Hiebert, G. W., & Fouad, K. (2006). BDNF promotes connections of corticospinal neurons onto spared descending interneurons in spinal cord injured rats. Brain, 129(6), 1534–1545.

Viganò, L., Fornia, L., Rossi, M., Howells, H., Leonetti, A., Puglisi, G., Bellacicca A., Grimaldi M., Bello L., Cerri, G. (2019). Anatomo-functional characterisation of the human “hand-knob”: A direct electrophysiological study. Cortex; a Journal Devoted to the Study of the Nervous System and Behavior, 113, 239–254.

Witham, C. L., Fisher, K. M., Edgley, S. A., & Baker, S. N. (2016). Corticospinal inputs to primate motoneurons innervating the forelimb from two divisions of primary motor cortex and area 3a. Journal of Neuroscience, 36(9), 2605–2616.

Woolsey, C. N., Settlage, P. H., Meyer, D. R., Sencer, W., Pinto Hamuy, T., & Travis, A. M. (1952). Patterns of localization in precentral and supplementary motor areas and their relation to the concept of a premotor area. Research Publications - Association for Research in Nervous and Mental Disease, 30, 238–264.

Yamawaki, N., Borges, K., Suter, B. A., Harris, K. D., & Shepherd, G. M. G. (2014). A genuine layer 4 in motor cortex with prototypical synaptic circuit connectivity. ELife, 3, e05422.

GENERAL MATERIAL AND METHODS

1 Patients enrolled

Intraoperative neurophysiological, imaging, clinical and neuropsychological data of 155 patients who underwent an asleep-awake-asleep or asleep-asleep neurosurgical resection of tumours according to functional boundaries by means of brain mapping technique in Humanitas Research Hospital between 2016 and 2019 (Prof. Bello, University of Milan, Neurosurgical Oncology Unit) were analysed. All patients gave written informed consent to the surgical and mapping procedure, which followed the principles outlined in “World Medical Association Declaration of Helsinki: Research involving human subjects". The study was performed with strict adherence to the routine procedure used for surgical tumour removal. Handedness was assessed in each patient using the Zappala Handedness Inventory. For detailed demographic information and features of the samples used in the different studies see the specific chapters.

2 MR data acquisition

2.1 *Preoperative neuroradiological evaluation*

Preoperative MRI imaging was performed on a Philips-Intera-3T scanner (Koninklijke Philips N.V. Amsterdam, Netherlands), and acquired for lesion morphological characterization and volumetric assessment. A post-contrast gadolinium T1-MPRAGE sequence was performed using the following parameters TE: 2.7ms, TR:95.4s, FOV: 176 slices, slice thickness: 1mm and a T2-FLAIR, as part of the clinical routine. DWI and ADC diffusion weighted images were acquired. Volumetric analysis was used to define tumour volume using BrainLab software. A subset of patients, for clinical reasons, performed a preoperative HARDI-optimised diffusion imaging sequence using an 8 channel head coil. A spin echo, single shot EPI sequence was performed with 73 directions collected using a b-value of 2000s/mm3, and seven interleaved non-diffusion weighted (b0) volumes (TE:96ms, TR 10.4ms). This acquisition had a matrix size of 128x128 with an isotropic voxel size of 2mm3.

If requested by the surgical procedure, fMRI images were acquired with T2-weighted sequences by means of BOLD (blood oxygenation level dependent) technique. Tasks

performed were finger tapping task to localize M1, two language tasks (covert visual naming and fluency task or covert auditory verb generation) to localize language-related areas, and an action execution-observation grasping task performed with the hand and the mouth to localize vlPM/BA6 (see Cerri et al. 2015).

2.2 *Postoperative neuroradiological evaluation*

All patients underwent a clinical magnetic resonance sequence immediately after the surgery (within 48 hours) at the one-month and three-months follow-up (volumetric FLAIR and post-gadolinium-T1-weighted images) to estimate the extent of resection (EOR). EOR corresponded to the percentage of the volume resected with respect to the pre-operative volume: (preoperative volume-postoperative volume / preoperative volume). We considered total resection a case in which EOR was 100% while subtotal when ranged between 90-100%. A supratotal resection was defined post-operatively on MRI as the complete removal of any signal abnormalities with a volume of the postoperative cavity larger (>100%) than the pre-operative tumour volume. Postoperative diffusion-weighted MRI scans were also performed to check for ischemic damage.

3 Neuropsychological assessment

All patients were extensively evaluated with a pre-operative and post-operative neuropsychological assessment of motor and cognitive functions. All patients were evaluated 5-7 days before the surgery, at 1 month, 3 months and finally 6 months after the surgical treatment. All the standardized tests used were sensible to detect severe as well as mild deficits. The cognitive domains tested for all patients were language (*verbal fluency on phonemic and semantic cue,* Novelli et al. 1986; *object picture naming* Catricalà et al. 2012; *token test,* Spinnler et al. 1987), attentive and executive functions (*attentive matrices,* Spinnler et al. 1987; *trail making test,* Giovagnoli et al. 1996; *stroop test,* Caffarra et al. 2002; *colored raven's progressive matrices,* Basso et al. 1996), memory (*digit span forward and backward*, Monaco et al. 2012; *rey auditory verbal learning test, RAVLT*, Carlesimo et al. 1996; *rey-osterrieth complex figure test recall, ROCF*, Cafarra et al. 2002), praxis and visuo-constructional abilities (*rey-*

osterrieth complex figure test copy, Cafarra et al. 2002; *ideomotor apraxia,* De Renzi et al.1980).

4 Surgical procedure and anaesthesiologic protocol

Resection was accomplished according to functional boundaries assessed by intraoperative motor (Bello et al. 2014; Rossi et al. 2018), language (Bello et al. 2014) and cognitive tasks (Puglisi et al. 2018) at cortical and subcortical level. Surgery was performed in asleep-awake-asleep anaesthesia (study 1and 3) or in asleep anaesthesia for tumours within the primary motor cortex (study 2). Total intravenous anaesthesia with propofol and remifentanil was used, and no muscle relaxants were employed during surgery to allow during asleep phase the execution of motor evoked potentials (Bello et al 2014). A craniotomy was performed to expose the tumour area and a limited amount of surrounding tissue, including the central sulcus for surgical needs. During the awake phase, the intravenous infusion of propofol was suspended, while the administration of remifentanil to guarantee analgesia are maintained, in addition to local anaesthesia. The time necessary for the awakening vary between 20 and 50 minutes. Particular attention was given to the prevention of seizures onset during the surgical procedure through a continuous monitoring of ECoG and EMG recordings. At the first sign of seizure onset, the stimulation was immediately interrupted, and the cerebral cortex irrigated with cold water, effective enough to block any ongoing crisis. When not sufficient, a bolus of propofol was administered.

5 Neurophysiological monitoring and mapping

5.1 *Neurophysiological monitoring*

During surgery, cortical activity was monitored by electroencephalography and electrocorticography (EEG, ECoG, Comet, Grass); ECoG from a cortical region adjacent the area to be stimulated was recorded by subdural strip electrodes (4-8 contacts, monopolar array referred to a mid-frontal electrode) throughout the whole procedure, to monitor the basal electrical activity of the brain and to detect after-discharges or electrical seizures during the resection. EEG was recorded with electrodes placed over the scalp in a standard array. EEG and ECoG signals were filtered (bandpass 1-100 Hz), displayed with high sensitivity (50-150 μV/cm and 300-

500 μV/cm, respectively) and recorded. The integrity of the descending motor pathways was monitored throughout the procedure by using a "train-of-five" monitoring technique delivered to the primary motor (M1) cortex to elicit MEPs in a sample of contralateral muscles (face, upper and lower limbs). To this aim, a 4-contact subdural strip electrode was placed over the precentral gyrus; each contact was tested against a vertex reference, with trains of 3-5 constant current anodal pulses (pulse duration: 0.5-0.8ms; inter-stimulus interval within the train (ISI): 2-4ms) at a repetition rate of 1 Hz. Train-of-five monitoring was suspended during cortical and subcortical mapping performed during resection to avoid interference.

Electromyographic (EMG) responses to stimulation of the motor areas, as well as the voluntary motor activity, were recorded throughout the procedure by pairs of subdermal hook needle electrodes (Technomed) inserted into 20 muscles (face, upper and lower limb) contralateral to the hemisphere to be stimulated, plus 4 ipsilateral muscles, all connected to a multichannel EMG recording (2000 Hz sample frequency, ISIS-IOM, InomedGmbH) (Bello et al 2014). Free-running EMG was used to record responses to stimulation and to distinguish between electrical and clinical seizures. The continuous monitoring of the ECoG and free-running EMG allowed to detect and avoid intraoperative seizures: at the first ictal sign, stimulation was stopped and cold irrigation of the cortex applied, generally successfully, to abort the seizure. Whenever the seizures spread to the whole hemibody, a bolus infusion of propofol (4 ml on average) was delivered.

5.2 *Neurophysiological brain mapping*

Two stimulation techniques were used to perform brain mapping: The Low Frequency (LF-DES) and the High Frequency (HF-DES) protocol, according to the frequency of stimulation delivered (Bello et al. 2014). HF-DES was delivered through a constant current monopolar stimulator (straight tip, 1.5 mm diameter (Inomed), with reference/ground on the skull overlying the central sulcus). Trains of 1 to 9 constant anodal current pulses (pulse duration 0.5 ms; interstimulus interval, ISI: 3-4 ms) were delivered at variable intensity (intensity range 1-25 mA), depending on the patient's cortical excitability and clinical condition. LF-DES consisted of trains, lasting 2 to 5 seconds, of biphasic square wave pulses (0.5 ms each phase) at 60 Hz (ISI 16.6 ms) delivered by a constant current stimulator (OSIRIS-NeuroStimulator) integrated into

the ISIS-System through a bipolar probe (2 ball tips, 2 mm diameter, separation 5 mm). As a general rule, the choice of HF or LF-DES paradigm to perform brain mapping depends on several factors among which critical are the function to be preserved and the clinical context possibly affecting the excitability of the tissue. The HF-DES, by eliciting MEPs, is indeed particularly (not exclusively see Riva et al 2016) effective in mapping the motor areas/pathways (Bello et al 2014; Fornia et al. 2016; Viganò et al. 2019). The LF-DES, by inducing a "transient interference" on a small amount of surrounding tissue around the probe affects the execution of complex tasks (i.e. the language tasks) only when applied on the structures belonging to the neural network underlying the function tested allowing its identification and preservation. In patients enrolled in this study, during LF-DES, and independently by the tumor location, the language assessment (performed with counting and naming tasks, see Bello et al. 2006) was tested at beginning, followed by the hand-manipulation task (HMt). As a routine procedure, the first cortical sites to be explored were the primary motor cortex (M1) in order to set the current intensity threshold (the so called "working current", WC), i.e. the lowest intensity of stimulation needed to disrupt/arrest the counting/naming and/or to evoke a hand muscle contraction. LF-DES during the following mapping was performed by using the same WC intensity delivered for language.

6 Hand-Manipulation Task (HMt)

LF-DES was applied while patients performed the hand-manipulation task with a specific tool made for this purpose (Rossi et al. 2018). The tool's rectangular base was kept stable close to the patient's hand along the armrest of the operating table, while the patient grasped, hold, rotated and released the cylindrical handle with the thumb and the index finger, likely resembling a precision grip rhythmically performed. Proximity between the hand and the cylindrical handle allowed the patients to perform the movement using just the fingers, avoiding a possible reaching movement. Each patient, opportunely trained one day before surgery, was asked to perform the task continuously, following an internal generated rhythm without any external cue to instruct the phases of movement nor visual information about the hand or the cylindrical handle movement (i.e. the movement was "haptically driven"). These experimental parameters were selected to satisfy the clinical setup and needs. No

external stimuli were added to disentangle between a planning and execution phase because the continuous mapping (especially subcortically where DES is applied simoultaneosly to the progression of resection) requires an incessant execution of the movement to evaluate possible disruptions. Therefore, a planning phase prior to action execution showing the object to be manipulated was not evaluable with this task. Moreover, the position of the head during surgery doesn't allow a reliable self visual monitoring of the moving hand, leading us to choose an haptically driven movement. This setup allows to evaluate selectively object-manipulation neurons and pathways and to compare the eloquent areas found with the so-called 'grasping in the dark' activations (Binkofski et al. 1999; Marangon et al. 2016; Nelissen et al. 2017), avoiding the neural modulations triggered in fronto-parietal areas by the visual feedback of the hand and the interacting object (Murata et al. 1997; Murata et al. 2000; Raos et al. 2006; Fattori et al. 2009).

During HMt execution, neuropsychologists performed a real-time monitoring of the patients' behavioural outcome, reporting to the surgeons any arrest, decrease of performance and/or any somatic sensation. During its execution up to 24 muscles were simultaneously recorded including bilateral upper body, lower body and oro-facial muscles. The hand-object interaction during the task execution was video-recorded and synchronized off-line with the EMG signals. At the beginning of the HMt session, 10 seconds (in some cases even longer) of baseline movement (without stimulation) was required to reach stable task execution. When good stability was reached (as assessed based on behavioural outcome and ongoing EMG activity real time monitoring), the surgeon started the stimulation of the investigated areas randomly during task performance. An interval of 3-4 seconds among different stimulation and among different sites was observed to avoid dragging-effects. The effect of the LF-DES-HMt was assessed by means of online and offline observation (behavioural outcome) and confirmed by qualitative EMG-pattern inspection (Study 1) and quantitative analysis of the EMG patterns (Study 3).

7 Data analysis

7.1 *Reconstruction of stimulation sites.*

During the surgery, the brain mapping technique was videotaped and MRI coordinates of all the stimulated sites were acquired by the neuronavigation system (Brainlab). The reconstruction of the exact position of all sites was then computed for each patient with the following procedure:

- Cortical sites (Study 1): the cortical surface extraction and surface volume registration was computed using the T1 with or without contrast according to the sequence loaded into the neuronavigation system during surgery, by means of Freesurfer software (Fischl 2008). Subsequently the results were loaded onto Brainstorm (a MATLAB toolbox; Tadel et al. 2011), an open source software downloadable under the GNU general public license. The exact position of all the sites was marked as a scout on the patient's 3D MRI with the aid of Brainstorm. Subsequently, using the same software, each patient's 3D MRI with the respective labelled scouts were co-registered in the MNI space (Ashburner & Friston, 2005). Finally, all the stimulation sites were plotted on the FSAverage template to create a 3D reconstruction of the stimulated hemisphere.
- Subcortical sites (Study 3): all the stimulated sites registered intraoperatively by the Brainlab system were individuated on the post-operative structural scan. Enantiomorphic normalisation was used from within the Clinical Toolbox in SPM (Rorden, 2012) to register this site to both a standard template for group visualisation (Montreal Neurological Institute "MNI"), and to the preoperative T1. Both the pre- and postoperative T1 were registered to the HARDI-derived map (Dell'Acqua et al. 2012). Reliability of the normalisation process was visually inspected case-by-case and corrected if needed.

The localization of the stimulated sites was finally confirmed by operating neurosurgeons (L.B. and M.R.).

REFERENCES

Ashburner J, Friston KJ. 2005. Unified segmentation. Neuroimage. 26(3):839-51.

Basso A, Capitani E, Laiacona M. 1987. Raven's coloured progressive matrices: normative values on 305 adult normal controls. Funct Neurol. 2(2):189-194.7.

Bello L, Acerbi F, Giussani C, Baratta P, Taccone P, Songa V. 2006. Intraoperative language localization in multilingual patients with gliomas. Neurosurgery. 59:115-125.

Bello L, Riva M, Fava E, Ferpozzi V, Castellano A, Raneri F, Pessina F, Bizzi A, Falini A, Cerri G. 2014. Tailoring neurophysiological strategies with clinical context enhances resection and safety and expands indications in gliomas involving motor pathways. Neuro Oncol. 16:1110-1128.

Binkofski F, Buccino G, Posse S, Seitz RJ, Rizzolatti G, Freund H. 1999. A fronto-parietal circuit for object manipulation in man: evidence from an fMRI-study. Eur J Neurosci. 11:3276–3286.

Caffarra, P., Vezzadini, G., Dieci, F., Zonato, F., & Venneri, a. (2002). Rey-Osterrieth complex figure: normative values in an Italian population sample. Neurological Sciences : Official Journal of the Italian Neurological Society and of the Italian Society of Clinical Neurophysiology, 22(6), 443–447.

Carlesimo, G. A., Caltagirone, C., Gainotti, G., Facida, L., Gallassi, R., Lorusso, S., Parnett, L. (1996). The mental deterioration battery: Normative data, diagnostic reliability and qualitative analyses of cognitive impairment. European Neurology, 36(6), 378–384.

Cerri G, Cabinio M, Blasi V, Borroni P, Iadanza A, Fava E, Fornia L, Ferpozzi V, Riva M, Casarotti A, Martinelli Boneschi F, Falini A, Bello L. 2015. The mirror neuron system and the strange case of Broca's area. Hum Brain Mapp. 36(3):1010-27.

De Renzi, E., & Faglioni, P. (1978). Normative Data and Screening Power of a Shortened Version of the Token Test. Cortex, 14(1), 41–49.

Dell'acqua F, Scifo P, Rizzo G, Catani M, Simmons A, Scotti G, Fazio F. 2010. A modified damped Richardson-Lucy algorithm to reduce isotropic background effects in spherical deconvolution. Neuroimage. 49(2):1446-58.

Dell'Acqua F, Simmons A, Williams SC, Catani M. 2012. Can spherical deconvolution provide more information than fiber orientations? Hindrance modulated orientational anisotropy, a true-tract specific index to characterize white matter diffusion. Hum Brain Mapp. 34(10):2464-83.

Fischl B, Rajendran N, Busa E, Augustinack J, Hinds O, Yeo BT, Mohlberg H, Amunts K, Zilles K. 2008. Cortical Folding Patterns and Predicting Cytoarchitecture. Cereb Cortex. 18:1973—1980.

Fornia L, Ferpozzi V, Montagna M, Rossi M, Riva M, Pessina F, Martinelli Boneschi F, Borroni P, Lemon RN, Bello L, Cerri G. 2018. Functional characterization of the left ventrolateral premotor cortex in humans: a direct electrophysiological approach. Cereb Cortex. 1-17.

Giovagnoli, A. R., Del Pesce, M., Mascheroni, S., Simoncelli, M., Laiacona, M., & Capitani, E. (1996). Trail making test: normative values from 287 normal adult controls. The Italian Journal of Neurological Sciences, 17(4), 305–309.

Leemans A, Jeurissen B, Sijbers J, Jones DK .2009. ExploreDTI: a graphical toolbox for processing, analyzing, and visualizing diffusion MR data. Proc Int Soc Magn Reson Med. 17: 3537.

Marangon M, Kubiak A, Króliczak G. 2016. Haptically guided grasping. fMRI shows right-hemisphere parietal stimulus encoding, and bilateral dorso-ventral parietal gradients of object-and action-related processing during grasp execution. Front Hum Neurosci. 9:691.

Monaco, M., Costa, A., Caltagirone, C., & Carlesimo, G. A. (2013). Forward and backward span for verbal and visuo-spatial data: Standardization and normative data from an Italian adult population. Neurological Sciences, 34(5), 749–754.

Nelissen K, Fiave PA, Vanduffel W. 2017. Decoding grasping movements from the parieto-frontal reaching circuit in the nonhuman primate. Cereb Cortex. 1–15

Novelli, G., Papagno, C., Capitani, E., Laiacona, M., Vallar, G., & Cappa, S. F. (1986). Tre test clinici di ricerca e produzione lessicale. Taratura su sogetti normali. Archivio Di Psicologia, Neurologia e Psichiatria, 47, 477–506.

Puglisi G, Sciortino T, Rossi M, Leonetti A, Fornia L, Conti Nibali M, Casarotti A, Pessina F, Riva M, Cerri G, Bello L. Preserving executive functions in nondominant frontal lobe glioma surgery: an intraoperative tool. J Neurosurg. 28:1-7.

Riva M, Fava E, Gallucci M, Comi A, Casarotti A, Alfiero T, Raneri FA, Pessina F, Bello L. 2016. Monopolar high-frequency language mapping: can it help in the surgical management of gliomas? A comparative clinical study. J Neurosurg. 124(5):1479-89.

Rorden C, Bonilha L, Fridriksson J, Bender B, Karnath HO. 2012. Age-specific CT and MRI templates for spatial normalization. Neuroimage. 61(4):957-65.

Rossi M, Fornia L, Puglisi G, Leonetti A, Zuccon G, Fava E, Milani D, Casarotti A, Riva M, Pessina F, Cerri G, Bello L. 2018. Assessment of the praxis circuit in glioma surgery to reduce the incidence of postoperative and long-term apraxia: a new intraoperative test. J Neurosurg. 23:1-11

Spinnler H, T. G. (1987). Taratura e standardizzazione italiana di test neuropsicologici. Ital J Neurol Sci Suppl, 8.

Tadel F, Baillet S, Mosher JC, Pantazis D, Leahy RM. 2011. Brainstorm: a user-friendly application for MEG/EEG analysis. Comput Intell Neurosci. 2011:879716.

Viganò L, Fornia L, Rossi M, Howells H, Leonetti A, Puglisi G, Conti Nibali M, Bellacicca A, Grimaldi M, Bello L, Cerri G. 2019. Anatomo-functional characterisation of the human "hand-knob": A direct electrophysiological study. Cortex. 113:239-254

RESULTS SECTION

STUDY 1:

"ROSTRO-CAUDAL SUBDIVISION WITHIN THE HUMAN HAND-KNOB: A DIRECT ELECTROPHYSIOLOGICAL STUDY"

STUDY 2:

"ONCOLOGICAL AND FUNCTIONAL EFFICIENCY OF HIGH-FREQUENCY STIMULATION MAPPING FOR PRIMARY MOTOR TUMOURS RESECTION".

STUDY 3:

"CONTRIBUTION OF FRONTAL LOBE AREAS IN CONTROL OF DEXTERITY: DISSOCIATING SUBCORTICAL TRACTS COMBININING DIRECT ELECTRICAL STIMULATION AND TRACTORGRAPHY IN AWAKE NEUROSURGERY"

STUDY 1: "ROSTRO-CAUDAL SUBDIVISION WITHIN THE HUMAN HAND-KNOB: A DIRECT ELECTROPHYSIOLOGICAL STUDY"

Paper:

Viganò L. & Fornia L., Rossi M., Howells H., Leonetti A., Puglisi G., Conti Nibali M., Bellacicca A., Grimaldi M., Cerri, G. (2019). Anatomo-functional characterisation of the human "hand-knob": A direct electrophysiological study. Cortex.113, 239–254. doi: 10.1016/j.cortex.2018.12.011

INTRODUCTION

In both human and non-human primates, the hand representation in the primary motor cortex (M1) and its descending fibres are crucial in the realization of voluntary movements (Lemon et al. 2008). Intracortical microstimulation (ICMS) and cytoarchitectonic investigations in the Old-World monkey revealed an anatomo-functional subdivision in two different sectors within M1 itself (Strick & Preston 1982; Rathelot & Strick 2008; Witham et al., 2016). The caudal, so-called "new-M1", incorporates the bank of the central sulcus, showing dense cortico-motoneuronal (CM) projections whereas the rostral, so-called "old-M1", shows few and slower CM projections (Rathelot & Strick 2008; Witham et al. 2016, see Introduction). As stated in the Introduction, from an evolutionary point of view, direct connections between corticofugal fibres and spinal motoneurons are correlated with skilled hand actions such as different precision grips, gestures not achievable by species in which the corticospinal neurons projects mainly on interneurons on the intermediate zone of the spinal cord (cats, rodents, squirrel monkeys etc.).

Moreover, the hand region of M1 could be heterogeneous also in cortico-cortical connectivity. Although a clear network for fine control of hand movements has been described for the Old-World monkey (Borra et al. 2017), a direct investigation of a possible differentiation in local connectivity between the 'new-M1' and the 'old-M1' was not yet performed. In the New World monkey, instead, in which the whole M1 is unfolded on the convexity, a different pattern of cortico-cortical connectivity has been shown in the rostro-caudal direction: the posterior M1 mainly projects to

somatosensory cortices, while the anterior M1 is mostly connected the caudal dorsal premotor (dPM) and ventral premotor (vPM) cortex (Stepniewska et al. 1993, 2006; Dea et al. 2016).

In human, the representation of the hand in M1 is localised in the *pli de passage fronto-pariétal moyen* (Broca 1888), nowadays called the 'hand-knob' region due to its visible omega or epsilon shaped bulge in axial MR images (Yousry et al. 1997, Boling et al. 1999, Caulo et al. 2007). However no data are available about the possible existence of human homologous of the new-M1 and the old-M1, cytoarchitectonic and functional studies of the human hand-knob showed a subdivision, along the rostro-caudal direction, in different architectonic districts suggested to subserve different roles in motor control (Geyer et al. 1996; Binkofski et al. 2002; Bastiani et al. 2016; Glasser et al. 2016). Brodmann area 4 was proposed by Geyer and colleagues (1996) to be organized in two sectors with different anatomical, neurochemical and functional features. The posterior region, area 4p, completely buried in the central sulcus, was significantly higher activated in a roughness discrimination task compared to a control inner-generated voluntary hand movement respect to the more anterior area 4a, which, from the central sulcus, reaches the convexity of the gyrus. A recent fMRI study (Amiez and Petrides 2018) confirmed a crucial role of the caudal region of the hand representation in M1 in the control of simple hand movements and suggested the most rostral region, corresponding to the dorsal portion of the superior precentral sulcus, to be involved in the selection of hand movements.

For what concerns the human short-range projections, two sets of U-shaped fibres were described: one connecting the M1 hand motor area to the superior and middle frontal gyri (more anterior premotor cortex) and the other one projecting to the hand somatosensory representation of the postcentral gyrus (Post-CG) (Rosett 1933; Catani et al. 2012; Thompson et al. 2017). However, no conclusive evidence of a different connectivity between M1 subsectors has yet been shown.

In the present study we investigated the anatomo-functional rostro-caudal organization within the human hand-knob analysing the neurophysiological data recorded intraoperatively in 17 patients undergoing awake surgery for right brain tumour resection with the aid of the Brain Mapping Technique and Direct Electrical Stimulation (DES). Data from high frequency stimulation in resting condition, low

frequency stimulation during the hand-manipulation task and diffusion tractography data (Diffusion Tensor, DTI, and High Angular Resolution Diffusion Imaging, HARDI) were combined to highlight possible functional and anatomical differences between the sector close the central sulcus, here defined caudal hand-knob, and the one close to the precentral sulcus, here defined rostral hand-knob.

HF stimulation of the two sectors, evoking MEPs, allowed to evaluate differences in cortical excitability. The assessment of differences in cortical excitability might point to anatomo-functional subdivisions, as showed in the macaque for M1, the ventral and dorsal premotor cortex (Cerri et al. 2003; Raos et al. 2003; Shimazu et al. 2004; Boudrias et al. 2010a, 2010b). As expected by monkeys microstimulation studies (Strick & Preston 1982; Rathelot & Strick 2008; Witham et al., 2016) the posterior region, close to the central sulcus, which is supposed to be dense of corticomotoneuronal cells, was the most excitable.

The second set of data available from the awake surgical procedure was the evaluation of the behavioural outcome and of the EMG pattern during the application of LF-DES while patients were performing the hand-manipulation task (HMt). This task requires adequate coordination of muscles synergies to achieve the proper hand-object interaction to correctly perform the movement. Given that, the analysis of the specific behavioural and electromyographic features characterizing the impairment elicited by DES during task realization was aimed at discovering possible differences between the two sectors in shaping the motor output during skilled hand-object interaction. Stimulation of the caudal sector always resulted in in hand-arm muscle recruitment, while stimulation of the rostral region resulted in both recruitment and movement suppression phenomena.

Finally, we evaluated long and short-range white matter connectivity of the hand-knob in a cohort of six patients. Specifically, we virtually dissected and correlated with stimulation sites the corticofugal tract and the U-shaped short projections (Catani et al. 2012). The hypothesis was that the functional differences within the hand-knob highlighted by our electrophysiological results may correspond also with different patterns of anatomical connectivity.

MATERIALS AND METHODS

All the surgical resections were performed according to functional boundaries by means of the brain mapping technique and Direct Electrical Stimulation (DES) (Bello et al. 2014). Two stimulation paradigms were available during the procedure:

- *High Frequency Monopolar Stimulation at rest (HF-DES-Rest)*, i.e. in absence of voluntary movement, was applied at the beginning of the procedure. HF-DES-Rest was used to identify the most excitable site on the precentral gyrus (evaluating the cortical motor threshold and the amplitude of the MEPs) in order to place the grid electrodes over M1 from which the integrity of the corticospinal tract can be monitored for all the procedure.
- *Low Frequency Bipolar Stimulation during the hand manipulation task (LF-DES-HMt).* This phase followed the mapping at rest with HF and it's clinically relevant in identifying the safe cortical entry zone and the subcortical functional boundaries (posterior margin of the resection for frontal tumours as all the cases included in the study) (Rossi et al. 2018). The effect of DES on task realization was performed by a classification in 'behavioural outcomes' and by the qualitative observation of the correspondent EMG patterns of distal and proximal upper-limb muscles. The cortical mapping required mainly stimulation on the rostral sector of the hand-knob because, in the patients selected, the caudal region was usually easily excitable and thus already identified with HF-DES-Rest. We thus included in the following analyses only LF-DES-HMt sites of the rostral sector, representing the stimulations in the posterior area less than the 10% of the sample. However, these stimulations were discussed according to neurosurgical experience/literature and in comparison to the rostral ones.

For a detailed specification of the two paradigms of stimulations see the Introduction and the General Materials and Methods.

Table 1

Pt	*Age range*	*Hand dominance*	*Apraxia**	*Lesion site Right hem*	*WHO grade*	*HF-DES -Rest*	*LF-DES- HMt*	*Diffusion Tract.*
1	50-55	Right	Normal	Frontal	AstroIII	X		
2	50-55	Right	Normal	Frontopar	Other**	X		
3	30-35	Left	Normal	Frontal	OligoIII	X		
4	40-45	Right	Normal	Frontal	AstroIII	X	X	
5	35-40	Right	Normal	Frontal	OligoII	X	X	X
6	60-65	Right	Normal	Frontal	AstroIII	X	X	X
7	30-35	Right	Normal	Frontal	OligoII	X	X	
8	25-30	Right	Normal	Frontal	AstroII	X		X
9	25-30	Left	Normal	Frontal	OligoIII	X	X	X
10	30-35	Right	Normal	Parietal	OligoIII	X	X	X
11	30-35	Right	Normal	Frontal	AstroIII	X	X	
12	15-20	Right	Normal	Frontal	Other**		X	
13	55-60	Right	Normal	Frontopar	AstroIII		X	
14	45-50	Right	Normal	Frontotemp	GBMIV	X	X	
15	20-25	Right	Normal	Frontal	Other***	X	X	
16	60-65	Right	Normal	Frontal	AstroIII		X	
17	40-45	Right	Normal	Frontal	OligoII		X	X

* Apraxia = bucco-facial/ideomotor

** Inflammatory lesion

*** Cystic lesion

1 Patients selection

17 patients (15 right-handed and 2 left-handed) who underwent an awake surgical resection of right hemisphere tumour were enrolled (see Table 1 for detailed information). We excluded all patients with lesions infiltrating the hand-knob region in the precentral gyrus, the postcentral gyrus, the posterior limb of the internal capsule and the cerebral peduncle hosting the corticospinal tract. As inclusion criterion, tumours (posterior or anterior border) must had a distance from the central or precentral sulcus ≥10 mm (Quiñones-Hinojosa et al. 2003; Fornia et al. 2016), parameter computed with Brainlab software. Patients with pre-operative sensory-motor and/or cognitive deficits and with not-welled controlled seizures were not included.

2 Intraoperative individuation of stimulation sites

Number of stimulations and their anatomical localization were constrained only by the surgical procedure, i.e. determined by the need to individuate the safe cortical entry zone and according to the morphology of the hand-knob. The central sulcus and the precentral sulcus were used intraoperatively as anatomical landmarks useful to distinguish between caudal and rostral stimulations. Resection of tumours included in this study required application of HF-DES from the central sulcus to the precentral sulcus along the antero-posterior axis. This was useful to obtain a map of the cortical motor threshold for the hand region useful to place the subdural electrode grid to monitor constantly the corticospinal tract (see General Materials and Methods, Neurophysiological monitoring). According to the extensive surgical experience (L.B. and M.R.) and to the results of the present work (see Results), the site with the lowest motor threshold is always located close to the central sulcus. Given that the motor output of the rostral sector is consistently lower compared to the caudal region (assess both with motor threshold and evaluation of MEPs amplitude), this sector was also tested during the Hand-Manipulation task delivering LF-DES to establish its possible role in action execution despite its lower excitability at rest. In the patients included in this study, the caudal region was rarely stimulated with LF-DES, thus the definition of the rostral sites was, at the single subject level, relative to the caudal site as identified with HF-DES (i.e. rostral site = localized anterior and approximately at same medio-

lateral of the caudal site, defined based on the proximity to the central sulcus) and verified using the precentral sulcus as anatomical landmark. In patients 12-13-16-17 (Table 1), HF-DES data of the rostral hand-knob were not included in the analysis (or because the procedure required only the application of LF-DES in this area or because number of MEPs collected was not adequate for a statistical comparison).

3 Data analysis

3.1 *Analysis of MEPs (high frequency at rest)*

Raw electromyography (EMG) of hand/forearm muscles was recorded with specific software (ISIS, INOMED, sampling rate 20 kHz, notch filter at 50 Hz). For each patient, the raw data, i.e. all the Motor Evoked Potentials (MEPs) recorded during the procedure, were extracted from the acquisition system and resampled at 4 kHz and analysed offline by means of dedicated MATLAB software. For each trial, a window of interest of 100 ms from the stimulus onset was defined. The average background EMG activity and its SD (±1 SD) were then calculated from the last 25 ms of the record (i.e., from 75 to 100 ms). A MEP was considered reliable only when the EMG voltage signal exceeded the average background ±1 SD (Fornia et al. 2018). All the MEPs were stored based on the location of the stimulating site within the hand-knob sectors (caudal vs rostral). We focused our analysis on the most represented forearm-hand muscles in the data sample (i.e. Extensor Digitorum Communis, EDC; First Dorsal Interosseous, FDI; Abductor Pollicis Brevis, APB; Abductor Digiti Minimi, ADM and Flexor Carpi Radialis, FCR). We visually inspected the raw EMG activity to evaluate the background activity at rest and thus exclude from the analysis any MEPs facilitated by unforeseen muscle contraction.

We selected two main parameters to assess differences in cortical excitability between caudal and rostral hand-knob:

- the caudal motor threshold (cMT), i.e. the minimum stimulation parameters [minimum intensity with a fixed number of pulses and minimum number of pulses with a fixed intensity] necessary to elicit MEPs in the caudal region. An offline analysis was performed at single subject level to assess if cMT stimulation parameters were successful also in evoking MEPs in the rostral sector.

- The amplitude of MEPs elicited with the same stimulation parameters (number of pulses and intensity) in the two sectors of the same patient.

3.2 Behavioural outcome classification (hand-manipulation task)

The evaluation of the effect of DES on HMt performance was always blind to the stimulation sites. All stimulations for each patient were inspected offline analysing the video-recording of the task realization during the surgery. Different outcomes occurred after delivering DES during the HMt, enabling a classification into distinct "behavioural outcomes". Finally, for each stimulation analysed the correspondent EMG pattern (upper-limb muscles) was qualitative inspected to confirm the behavioural classification.

3.3 Statistical analysis

To assess differences in cortical excitability between the two subsectors, a statistical analysis on the amplitude of MEPs evoked with the same stimulation parameters in the forearm-hand muscles (EDC, APB, FDI, ADM and FCR) was performed. We included in the analysis only muscles responsive to at least five HF-DES-Rest trials in both areas. MEPs were grouped by area (caudal vs rostral). MEPs amplitudes were standardized (z-score) within area and between muscles. To compare amplitude of MEPs elicited in the two sector, direct comparisons at single subject level were performed by means of Mann-Whitney U tests (non-parametric data distribution).

3.4 *Diffusion tractography dissections*

We corrected the diffusion MRI collected in the six patients for head motion, eddy current distortion and susceptibility artefacts using ExploreDTI (Leemans et al. 2009). This data was then processed for both whole brain diffusion tensor and spherical deconvolution tractography, using StarTrack software (www.mr-startrack.com; Dell'Acqua et al. 2010). For spherical deconvolution modelling, a damped Richardson-Lucy algorithm was used with a fibre response parameter of 1.5, 200 iterations, and threshold and geometrical regularisation parameters of 0.04 and 15 respectively (Dell'Acqua et al. 2012). An absolute threshold of 0.0038 was used to exclude spurious local maxima. For both tensor and HARDI models, Euler integration was used for streamline reconstruction, using an angle threshold of 45 and a step-size of 1 (with tensor FA threshold of 0.12). Tractography dissections were performed

using a region-of-interest approach by an experienced dissector (H.H.). The corticospinal (corticofugal) projection tracts were dissected using the methods detailed in Catani & Thiebaut de Schotten (2012) and Howells et al. (2018). One inclusion ROI was composed of the entire precentral gyrus, and a second inclusion ROI was used in the brain stem, below the cerebellar peduncles, to constrain the resulting streamlines to display those descending to the brain stem. The U-shaped connections between the precentral gyrus, superior and middle frontal gyrus, and precentral to postcentral gyri were dissected according to Catani et al. (2012). The entire precentral, postcentral, superior frontal and middle frontal gyri were delineated and used as inclusion ROIs for the relevant tracts in all six patients.

Detailed information on the hand-manipulation task, on the reconstruction of the stimulated sites and on the diffusion tractography acquisition and are reported in the General Materials and Methods.

RESULTS

1 High Frequency at rest – Cortical excitability

Cortical excitability comparisons between rostral and caudal sector were performed in 13 patients out of 17 (Table 1). A total of 30 stimulation sites was reported. 14 sites were recorded in the caudal region (1.1 mean per patient, SD 0.3), while 16 sites in the rostral hand-knob (1.2 mean per patient, SD 0.6) (Fig. 1A). Two main parameters were used to assess differences in cortical excitability:

1) **Caudal motor threshold** we verified if the stimulation with cMT parameters (intensity and number of pulses) effective in caudal hand-knob was equally efficient in the rostral hand-knob. cMT stimulation parameters (mean intensity = 5.8mA; mean number of pulses = 5; Fig 1C), elicited MEPs in all the muscles considered for analysis (APB, FDI, EDC, ADM, FCR) when applied to caudal region, while failed to evoke any MEPs in the rostral region. This result suggests a non-homogeneous distribution of excitability in the two subsectors, with the caudal one more excitable than the rostral.

2) we performed a direct **comparison between amplitude of MEPs** evoked with an over-threshold stimulation on the two subsectors with the same parameters (in 8 patients): DES on the caudal hand-knob evoked MEPs from all the hand-arm muscles analysed, while on rostral hand-knob DES elicited responses in fewer muscles. This meant that amplitude comparisons were not performed in all the recorded muscles, but in combination of them considering the occurrence in the rostral region. MEP amplitudes elicited in the rostral hand-knob were, at single subject level, always significantly lower respect to MEP amplitudes evoked in the caudal sector. Single subject results (Fig. 1E): patient 5 (muscle analysed: EDC – FDI): $p<.001$; patient 6 (muscle analysed: FCR): $p<.001$; patient 7 (muscle analysed: APB): $p<.01$; patient 8 (muscle analysed: ADM, FDI, APB): $p<.001$; patient 9 (muscle analysed: FDI): $p<.001$; ; patient 10 (muscle analysed: APB): $p<.01$; ; patient 11 (muscle analysed: EDC, APB): $p<.001$; ; patient 15 (muscle analysed: EDC, ADM, FDI): $p<.001$. Amplitude comparisons results strongly supports results obtained with the cMT

protocol. Fig. 1D shows an example of amplitude difference between MEPs elicited in the two sectors of a single patient.

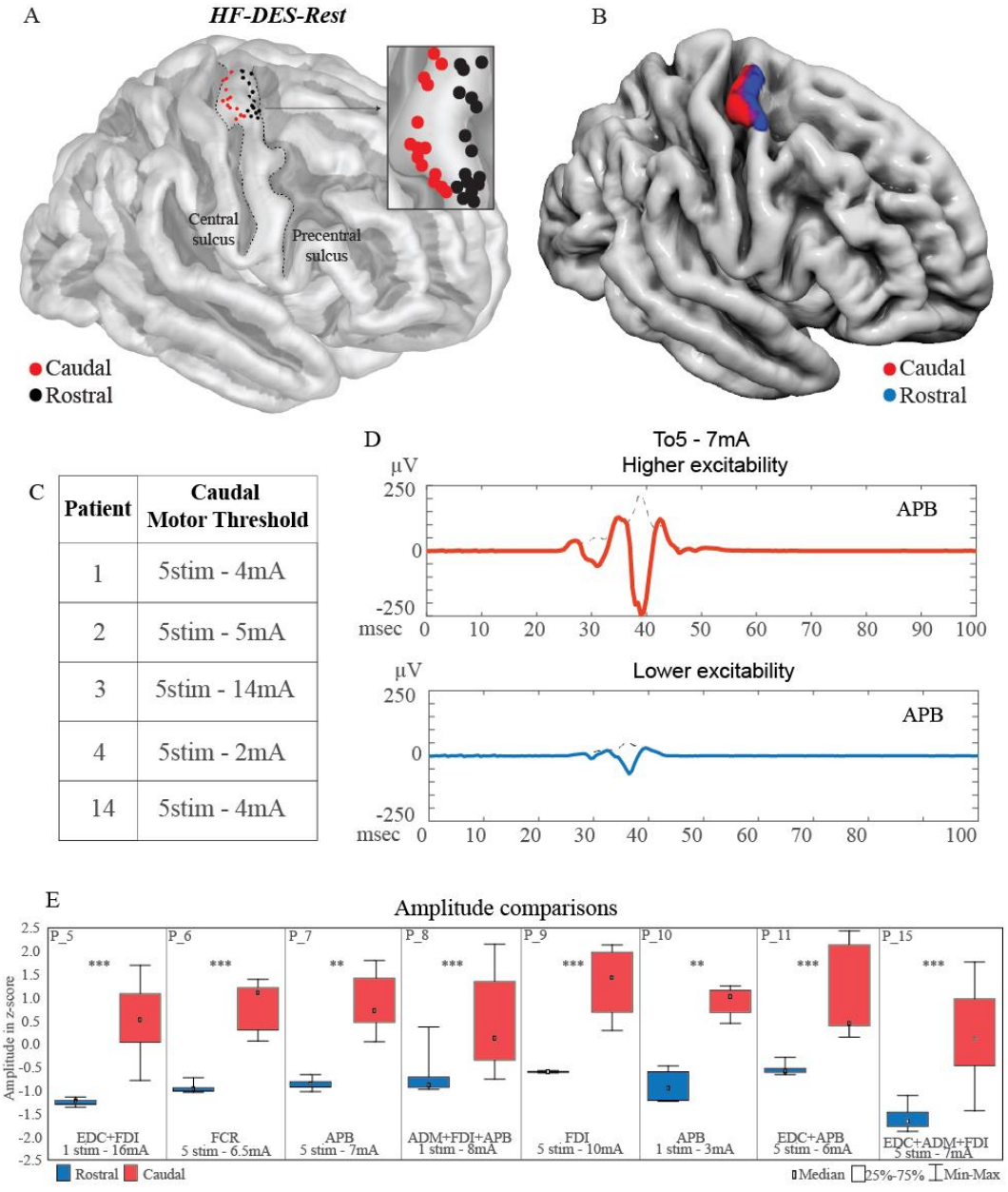

Patient	Caudal Motor Threshold
1	5stim - 4mA
2	5stim - 5mA
3	5stim - 14mA
4	5stim - 2mA
14	5stim - 4mA

Fig. 1: A) Cortical distribution of the HF-DES-Rest sites on caudal sector (red) and rostral sector (black) of the hand-knob on the 3D FSAverage template. B) Probability density estimation of the two HF-DES-Rest subsectors (caudal hand-knob in red and rostral hand-knob in blue). C) Caudal Motor Threshold (cMT) parameters (number of pulses and intensity) that, applied to the rostral sector of hand-knob failed to elicit motor responses within the same patients. D) MEP average of 10 trials elicited by stimulating caudal (red) and rostral (blue) hand-knob in a single subject (patient 7). The grey dashed lines represent the MEP root mean square. The 10 trials for averaging were selected among a sequence obtained over the same site in the same run. E) Comparison of MEP amplitude evoked with the same stimulation parameters (number of pulses and intensity) in the caudal and rostral hand-knob. All MEP amplitude values were standardised within the area and between muscles. Boxplots indicate the median value (small rectangles), 25th-75th (edge of the box) and the most extreme datapoints (whiskers). *p<.5;**p<.01;***p<.001. Modified from Viganò et al. (2019).

2 Low frequency – Hand Manipulation Task

LF during the HMt was applied in the hand-knob region in 13 patients out of 17 (table 1). All stimulations sites resulted in an impairment of the HMt. The behavioural outcome and the correspondent EMG pattern of 20 sites in the rostral hand-knob were analysed (mean 1.54 per patient, sd 1) (Fig. 2A). DES on the rostral hand-knob altered the HMt performance causing two main behavioural outcomes:

1) **Dysfunctional Hand Movement (dHM)** (10 sites out of 20 (50%), Fig. 2A-F:

DES induced involuntary movements in the hand-arm district. These muscle activations were completely dysfunctional to the hand-object interaction required by the task. Precisely, two possible involuntary configurations of the hand induced by stimulation were observed: closure/contraction of the hand/fingers; progressive aperture of the hand. Recruitment of distal muscles not required to perform the HMt was observed by inspection of EMG recording in all cases. An involuntary recruitment in the forearm and/or proximal muscles occurred in 50% of stimulations (5 out 10).

2) **Suppression of Hand Movement (sHM)** (10 sites out of 20 (50%), Fig. 2A-G-H:

Delivery of DES during the HMt caused an arrest of hand and finger movement, with a loss of postural tone. In 50% of stimulations (5 out 10 sites) the suppression of the movement was simultaneously coupled with a recruitment in the forearm/proximal muscles leading to a flexion or an extension of the arm (confirmed also with EMG recording when this phenomenon was not clearly observable).

The clinical cortical mapping on the rostral area provided 4 stimulations that we can consider as ‘control stimulations’, which suggest that DES during the HMt produced some task-dependent outcome rather than being the result of recruitment of muscle represented in this cortical zone, irrespective to their reciprocal action (e.g. agonist and antagonists) in the ongoing task: 3 sites classified as sHM (suppression of hand movement during the HMt) and one classified as dHM (dysfunctional hand muscle recruitment during the HMt) were indeed stimulated in resting condition and did not produce any upper-limb muscle activation with the same intensity used for the HMt. Finally, 1 site in which DES during the HMt resulted in a suppression of hand movement with a concurrent biceps activation, was stimulated during an opening and

closing of the hand, without any behavioural and EMG interference. These results suggest that HMt execution shaped the excitability of this cortical area leading to dHM and sHM outcome, which are DES-related effect not reproducible in resting condition and during other hand movement task. Finally, LF-DES during the HMt, when applied close to the central sulcus in the caudal sector, always resulted in dysfunctional hand-arm muscle recruitment (Fig. 2 D-E) No movement inhibition phenomena were observed in this area.

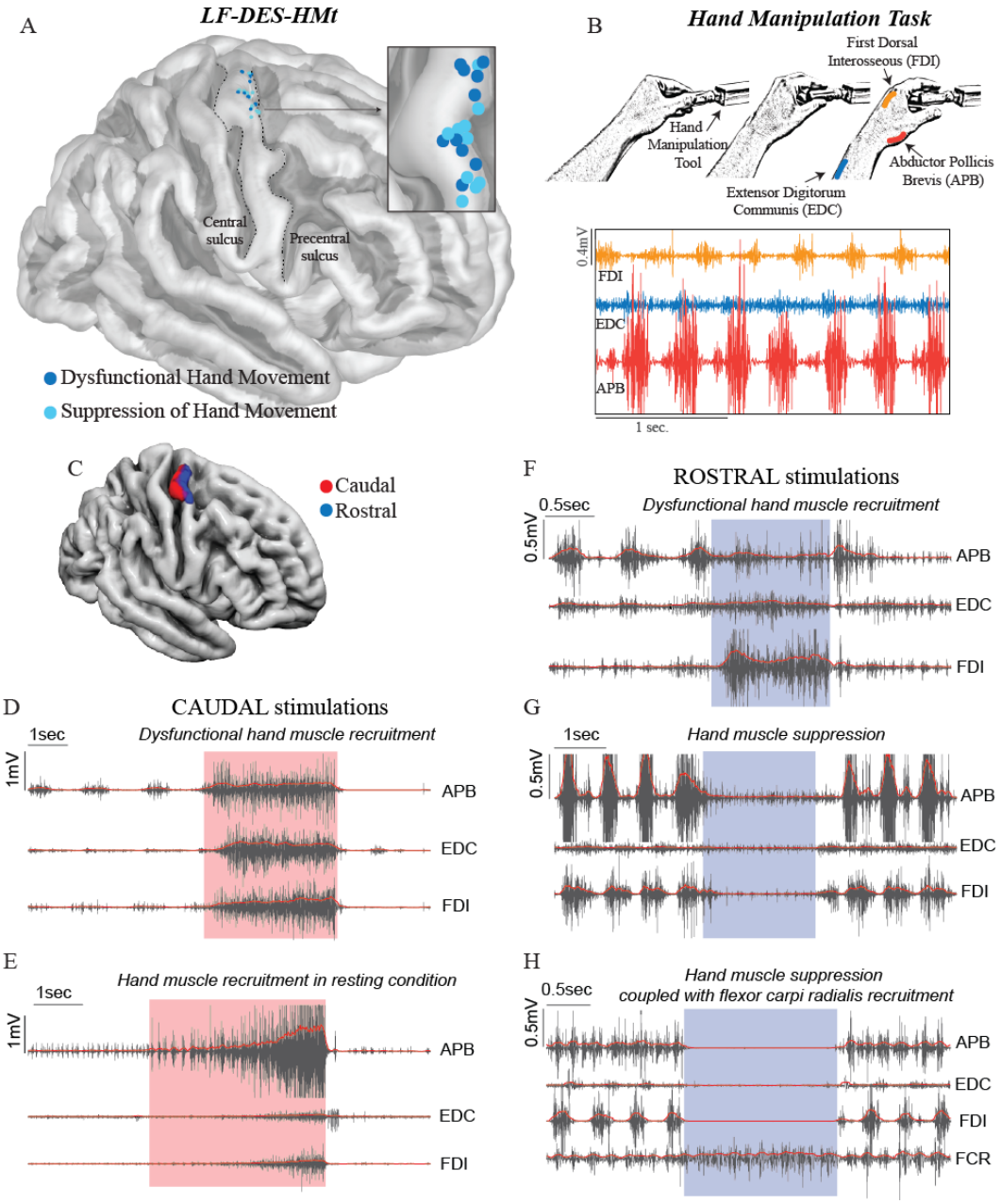

Fig. 2: A) Distribution of the cortical stimulation sites associated with the two behavioural outcomes mapped on the 3D FSAverage template: Dysfunctional Hand Movement (dHM) (blue) and Suppression

of hand movement (sHM) (pale-blue). B) Schematic representation of the HMt execution. C) Probability density estimation of caudal (red) and rostral (blue) LF-DES stimulation sites. D-E) Examples of EMG patterns of dHM caused by stimulation over the caudal sector, which consists in progressive recruitment of the muscles represented in the area. F-G-H) EMG pattern caused by stimulation on the rostral hand-knob: dHM (E); sHM (G); suppression of hand-muscles activity coupled with an involuntary increase in muscle activity in the forearm (FCR muscle) (H). The shadows (red for caudal and blue for rostral) represent the onset and the offset of the stimulations. Modified from Viganò et al. (2019).

3 Diffusion tractography

Virtual dissection of the corticofugal tract and the U-shaped tracts between the hand-knob area in the precentral gyrus and middle/superior frontal gyri and postcentral gyrus were performed in a subset of six patients (table 1) (Fig. 3). Regarding the corticofugal tract, no differences with the diffusion tensor and spherical deconvolution (Fig. 3) were detected between the rostro-caudal line: it projects equally into rostral and caudal hand-knob. In all patients, the U-shaped connections projecting to the posterior middle and superior frontal gyrus (dorsal premotor region) terminate solely within the rostral-hand knob. Conversely, the U-shaped fibres projecting to the primary somatosensory cortex in the postcentral gyrus terminate solely in the caudal hand-knob. 'Frontal' U-fibres connections always correlate with rostral hand-knob stimulations, area defined with DES as the one with the lowest cortical excitability, while 'postcentral' U-fibres correlate with stimulations in the caudal hand-knob, the region with the highest cortical excitability (Fig. 4).

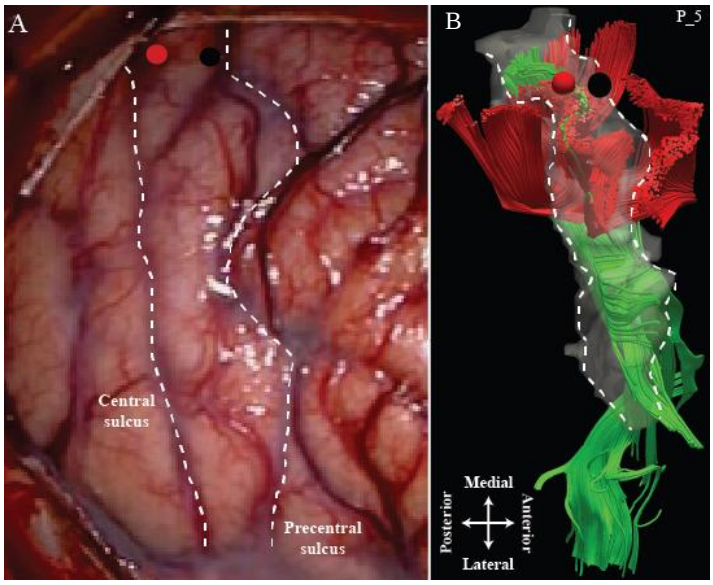

Fig. 3: A) Anatomical localisation of the caudal (red) and the rostral (black) HF-DES stimulation sites in patient 5 shown on photograph of the surgical flap. The black dot was also stimulated with LF-DES during HMt (resulting in sHM). Right panel shows the diffusion tractography reconstruction of the corticofugal tract (green), the precentral-postcentral and intra-frontal tracts (red).
These connections form a 'poppy flower' formation, described in Catani et al. (2012). Modified from Viganò et al. (2019).

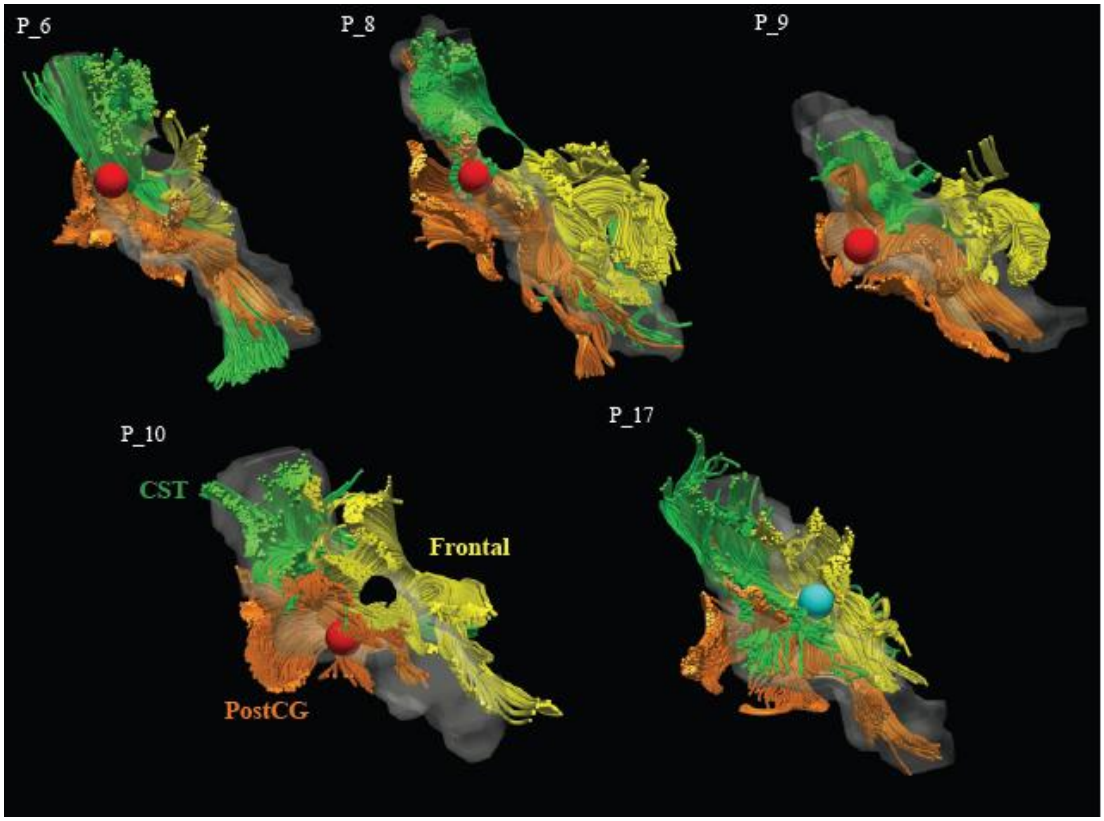

Fig. 4: Diffusion tractography reconstruction of corticofugal (green), precentral/postcentral (orange) and precentral/frontal (yellow) tracts of each single subject plotted in the 3D native space. All the stimulation sites have a diameter of 5 mm (Haglund et al., 1993). Red and black dots represent respectively caudal and rostral HF-DES-Rest sites. In patient 17 is shown the anatomical localisation of LF-DES-HMt site of stimulation resulted in a suppression of the hand movement (sHM). Modified from Viganò et al. (2019).

DISCUSSION

1 Rostro-caudal gradient of cortical excitability

Both the analyses used to assess differences in cortex excitability (caudal motor threshold and MEPs amplitude comparison) indicated univocally that the caudal sector, close to the central sulcus, had significantly a higher excitability. MEPs amplitude analysis provided also another interesting data supporting this result: over-threshold stimulations (same parameters in the two sectors) elicited responses of a higher number of muscles when applied to the caudal hand-knob (mean of 5 muscles/patient) compared to the rostral one (mean of 1.6 muscles/patient). However interesting, only a future study focused on the muscle synergies implemented by the two sectors will clarify this observation.

The gradient of cortical excitability revealed by MEPs analysis should reveal an anatomo-functional differentiation between the posterior and the anterior sector of the hand-knob: in this light, the functional organization of monkeys' M1 and dorsal premotor cortex could be used as comparison, since data on cortical excitability are available, mainly from intracortical micro-stimulation. Using the monkey model as benchmark, we advanced two hypotheses:

1) The caudal sector might correspond to the new-M1 buried in the central sulcus, while the rostral sector might correspond to the old-M1, on the crest of the precentral sulcus. In the monkey, the highest excitability was observed within the central sulcus, in the new-M1. Injections of retrograde trans-synaptic transport of rabies virus (finger, elbow and shoulder muscles) showed that corticomotoneuronal (CM) cells correspond selectively with the low-threshold stimulation site of the new-M1 (Rathelot and Strick 2008). More recent data (Whitam et al. 2016) advanced that both the monkeys' M1 sectors has direct access to the spinal cord motoneurons via CM cells, however from the old-M1 originate slower corticospinal fibres compared to the faster fibres of the new-M1. Since a higher excitability correlated with a direct access to the motoneurons in the ventral horn of the spinal cord, we can speculate that the cells of the human hand-knob close to the central sulcus might contribute in a different way (i.e. monosynaptic connection with motoneurons in the spinal cord or faster fibres) to the

CST compared to the cells located anteriorly with a lower excitability (interneurons in the spinal cord or slower fibres). This hypothesis cannot obviously be grounded in an architectonic investigation of the caudal and rostral sector of the hand-knob in our patients, therefore remains not conclusive. Another limitation comes from architectonic data in human which indicates that M1 is completely buried on the bank of the central sulcus (Geyer et al. 1996). For clinical constraints, in the selected patients, the central sulcus was never unfolded, and HF-DES was never applied directly on its bank (in all patient M1 and its projections were never infiltrated by tumour). If all the CM cells are located deep in the central sulcus, HF-DES on the convexity could easily excite them when applied in the posterior sector (caudal hand-knob), while more intensity of current would be needed when DES is applied moving anterior (rostral hand-knob). This consideration could explain the lower excitability of the area close the precentral sulcus, challenging the idea of a functional subdivision in two anatomo-functional sectors within M1 itself, and, finally, led us to a second hypothesis.

2) fMRI metanalysis in humans showed a partial overlap between M1 and dorsal premotor cortex (dPM) on the surface of the precentral gyrus (Mayka et al. 2006; Fan et al. 2016; Glasser et al. 2016). Anatomically, the caudal and rostral hand-knob individuated with DES in this study, could correspond respectively to area 4 and area 6d. From a functional point of view, the rostral sector could represent a transition area from M1 toward dPM. Again, a comparison with the Old World monkey is feasible: F2, which is the most caudal sector of dPM (Matelli et al. 1991) and has connections with M1 and the spinal cord (He et al. 1993; Geyer et al. 2000; Dum & Strick 2005), when stimulated, showed a clear motor output in distal and proximal upper-limb muscles, however with a significative lower excitability compared to M1 (Raos et al. 2003, 2004; Dum & Strick 2005). Moreover, the F2 contribution to the CST is lower in respect to M1 (He et al. 1993). The cortical excitability along the human hand-knob here demonstrated might reflect the transition between M1 and caudal dPM, since the rostral hand-knob, compared to the caudal one, shares functional similarities to monkeys' F2 compared to M1.

2 Rostral hand-knob involvement in action execution

Despite its lower excitability at rest during HF delivery, LF stimulations of the rostral hand-knob during the intraoperative object manipulation task always disrupted its execution, either evoking or suppressing movement. This data led us to hypothesize the involvement of that sector in the neural network controlling hand action execution (idea also supported by stimulations in control conditions, not able to evoke any upper-limb muscle activation). Main result of DES during the HMt in the rostral hand-knob was the occurrence of two different behavioural outcomes: an involuntary recruitment of distal muscles (Dysfunctional Hand Movement, dHM) and an arrest of hand movement (Suppression of Hand Movement, sHM). In the sample selected for the study the two responses were represented in the same proportion (50% dMH, 50% sHM) and were not segregated, but distributed in the hand area along the precentral sulcus. Both responses were coupled in half stimulations with recruitment in forearm and/or proximal districts. From a physiological prospective, LF-DES in this area disrupted the task changing the muscle synergies activated and sub-serving HMt execution (in both dHM and sHM, when coupled when proximal activation) or suppressing the ongoing movement (sHM without proximal activation). Differently, LF-DES on the caudal sector, close to the central sulcus, always resulted in a clear progressive muscles recruitment both at rest (see also Penfield et al. 1937; Bello et al. 2014) and during the HMt, activating a number of muscles proportional to the amount of current delivered. This response is coherent with direct stimulation of pure M1 (Park et al. 2004; Boudrias et al 2010; Bello et al. 2014). However, despite a direct comparison between stimulations of the caudal and rostral sector was not allowed (the caudal one was not systematically investigated in this data sample for clinical reasons), is mandatory to observe how stimulations in the rostral sector were never coherent with a-specific hand muscles recruitment described in literature after direct delivery of current in the M1 hand area (Park et al. 2004; Boudrias et al 2010; Rech et al. 2016; 2017). This data points to the rostral hand-knob as an area involved in shaping the motor output rather than in hosting the muscle representations used for the transmission of the motor command to the spinal motoneurons.

As already observed, both dHM and sHM stimulations were coupled in half cases with forearm and/or proximal activations (biceps or triceps). This result seems coherent

with the M1 somatotopical organization both in monkeys and humans: a central core of distal muscles, represented in the central sulcus, is surrounded first by an area with an intermingle distal and proximal representation and finally by a horseshoe-shaped proximal muscle zone in the Old-World monkey (Park et al 2001; Hudson et al. 2017); while in humans a central district of digits representation is enclosed by a wrist and forearm area (Meier et al. 2008). If the rostral hand-knob shares functional similarities with monkeys F2 in terms of cortical excitability when compared to M1 (see Rostro-caudal gradient of cortical excitability), the forearm/proximal involvement during DES-HMt could lead again to hypothesize that this sector represents a transitional area between M1 and dPM. In fact, F2 showed an overlapped representation between distal and proximal upper limb muscles (Dum & Strick, 2005; Boudrias et al 2010). Moreover, its involvement in reaching and grasping movements is well demonstrated in non-human (Kalaska et al. 1997; Cisek et al 2003; Raos et al. 2004; Nelissen et al. 2017) and human primates (Davare et al. 2006; Genon et al. 2017). The co-occurrence of both recruitment and suppression distal phenomena simultaneously coupled with more proximal activations (50% of stimulations) in the same rostral sector may let us speculate the attribution to this area along the precentral sulcus of a functional role in the computation of the synergies required for the integration between distal and proximal muscles during upper-limb gestures.

In the macaque both M1 and dPM, responsible for the motor output, are interconnected by cortico-cortical connections with the hand-dominnant and the sensorimotor domain of the superior parietal lobule (SPL), devoted to convert the sensory signals into motor commands. These projections give rise to the dorsal reaching system, which is supposed to encode the hand transport toward objects and the hand pre-shaping before grasping (Caminiti et al. 1996; Jhonson et al 1996; Battaglia-Mayer et al. 2000; Marconi et al. 2001; Fattori et al. 2010). Battaglia-Mayer et al. (2016) reviewed its functional-architechtonic organisational matrix of hand and eye representational cells allowing space exploration and coordinated hand movement toward the targets. A double rostro-caudal gradient in effector-dominance and distribution of signals related to different stages of motor behaviour emerged: in the frontal lobe F7 hosts eye cells, F2 an intermingle representation of eye and hand, while M1 represents the pure hand area. Accordingly to this architecture, from anterior to posterior, is ecoded the target

location (F7), the movement preparation (F2) and finally the action execution (M1) (in the parietal lobe these gradients are inverted from caudal to rostral). Again, both from cortical excitability analysis and pattern of interference during the object manipulation task, our results support this idea of a progressive encoding from higher-order motor computation toward the actual movement execution moving from frontal premotor regions to the central sulcus.

3 White matter connectivity of the hand-knob: considerations in light of the electrophysiological result

With the aim of evaluating if the functional differences detected between the rostral and the caudal sector corresponded also with differences in white matter connectivity, we performed (in a subset of six patients) virtual dissections of the corticofugal tracts projecting to the brainstem and the local connections between the hand-knob region ('poppy-flower' like formations, Catani et al. 2012), the more anterior premotor cortex (superior and middle frontal gyri) and the more posterior primary somatosensory area (postcentral gyrus).

Evaluating the corticofugal tracts, no differences in rostral or caudal terminations could be detected, however previous histological and ex-vivo diffusion imaging studies highlighted a gradient in laminar structure (Geyer et al. 1996, Bastiani et al. 2016). The possible conclusion that the two hand-knob regions share the same corticospinal components with the same subcortical targets and do not present any microstructural differences, must take into account the lack of sensitivity of the technique: we used a voxel size of 2mm voxel, which may contain up to 5 million axons (Walhovd et al. 2014).

As main results, we detected differences in local connectivity: the U-shaped connection between M1 and the PostCG projected exclusively to the caudal portion of the hand-knob, while the u-shaped connection between M1 and the superior and middle frontal gyrus projected solely the rostral hand-knob (Fig. 3-4). The owl and the squirrel monkeys present a similar pattern of cortical connectivity (Stepniewska et al. 1993, 2006; Dea et al. 2016).

The observed differences in local connectivity may reflect the functional role that each sector plays in control of the hand. The rostral hand-knob and the frontal regions connected via U-shaped tracts were suggested as a hub in mediating motor planning and execution (Catani et al. 2012), and considered as part of the dorsal premotor cortex characterized by a posterior to anterior gradient from movement execution to higher level motor functions (Genon et al. 2017). Physiological result of the present study, both from cortical excitability and stimulations during the intraoperative object manipulation task, led us to identify the rostral sector a transitional zone between M1 and dPM: this hypothesis is supported by anatomical result. Remains to be investigated with a dedicated study the role of the postcentral-M1 U-shaped tracts.

4 Limitations

The main result of the study, based on the quantitative analysis of the motor output elicited with HF-DES-Rest, shows a non-homogeneous rostro-caudal distribution of cortical excitability, with the caudal hand-knob being the most excitable sector. Although we show consistency in this result across the patients studied, some limitations should be considered. Concerning the hemisphere investigated, the pattern of cortical excitability of the hand-knob region must be verified also in the left hemisphere, particularly when considering the left-lateralization of the corticospinal tract (Thiebaut de Schotten et al. 2011; Catani & Thiebaut de Schotten 2012; Howells et al. 2018). Moreover, due to clinical constraints, the central sulcus cannot be unfolded preventing a direct investigation of the cortex localized on its anterior bank, an area that, from architectonic studies, might suggest the presence of the highest concentration of corticomotoneuronal cells (Geyer et al. 1996). The existence of different patterns of short-range cortico-cortical U-shaped connections according to rostro-caudal directions must be considered a preliminary result, given the low number of patients with HARDI acquisition. Investigating these functions in non-neurotypical brain tissue has potential limitations, considering the possible reorganization of function with respect to the healthy brain (especially for low-grade gliomas). To account for this, we applied strict inclusion criteria for each patient in order to avoid possible confounding results.

REFERENCES

Amiez C, Petrides M. 2018. Functional rostro-caudal gradient in the human posterior lateral frontal cortex. Brain Struct Funct. 223(3):1487-1499.

Bastiani M, Oros-Peusquens AM, Seehaus A, Brenner D, Möllenhoff K, Celik A, Felder J, Bratzke H, Shah NJ, Galuske R, Goebel R, Roebroeck A. 2016. Automatic Segmentation of human cortical layer-complexes and architectural areas using ex vivo diffusion MRI and its validation. Front Neurosci. 10:487.

Battaglia-Mayer A, Ferraina S, Mitsuda T, Marconi B, Genovesio A, Onorati P, Lacquaniti F, Caminiti R. 2000. Early coding of reaching in the parieto-occipital cortex. J Neurophysiol 83:2374–2391.

Battaglia-Mayer A, Babicola L, Satta E. 2016. Parieto-frontal gradients and domains underlying eye and hand operations in the action space. Neuroscience. 334:76-92.

Bello L, Riva M, Fava E, Ferpozzi V, Castellano A, Raneri F, Pessina F, Bizzi A, Falini A, Cerri G. 2014. Tailoring neurophysiological strategies with clinical context enhances resection and safety and expands indications in gliomas involving motor pathways. Neuro Oncol. 16:1110-1128.

Binkofski F, Fink GR, Geyer S, Buccino G, Gruber O, Shah NJ, Taylor JG, Seitz RJ, Zilles K, Freund HJ. 2002. Neural activity in human primary motor cortex areas 4a and 4p is modulated differentially by attention to action. J Neurophysiol. 88(1):514-9.

Boling W, Olivier A, Bittar RG, Reutens D. 1999. Localization of hand motor activation in Broca's pli de passage moyen. J Neurosurg. 91(6):903-10.

Borra E, Gerbella M, Rozzi S, Luppino G. 2017. The macaque lateral grasping network: a neural substrate for generating purposeful hand actions. Neurosci Biobehav Rev. 75:65-90.

Boudrias MH, McPherson RL, Frost SB, Cheney PD. 2010. Output properties and organization of the forelimb representation of motor areas on the lateral aspect of the hemisphere in rhesus macaques. Cereb Cortex. 20(1):169-86.

Boudrias MH, Lee SP, Svojanovsky S, Cheney PD. 2010. Forelimb muscle representations and output properties of motor areas in the mesial wall of rhesus macaques. Cereb Cortex. 20(3):704-19.

Broca P. 1888. Description ele´mentaires des circonvolutions ce´re´brales de l'homme. Me´moires d'Anthropologie. Memo Paris: C. Reinwald. 707–804.

Caminiti R, Ferraina S, Johnson PB (1996) The sources of visual information to the primate frontal lobe: a novel role for the superior parietal lobule. Cereb Cortex 6:319–328.

Catani M, Thiebaut de Schotten M. 2012. Atlas of human brain connections. Oxford. New York, NY: Oxford University Press.

Catani M, Dell'acqua F, Vergani F, Malik F, Hodge H, Roy P, Valabregue R, Thiebaut de Schotten M. 2012. Short frontal lobe connections of the human brain. Cortex. 48(2):273-91.

Caulo M, Briganti C, Mattei PA, Perfetti B, Ferretti A, Romani GL, Tartaro A, Colosimo C. (2007). New morphologic variants of the hand motor cortex as seen with MR imaging in a large study population. AJNR Am J Neuroradiol. 28(8)1480-5.

Cerri G, Shimazu H, Maier MA, Lemon RN. 2003. Facilitation from ventral premotor cortex of primary motor cortex outputs to macaque hand muscles. J Neurophysiol . 90:832–842.

Cisek P, Crammond DJ, Kalaska JF. 2003. Neural activity in primary motor and dorsal premotor cortex in reaching tasks with the contralateral versus ipsilateral arm. J Neurophysiol. 89(2):922-42.

Davare M, Andres M, Cosnard G, Thonnard JL, Olivier E. 2006. Dissociating the role of ventral and dorsal premotor cortex in precision grasping. J Neurosci. 26(8):2260-8.

Dea M, Hamadjida A, Elgbeili G, Quessy S, Dancause N. 2016. Different patterns of cortical inputs to subregions of the primary motor cortex hand representation in cebus apella. Cereb Cortex. 26(4):1747-61.

Dell'acqua F, Scifo P, Rizzo G, Catani M, Simmons A, Scotti G, Fazio F. 2010. A modified damped Richardson-Lucy algorithm to reduce isotropic background effects in spherical deconvolution. Neuroimage. 49(2):1446-58.

Dell'Acqua F, Simmons A, Williams SC, Catani M. 2012. Can spherical deconvolution provide more information than fiber orientations? Hindrance modulated orientational anisotropy, a true-tract specific index to characterize white matter diffusion. Hum Brain Mapp. 34(10):2464-83.

Dum RP, Strick PL. 2005. Frontal lobe inputs to the digit representations of the motor areas on the lateral surface of the hemisphere. 9;25(6):1375-86.

Fan L, Li H, Zhuo J, Zhang Y, Wang J, Chen L, Yang Z, Chu C, Xie S, Laird AR, Fox PT, Eickhoff SB, Yu C, Jiang T. 2016. The human brainnetome atlas: a new brain atlas based on connectional architecture. Cereb Cortex. 26:3508-3526.

Fornia L, Ferpozzi V, Montagna M, Rossi M, Riva M, Pessina F, Martinelli Boneschi F, Borroni P, Lemon RN, Bello L, Cerri G. 2018. Functional characterization of the left ventrolateral premotor cortex in humans: a direct electrophysiological approach. Cereb Cortex. 1-17.

Fattori P, Raos V, Breviglieri R, Bosco A, Marzocchi N, Galletti C (2010) The dorsomedial pathway is not just for reaching: graping neurons in the medial parieto-occipital cortex of the macaque monkeys. J Neurosci 30:342–349.

Genon S, Li H, Fan L, Müller VI, Cieslik EC, Hoffstaedter F, Reid AT, Langner R, Grefkes C, Fox PT, Moebus S, Caspers S, Amunts K, Jiang T, Eickhoff SB. 2017. The Right Dorsal Premotor Mosaic: Organization, Functions, and Connectivity. Cereb Cortex. 27(3):2095-2110

Geyer S, Ledberg A, Schleicher A, Kinomura S, Schormann T, Bürgel U, Klingberg T, Larsson J, Zilles K, Roland PE. 1996. Two different areas within the primary motor cortex of man. Nature. 382(6594):805-7.

Geyer S, Matelli M, Luppino G, Zilles K. 2000. Functional neuroanatomy of the primate isocortical motor system. Anat Embryol. 202(6):443-74.

Glasser MF, Coalson TS, Robinson EC, Hacker CD, Harwell J, Yacoub E, Ugurbil K, Andersson J, Beckmann CF, Jenkinson M, Smith SM, Van Essen DC. 2016. A multi-modal parcellation of human cerebral cortex. Nature. 536(7615):171-178.

He SQ, Dum RP, Strick PL. 1993. Topographic organization of corticospinal projections from the frontal lobe: motor areas on the lateral surface of the hemisphere. J Neurosci. 133:952–980.

Howells H, Thiebaut de Schotten M, Dell'Acqua F, Beyh A, Zappalà G, Leslie A, Simmons A, Murphy DG, Catani M. 2018. Frontoparietal tracts linked to lateralized hand preference and manual specialization. Cereb Cortex. 28(7):2482-2494.

Hudson HM, Park MC, Belhaj-Saïf A, Cheney PD. 2017. Representation of individual forelimb muscles in primary motor cortex. J Neurophysiol. 118(1):47-63.

Johnson PB, Ferraina S, Bianchi L, Caminiti R (1996) Cortical networks for visual reaching: physiological and anatomical organization of frontal and parietal lobe arm regions. Cereb Cortex 6:102–119.

Kalaska JF, Scott SH, Cisek P, Sergio LE. 1997. Cortical control of reaching movements. Curr Opin Neurobiol. 7(6):849-59.

Kleinschmidt A, Nitschke MF, Frahm J. 1997. Somatotopy in the human motor cortex hand area. A high-resolution functional MRI study. Eur J Neurosci. 9(10):2178-86.

Leemans A, Jeurissen B, Sijbers J, Jones DK .2009. ExploreDTI: a graphical toolbox for processing, analyzing, and visualizing diffusion MR data. Proc Int Soc Magn Reson Med. 17: 3537.

Lemon RN, 2008. Descending pathways in motor control. Annu Rev Neurosci. 31:195-218. doi: 10.1146/annurev.neuro.31.060407.125547.

Mayka MA, Corcos DM, Leurgans SE, Vaillancourt DE. 2006. Three-dimensional locations and boundaries of motor and premotor cortices as defined by functional brain imaging: a meta-analysis. Neuroimage. 31(4):1453-1474.

Marconi B, Genovesio A, Battaglia-Mayer A, Ferraina S, Squatrito S, Molinari M, Lacquaniti F, Caminiti R (2001) Eye–hand coordination during reaching. I. Anatomical relationships between parietal and frontal cortex. Cereb Cortex 11:513–527.

Matelli M, Luppino G, Rizzolatti G. 1991. Architecture of superior and mesial area 6 and the adjacent cingulate cortex in the macaque monkey. J Comp Neurol. 311(4):445-62.

Meier JD, Aflalo TN, Kastner S, Graziano MS. 2008. Complex organization of human primary motor cortex: a high-resolution fMRI study. J Neurophysiol. 100(4):1800-12.

Nelissen K, Fiave PA, Vanduffel W. 2017. Decoding grasping movements from the parieto-frontal reaching circuit in the nonhuman primate. Cereb Cortex. 1-15.

Park MC, Belhaj-Saïf A, Gordon M, Cheney PD. 2001. Consistent features in the forelimb representation of primary motor cortex in rhesus macaques. J Neurosci 21: 2784–2792.

Park MC, Belhaj-Saïf A, Cheney PD. 2004. Properties of primary motor cortex output to forelimb muscles in rhesus macaques. J Neurophysiol. 92(5):2968-84.

Penfield W, Boldrey E. 1937. Somatic motor and sensory representation in the cerebral cortex of man as studied by electrical stimulation. Brain. 9:389-443.

Quiñones-Hinojosa A, Ojemann SG, Sanai N, Dillon WP, Berger MS. 2003. Preoperative correlation of intraoperative cortical mapping with magnetic resonance imaging landmarks to predict localization of the Broca area. J Neurosurg. 99(2):311-8.

Raos V, Franchi G, Gallese V, Fogassi L. 2003. Somatotopic organization of the lateral part of area F2 (dorsal premotor cortex) of the macaque monkey. J Neurophysiol. 89(3):1503-18.

Raos V, Umiltá MA, Gallese V, Fogassi L. 2004. Functional properties of grasping-related neurons in the dorsal premotor area F2 of the macaque monkey. J Neurophysiol. 92(4):1990-2002.

Rathelot JA, Strick PL. 2008. Subdivisions of primary motor cortex based on cortico-motoneuronal cells. Proc Natl Acad Sci U S A. 106(3):918-23.

Rech F, Herbet G, Moritz-Gasser S, Duffau H. 2016. Somatotopic organization of the white matter tracts underpinning motor control in humans: an electrical stimulation study. Brain Struct Funct. 221(7):3743-53.

Rech F, Duffau H, Pinelli C, Masson A, Roublot P, Billy-Jacques A, Brissart H, Civit T. 2017. Intraoperative identification of the negative motor network during awake surgery to prevent deficit following brain resection in premotor regions. Neurochirurgie. 63(3):235-242.

Rosett J. 1933. Intercortical Systems of the Human Cerebrum. Columbia University Press, New York.

Rossi M, Fornia L, Puglisi G, Leonetti A, Zuccon G, Fava E, Milani D, Casarotti A, Riva M, Pessina F, Cerri G, Bello L. 2018. Assessment of the praxis circuit in glioma surgery to reduce the incidence of postoperative and long-term apraxia: a new intraoperative test. J Neurosurg. 23:1-11.

Shimazu H, Maier MA, Cerri G, Kirkwood PA, Lemon RN. 2004. Macaque ventral premotor cortex exerts powerful facilitation of motor cortex outputs to upper limb motoneurons. J Neurosci . 24:1200–1211

Stepniewska I, Preuss TM, Kaas JH. 1993. Architectonics, somatotopic organization, and ipsilateral cortical connections of the primary motorarea (M1) of owl monkeys. J Comp Neurol. 330:238 – 271.

Stepniewska I, Preuss TM, Kaas JH. 2006. Ipsilateral cortical connections of dorsal and ventral premotor areas in New World owl monkeys. J Comp Neurol. 495:691–708.

Strick PL, Preston JB. 1992. Two representations of the hand in area 4 of a primate. II. Somatosensory input organization. J Neurophysiol. 48(1):150-9.

Thiebaut de Schotten M, Ffytche DH, Bizzi A, Dell'Acqua F, Allin M, Walshe M, Murray R, Williams SC, Murphy DG, Catani M. 2011. Atlasing location, asymmetry and inter-subject variability of white matter tracts in the human brain with MR diffusion tractography. Neuroimage. 54(1):49-59.

Thompson A, Murphy D, Dell'Acqua F, Ecker C, McAlonan G, Howells H, Baron-Cohen S, Lai MC, Lombardo MV; MRC AIMS Consortium, and Marco Catani. 2017. Impaired communication between the motor and somatosensory homunculus is associated with poor manual dexterity in autism spectrum disorder. Biol Psychiatry. 81(3):211-219.

Walhovd KB, Johansen-Berg H, Káradóttird RT. 2014. Unraveling the secrets of white matter – Bridging the gap between cellular, animal and human imaging studies. Neuroscience. 276(100): 2–13.

Witham CL, Fisher KM, Edgley SA, Baker SN. 2016. Corticospinal inputs to primate motoneurons innervating the forelimb from two divisions of primary motor cortex and area 3a. J Neurosci. 36(9):2605-16.

Yousry TA, Schmid UD, Alkadhi H, Schmidt D, Peraud A, Buettner A, Winkler P. 1997. Localization of the motor hand area to a knob on the precentral gyrus. A new landmark. Brain. 1:141-57.

STUDY 2: ONCOLOGICAL AND FUNCTIONAL EFFICIENCY OF HIGH-FREQUENCY STIMULATION MAPPING FOR PRIMARY MOTOR TUMOURS RESECTION

Paper:

Rossi M. & Conti Nibali M., Viganò L., Puglisi G., Howells H., Gay L., Sciortino T., Leonetti A, Riva M., Fornia L., Cerri G., Bello L. 2019. Resection of tumors within the primary motor cortex using high-frequency stimulation: oncological and functional efficiency of this versatile approach based on clinical conditions. J Neurosurg. 9:1-13. doi: 10.3171/2019.5.JNS19453.

INTRODUCTION

Primary motor cortex (M1), representing the body with a somatotopic organization (Penfield and Boldrey 1937), and its descending pathways, play a crucial role in voluntary movement (Lemon 2008). Tumours removal in M1 was traditionally considered not feasible, since the high occurrence of permanent deficit with poor recovery after surgeries within this area (Penfield and Boldrey 1937; Ius et al.2011; Duffau et al. 2013). It follows that the surgical approach for M1 tumours was historically limited to partial biopsies, in order to avoid a long-term morbidity caused by more extended tumour resection (Duffau et al. 2013). Nowadays, intraoperative neurophysiology, with the multiple stimulations' paradigms available, is the most efficient tool to individuate the critical motor sites to be preserved (De Witt et al. 2012, Rossi et al. 2018). Preserving the eloquent motor cortical and subcortical structures allows to maintain the functional integrity of patients while reaching the maximus tumour resection possible (Sanai et al. 2008; Smith et. al 2008; Buckner et al. 2017). Some reports are available on limited series or anecdotal cases, mainly involving well demarcated tumours (Obermueller et al. 2014), in which traditionally available mapping paradigms are to a certain extent, quite efficient. Studies on larger series on different tumour type reported variable extent of resection (EOR) and post-operative permanent morbidity (Seidel et al. 2012; Han et al. 2018). However data on M1 tumour removal is limited, recent publications suggest that brain mapping technique with direct electrical stimulation allows excellent resection of lesions harbouring within M1

(Bello et al. 2014, Magill et al. 2017). Motor mapping could be managed with different stimulation paradigms and probes, which main features, clinical use and complications are well described in literature (Szelényi et al. 2011). Selecting the most appropriate neurophysiological tool is critical, being the preservation of patient's motor integrity strictly dependent from the ability in identifying motor tract during the progression of the resection (Han et al. 2018). Feasibility in the Operating Room, adaptability in different clinical conditions, low occurrence of false negative or false positive results are all crucial features that guide the choice of a specific neurophysiological protocol. Few data are available on the usage of high frequency (HF) stimulation paradigm to guide resection of tumours within the primary motor cortex and its descending projections. High frequency technique stimulation with the 'pulse technique' was suggested in a previous work of our group (Bello et al. 2014) as the most efficient tool to map motor pathways, allowing a high percentage of lesion removal with a low occurrence of post-operative deficits and showing also a high flexibility to different clinical conditions. According to this experience, in the recent years HF was selected as the main neurophysiological protocol for performing cortical and subcortical mapping to guide tumours' resection in patients harbouring lesions within M1 routinely submitted to surgery. Study 2 consists in a retrospective analysis of 102 brain tumour patients admitted between 2013 and 2018 affected by tumours harbouring within M1. A critical review of HF technique was obtained correlating the stimulations parameters with the patients' clinical features and the neuroradiological tumour properties. Feasibility of mapping, EOR and motor function assessment were used to evaluate the oncological and functional outcome correlated with the selected neurophysiological parameters used for guiding resection. Main aim was tailoring for each different clinical condition the most efficient and adaptable neurophysiological approach.

MATERIALS AND METHODS

1 Patients selection

We performed a retrospective study of 102 patients who underwent an asleep neurosurgical resection of brain lesion at Humanitas Research Hospital (prof. Bello, University of Milan, Neurosurgical Oncology Unit) between May 2013 and April 2018. Only patients with 75% or more of the tumour mass harbouring within M1 were included (as determined on axial-FLAIR images for low-grade gliomas (LGGs) and on axial-T1-post-gadolinium for high-grade gliomas (HGGs). All patients gave informed consent to the procedure, covered by Ethical-Committee-1299.

2 Surgical procedure

The surgical resection was performed according to functional boundaries (see General Materials and Methods). After the individuation of subcortical descending motor pathways and the functional disconnection of the lesion, the mass was finally removed. For pure Rolandic tumours, the peripheral functional motor borders were initially located all around the tumour, and then the tumour mass was removed. In case of tumours extending anteriorly or posteriorly, subcortical functional tumour disconnection was started at M1 level and continued anteriorly (in case of pre-M1) or posteriorly (in case of post-M1).

3 Neurophysiological monitoring and mapping

For a detailed description of brain monitoring protocols (EMG, EEG, ECoG) and the specification of the high frequency stimulation paradigm see the General Materials and Methods.

The standard To5 paradigm (HF, train of 5 pulses) was modified according to the clinical conditions. Number of stimuli (2 to 9), pulse duration (500-800 μs) and interstimulus interval (2-4 ms) were selected for the clinical needs. However stimulations were mainly delivered through a monopolar probe, a bipolar one was adopted when the procedure required an higher spatial focality. Anodal polarity was

used for cortical mapping, cathodal for the subcortical one. Reference electrode was placed close to M1 at the mesial border of the craniotomy. After the stimulation (cortical and subcortical) with the To5 protocol, the number of pulses, when required by the clinical context, was modified both decreasing (1 or 2 stimuli) or increasing (7 or 9 stimuli – in these cases pulse duration could be increased at 800 μs). Stimulation intensity was never higher than 25mA. Cortical motor threshold (cMT) was used to place the strip for continuous motor monitoring and to select the safe entry point, while subcortical motor threshold (sMT) was used to evaluate the distance from the corticofugal tracts and thus to establish the margins of the resection.

4 Variables considered for analysis

All the following listed factors, grouped by category, were considered for analysis.

1. *Demographic and clinical information*: age, gender, clinical history, symptoms at the entrance, previous treatments, seizure history and seizure control, previous and current drug uptake, neurological assessment (performed ad admission, 1 week and 1 month post-op, motor condition (MRC- Medical Research Council scale) before and after surgery, requirement of rehabilitation.

2. *Neuroradiological-imaging information*: tumour volume (computed on BrainLab software with the aid of the Smartbrush tool – the target of the resection was assessed for contrast enhancing lesions using the contrast-enhancing portion of the tumour while for low-grade gliomas using the FLAIR signal), zone location (assessed dividing M1 in 3 zones: zone 1 = lower limb; zone 2 = upper limb; zone 3 = face, see Magill et al. 2017), side, tumour border (distinguishing between well-defined or irregular; Bello et al. 2008; Aboian et al. 2017), presence or absence of contrast enhancement, outcrop of M1, extension outside M1 (both anteriorly in dorsal premotor regions and posteriorly invading the primary somatosensory area),

3. *Histological information*: histology and molecular profile of the tumour (IDH1-status, codeletion)

4. *Surgical variables*: duration of the surgery, intraoperative complications as ischemia-infection-bleeding, intraoperative mortality, asleep or awake anaesthesia

protocol, extent of resection (EOR). EOR consists in the percentage of volume resected compared to the pre-operative tumour volume: (preoperative tumour volume – resected tumour volume) / preoperative tumour volume. EOR was always calculated on the immediate post-operative MR performed within 48 hours. The outcome of the resection was classified as: -partial resection (postoperative volume > 5 cm); subtotal resection (postoperative volume between 1 and 5 cm); total resection (postoperative volume = 0 cm) (Bello et al. 2014). EOR was always calculated on the immediate post-op MRI (MR for enhancing lesion and FLAIR non non-enhancing) performed within 48 hours. To rule out ischemia and DWI abnormalities post-operative diffusion-weighted MRI scans were performed (Magill et al. 2017).

5. *DES mapping information*: mapping strategy used, type of probe, typology of motor responses obtained, minimum stimulation parameters useful in evoking motor evoked potentials, MEPs, both on the cortex (cortical motor threshold, cMT) and at subcortical level (subcortical motor threshold, sMT), changes in MEPs features (> 50% reduction of MEP amplitude; MEP loss assessed during the whole procedure with the To5 grid monitoring).

5 Statistical analysis

Statistical analysis was performed with SPSS-software (IBM). Chi-square (multiple categories) or Fisher exact (2 categories) tests were reported for categorical data. Univariate logistic regression was performed and used to calculate odds ratios. When comparing 2 variables two-tailed t tests for comparison between continuous variable were adopted. When comparing 3 or more variables ANOVA was used for comparisons between continuous variables.

RESULTS

1 Patients

102 patients were included (more than the 75% of the tumour bulk was located within M1, according to the inclusion criteria). Table 1 shows patients clinical and imaging features. Most patients experienced seizures, requiring at least 1 AED to be controlled. Poor seizure control was observed in 41.2% of cases. Most of the tumours had a small volume, were located prevalently in zone 1 and 2, and in half of cases reached the surface. 76.5% of lesions had irregular borders. In 38.2% of lesions contrast enhancement was present. In 20.6% of cases tumours extended outside M1 (anteriorly – 12 cases, or posteriorly – 9 cases, see Fig. 1).

Table 1 - Demographic, clinical, radiological and surgical features

102 patients	*n°*	*%*
Clinical and demographic features		
Sex		
Male	62	60.7%
Female	40	39.3%
Age		
Mean	42.7	
Range	17.2-75	
Clinical onset		
Focal seizure	91	89.2%
Other	11	12.8%
Duration of clinical history		
>6 months	62	60.8%
n. AED before surgery		
1	44	43.1%
>1	58	56.9%
Controlled pre-operative seizure	62	60.8%
Pt. with pre-op. motor deficit	10	9.8%

Preoperative MRC scale		
5	92	90.1%
4	10	9.9%
Radiological features		
Side		
Left	35	34.4%
Right	67	65.6%
Tumour volume		
Mean	10.13ml	
Median	5.6ml	
Range	1.3-65ml	
Contrast enhancing lesion		
Yes	39	38.2%
No	63	61.8%
Tumour motor zone (Berger classification)*		
1	40	39.3%
2	54	52.9%
3	8	7.8%
Tumour extension		
No	81	79.4%
anterior	12	11.8%
posterior	3	2.9%
Cortical outcrop	80	78.4%
Border		
Highly irregular	78	76.5%
Well defined	24	23.5%
Post-operative tumour volume		
Mean	1.06ml	
Median	0ml	
Range	0-29ml	
Resection		
Partial (residual tumour > 5 ml)	8	7.9%
Subtotal (residual tumour= 1-5 ml)	7	6.8%

Total (residual tumour =0 ml)	87	85.3%
Mean EOR	95.62%	
EOR = 100 %	87	85.3%
EOR 90-99%	2	1.9%
EOR <90 %	13	12.7%
DWI alteration		
Yes	6	5.9%
No	92	90.2%
NA	4	3.9%
Surgical features and Outcome		
Neurophysiological approach		
"Standard"	51	50%
"Reduced train"	43	42.1%
"Increased train"	8	7.9%
Worsening of motor deficit		
1 week	98	96.4%
1 month	2	1.9%
1 week MRC scale		
5	4	3.9%
4	68	66.6%
>=3	30	29.5%
1 month MRC scale		
5	100	98%
4	2	2%
Post-operative apraxia	2	2%
Post-operative rehabilitation	36	35.3%
Histology		
LGG	54	52.9%
HGG	41	40.2%
other	7**	6.9%
IDH1-2		
Wildtype	45	44.1%

Mutated	52	49%
NA	7	6.9%
1p/19 codeletion		
Yes	19	18.6%
NA	7	6.9%

* Zone 1: lower limb; zone 2: upper limb; zone 3: face.

** 7 metastasis (6 lung, 1 breast).

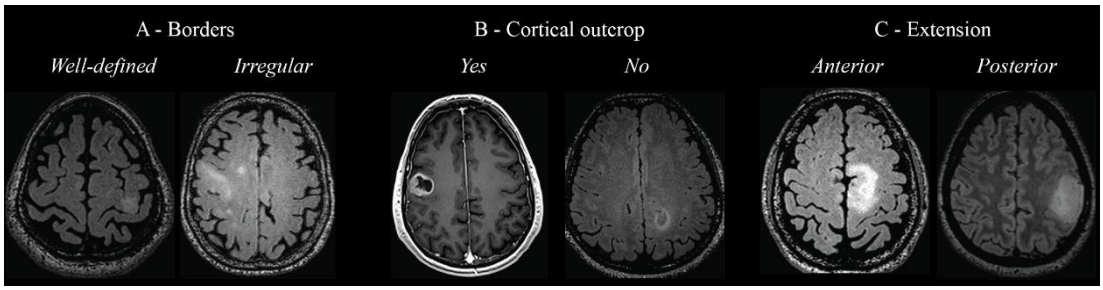

Fig. 1: Exemplificative cases of: (A) lesions' borders of a left LGG in zone 2 with well-defined borders (left) and a right LGG in zone 2 with irregular borders; (B) cortical outcrop of a right HGG in zone 2 with a visible cortical outcrop (left) and of a left LGG in zone 1 not reaching the surface; (C) tumours' extension of a left LGG in zone 1 which extends anteriorly respect to M1 and of a left LGG in zone 2 which extends posteriorly compared to M1. Modified from Rossi et al. (2019).

2 Surgical data and EOR

Surgery was performed in all cases under general anaesthesia. EEG and ECOG were used to monitor the level of anaesthesia, titrated to get for continuous EEG and ECOG activity, avoiding any burst suppression. High Frequency stimulation was used in all motor mapping. At cortical level, HF was useful to identify the safe entry zone. Subcortically, HF was used to define the functional boundaries of resection. Only in 2 cases out of 102 the MEP monitoring, recorded from the strip electrodes during the whole resection, detected abnormalities. These two cases were the only who experienced post-operative deficit. Intraoperative seizure never occurred. EOR was total in 87 cases (85.3%), subtotal in 7 (6.8%) and partial in the remaining 8 (7.8%). Mean EOR was 95.62%. In cases of subtotal and partial removal, mean and median EOR were 70.3% and 70.1% respectively. Complications (bleeding) were observed in

2 cases (1,96%). No postoperative mortality was documented. EOR was not affected by tumour-related factors deducible from conventional MR, neither by other clinical factors. A lower odd of achieving a total removal was associated with irregular borders, large volume and absence of contrast enhancement. Histology did not exert any effect, IDH1 mutation was associated with a lower odd of achieving a total resection (Table2).

Table 2 – Variables related to residual tumour (*total* vs *subtotal*).

	N. Pt	***Partial/subtotal***	***Total***	***Pearson Chi-Square***
Contrast enhancement				**0.004**
Yes	39	2 (5.1%)	37 (94.9%)	
No	63	18 (28.6%)	45 (71.4%)	
Extension outside M1				**0.000**
No	82	10 (12.2%)	72 (87.8%)	
Yes	20	10 (50%)	10 (50%)	
M1 outcrop				**0.045**
No	22	1 (4.5%)	21 (95.5%)	
Yes	80	19 (23.8%)	61 (76.2%)	
Borders				**0.029**
Well defined	24	1 (4.2%)	23 (95.8%)	
Highly irregular	78	19 (24.4%)	59 (75.6%)	
Pre-Operative mean volume		21.57	7.03	**0.000**
IDH1 status				**0.027**
Mutated	50	15 (30%)	35 (70%)	
Wild-type	45	5 (11.1%)	40 (88.9%)	
other	7	0 (0%)	7 (100%)	
Rehabilitation				**0.002**
No	66	7 (10.6%)	59 (89.4%)	
Yes	36	13 (36.1%)	23 (63.9%)	
Duration clinical history				0.346
>6 months	62	14 (22.6%)	48 (77.4%)	
<6months	40	6 (15%)	34 (85%)	

Previous treatment				0.856
Yes	39	8 (20.5%)	31 (79.5%)	
no	63	12 (19%)	51 (81%)	
Side				0.262
Right	67	11 (16.4%)	56 (83.6%)	
Left	35	9 (25.7%)	26 (74.3%)	
Motor Zone				0.280
1	40	7 (17.5%)	33 (82.5%)	
2	54	11 (20.4%)	43 (79.6%)	
3	8	2 (25%)	6 (75%)	
Pre-operative motor deficit				0.383
No	92	17 (18.5%)	75 (81.5%)	
Yes	10	3 (30%)	7 (70%)	
Histo-molecular diagn.				0.278
LGG	54	13 (24.1%)	41 (75.9%)	
HGG	41	7 (17.1%)	34 (82.9%)	
Other	7	0 (0%)	7 (100%)	

3 Motor functions

Immediately after surgery a decline in motor function was observed in 98 patients (69% of which experienced a mild deficit, MRC4; while a severe deficit, MRC< 4, occurred in the 31% of the sample) (Table.1). All post-operative deficits recovered at follow-up in all cases but in 2 patients in which a mild motor deficit (MRC4) persisted. Both cases were operated for HGGs. No permanent deficits were registered after resections of LGGs. Rehabilitation was needed for 35.5% of patients. Praxis was affected in 2% of patients.

Table 3 – Comparison between groups (dived by neurophysiological approach):

	Standard **51 pat.**	***Reduced*** **43 pat.**	***Increased*** **8 pat.**	***Pearson Chi-Square***
Previous treatment				**0.039**
Yes	15 (29.4%)	18 (41.9%)	6 (75%)	
No	36 (70.6%)	25 (58.1%)	2 (25%)	
Pre-operative deficit				**0.000**
Yes	1 (2%)	5 (11.6%)	4 (50%)	
No	50 (98%)	38 (88.4%)	4 (50%)	
Histo-molecular diagnosis				**0.000**
LGG	23 (45%)	31 (72.1%)	0 (0%)	
*HGG**	28 (55%)	12 (27.9%)	8 (100%)	
EOR				0.136
Total	37 (72.5%)	38 (88.4%)	7 (87.5%)	
Subtotal/partial	14 (27.5%)	5 (11.6%)	1 (12.5%)	
Post-operative deficit (1week)				0.566
Yes	48 (94.1%)	42 (97.7%)	8 (100%)	
No	3 (5.9%)	1 (2.3%)	0 (0%)	
Post-operative deficit (1month)				0.909
Yes	1 (2%)	1 (2.3%)	0 (0%)	
No	50 (98%)	42 (97.7%)	8 (100%)	
Rehabilitation				0.237
Yes	14 (27.5%)	19 (44.2%)	3 (37.5%)	
No	37 (72.5%)	24 (55.8%)	5 (62.5%)	

* Includes 7 patients with metastasis.

4.1 The standard approach

The standard approach consisted in the classic HF To5 paradigm (monopolar probe, train of 5 pulses). This approach was applied in 51 patients both at cortical (individuation of the safe entry zone) and subcortical (definition of the margins of the

resection by means of individuation of sites with an sMT of 3mA). Patients in which this paradigm was applied were diagnosed because of seizures, were neurologically intact in the pre-operative period and were taking AEDs with a well seizure control. Lesions of those patients were located in all M1 zones, reached in most cases the surface of M1, showed contrast enhancement and had well defined borders. Low-grade, high-grade and metastases were included. Cortical mapping with this approach was successful in all cases in the identification of the safe cortical entry zone (sites with a lower cortical excitability defined with cMT parameters) which corresponded with the outcrop area of the tumour when present. In all cases an sMT of 3mA was found during subcortical mapping without any alteration in MEPs parameters (recording strip electrodes). A complete resection was achieved in 72.5% of cases, a subtotal in 11.7% and a partial in 15.8%. In most cases a motor functions decline was observed in the immediate post-operative phase. All patients recovered within 1 month, except 1 patient (2%). Motor rehabilitation was applied in the 27.5% of the sample. Lesion analysis showed that surgeries of tumours characterised by contrast enhancement, well-defined borders and in most case diagnosed as high-grade gliomas, resulted in a total resection. On the contrary, when tumours were characterised by irregular borders with no contrast enhancement and diagnosed as low-grade gliomas, only a partial/subtotal resection was achieved (Table 3).

4.2 *The increased approach*

When the To5 approach resulted in a negative mapping (failed in evoking any reliable MEPs even increasing the stimulation intensity till 25mA), an increased train approach was used (Fig. 2). This one consisted of an increase both in number of pulses (from 5 to 7 or 9) both in pulse duration (from 500µs to 800µs) delivered with a monopolar probe. This approach was used in 8 patients (7.8%): in 2 patients was used a train of 7; in 6 patients was used a train of 9; in 5 patients the pulse duration was increased. Moreover in 3 cases a reversal of polarity from anodal to cathodal was requested to obtain MEPs. In all cases the application of the increased approach allowed a definition of a reliable cortical map useful for the definition of the safe cortical entry zone. The same paradigm defined at cortical level was adopted subcortically to guide resection. In all cases, the train was reduced to a To5 at the end of resection, allowing for complete tumour removal (sMT 5mA). An increased train approach was selected not

only for the monopolar probe but also for the MEPs monitoring from the grid electrodes. Only after tumour removal the standard To5 MEPs monitoring regained efficacy. When analysing the cases who requested intraoperatively this approach, it emerged that they were patients with a long clinical history, who received previous treatment (radiosurgery or surgery with radio-chemotherapy) in 75% of cases, characterised by a poor seizure control despite AEDs and presenting mild motor deficits before the admission (Table 3). EOR was complete in 87.5% of cases, subtotal in the remaining. Histology diagnosed high-grade gliomas or metastases. No motor deficit at 1 month were recorded.

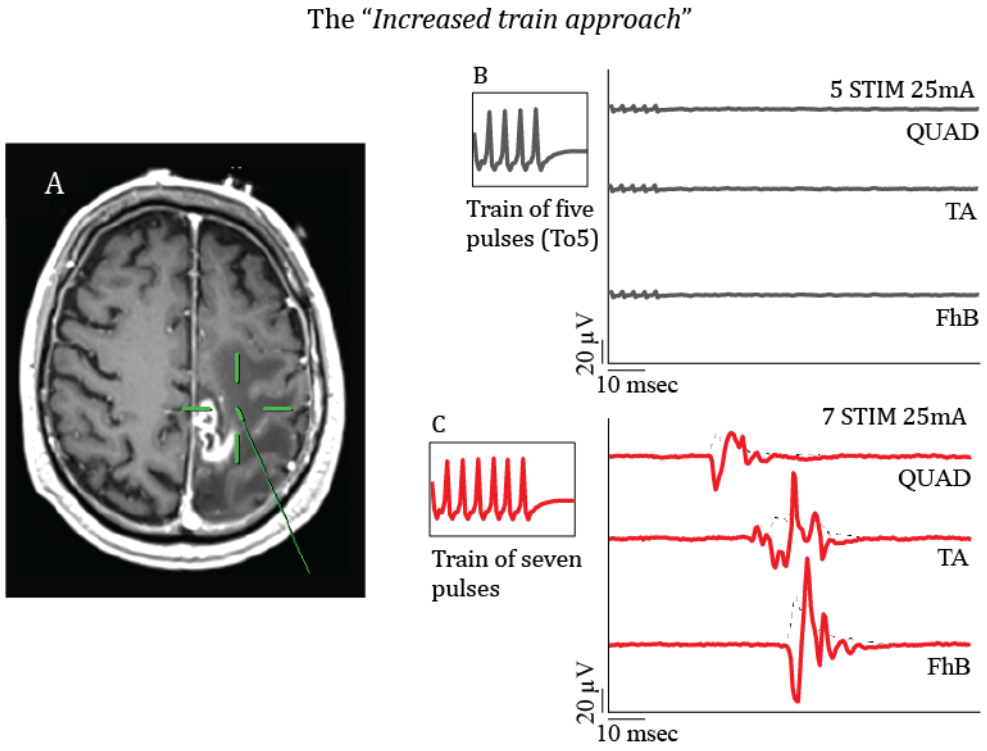

Fig. 2: Axial post-contrast T1 weighted image of a left metastasis (zone 1) previously treated with radiosurgery (A). The green cross indicates the subcortical site stimulated with the standard To5 approach which failed to evoke any MEPs even increasing the current intensity till 25mA (B) and subsequently with the *increased approach* (7 pulses) evoking reliable MEPs from the quadriceps femoris, QUAD, the tibialis anterior, TA, and the flexor hallucis brevis, Fhb. Grey dashed lines (B-C) represent the rectified signal. Modified from Rossi et al. (2019).

4.3 *The reduced approach*

When the standard To5 approach did not allow the individuation of a cortical negative site candidate as safe entry point for the resection (evoking MEPs from several muscles in each site stimulated on the convexity at cMT parameters), a further modified approach was adopted. This strategy, defined here as 'reduced approach', consisted in the delivery with a monopolar probe of train of 2 pulses (To2) always paralleled simultaneously with the To5 technique (Fig 3). This approach was administered to 43 patients (42.5%). In all cases, where the To5 paradigm did not discriminate between sites with higher or lower cortical excitability, the application of the To2 allowed to found sites with lower cMT and the negative sites where the corticectomy started. This protocol was particularly successful with tumours not reaching the surface. Both for cortical and subcortical mapping thresholds stimulation parameters were found for the two approaches (To5 and To2). The subcortical mapping usually started using the To5 since an sMT of 2mA was reached. With this intensity parameters responses from several muscles were detectable in each stimulated site. Application of the To2 paradigm in the same sites resulted or in no responses or in MEPs from fewer muscles, usually at higher current intensity (mean of 8mA). This allowed to extend the resection till an sMT of 2mA was found with the To2 in presence of a stable MEP recording performed with the To5 technique from the cortical grid electrodes. In some cases (12 patients, 27.9%) a bipolar probe was needed to increase the spatial resolution, despite requiring a higher current intensity (4-7mA), resulting an extended resection (Fig. 4). Total resection was reached in 88.4% of cases, and subtotal resection in the remaining (Fig.5). 97.7% of patients experienced a decline in motor function in the first post-operative week, all recovered but in one patient (2.3%, mild motor deficit), requiring two weeks rehabilitation in 44.2% of cases. Histological analysis diagnosed 72.1% of these tumours as Lower-grade (Table 3). Analysing the features of the patients who needed the reduced approach intraoperatively, it emerged that: they had a long clinical history; 50% of them showed not well controlled seizure despite a large number of AEDs at high doses; except for two cases, all of them were neurologically intact at admission; lesion, distributed in all M1 regions, were characterized by highly irregular margins, no contrast enhancement, resembling low-grade gliomas at standard clinical imaging; 40% of lesions did not reach M1 surface.

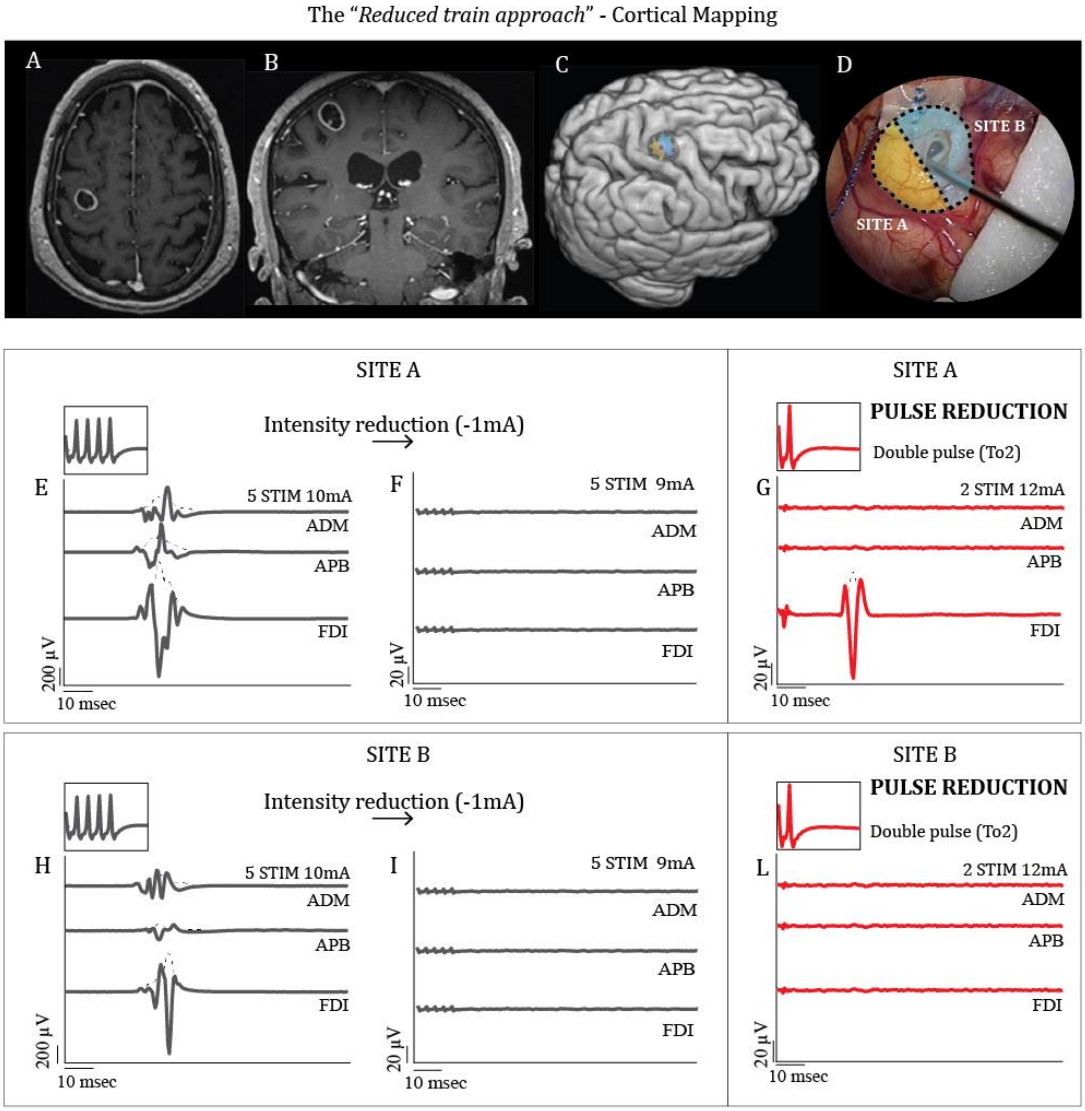

Fig. 3: Post-contrast T1 weighted image of a right HGG in zone 2 in axial (A) and coronal (B). Yellow area [site 1] on the 3D brain reconstruction (C) and on the picture of the surgical field (D) corresponds to the posterior sector of stimulation in the hand-knob region, close to the central sulcus, while pale-blue area corresponds to the anterior region of stimulation, close to the pre-central sulcus. Middle and low panel show the neurophysiological mapping strategy: stimulation of site A with the To5 approach at cMT (10mA) parameters evoked MEPs from several hand muscles (E) (here reported the abductor pollicis brevis, APB, the abductor digiti minimi, ADM, and the flexor carpi radialis, FDI). Decreasing the intensity of stimulation in the same site (-1mA) did not evoke any MEPs (F). Stimulation of the same site with the *reduced approach* (from 5 to 2 pulses) evoked reliable MEPs selectively from the FDI muscle, with a cMT of 12mA (G). Stimulation of site B with the To5 at cMT (10mA) evoked responses from several hand muscles, not allowing an intraoperative detection of any difference in cortical excitability compared to site A (H). Again, decreasing the intensity (-1mA), resulted in a negative stimulation also in site B (I). The application on site B of the same cMT stimulation parameters with the To2 useful to evoke motor responses in site A (2 pulses, 12mA) did not evoke any MEPs (L). The *reduced approach* was here able to detect a 'negative site' from which start the corticectomy (site B, see the intraoperative field in D). Grey MEPs were elicited with the standard approach (To5), while red MEPs were elicited with the To2. Grey dashed lines represent the rectified signal. Modified from Rossi et al. (2019).

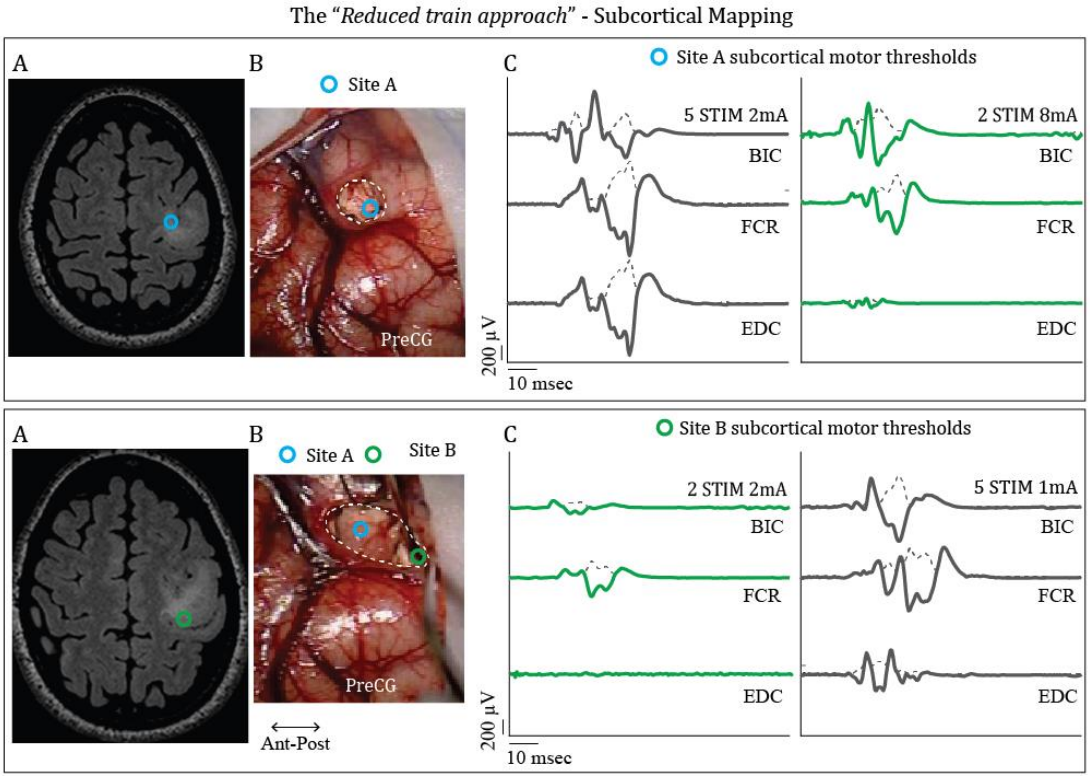

Fig. 4: Example of tailored neurophysiological subcortical mapping with the *reduced approach* in a left LGG in zone 2. Stimulation of site A [blue dot on axial pre-operative FLAIR (upper panel - A) and on the picture of the surgical field (upper panel - B)] at sMT parameters (2mA) with the To5 resulted in MEPs from several upper-limb muscles (upper panel - C-left) (here reported the biceps, BIC, the flexor carpi radialis, FCR, and the extensor digiti minimi, EDC). Application of the To2 in the same site at 2mA failed in evoking any MEPs. To obtain reliable responses was needed an increase in intensity (8mA) (upper panel - C-right). This strategy allowed to extend the resection from site A to the more inferior and posterior site B [in green on axial FLAIR (lower panel – A) and on the picture of the surgical field (lower panel – B)] in which an sMT with the To2 of 2mA was found (lower panel – C). Without moving the probe, site B was stimulated also with the To5 evoking responses with a greater amplitude in several muscles (BIC, FCR, EDC) also decreasing the intensity to 1mA (the minimum allowed by the Inomed machine). Modified from Rossi et al. (2019).

DISCUSSION

Recent studies suggest that surgical resection of tumours harbouring in M1 is feasible with an acceptable low morbidity (Magill et al. 2017), however these data are refereed mainly to the use of LF stimulations (Seidel et al. 2012; Schucht et al. 2014; Han et al. 2018). As previously demonstrated (Bello et al. 2014), a successful resection of a tumour infiltrating the motor pathways is obtained when the neurophysiological mapping approach was tailored to the specific clinical needs, as defined the patient clinical history and lesion imaging features. This study highlighted how HF stimulation paradigms are the most efficient strategy in identifying motor threshold parameters both at cortical and subcortical level according to the different clinical context (Bello et al. 2014). The present study extends this experience in surgical resection of tumours located mainly in M1, evaluating the EOR, the feasibility of mapping, the post-operative motor function assessment in correlation with the intraoperative neurophysiological mapping decided for guiding the resection. This retrospective analysis led to the identification of the most efficient mapping protocol to guide resection given the particular clinical condition.

Our series confirmed the feasibility of M1 tumours resection. Previous data reported that a complete resection (performed both in HGG and LGG) was achieved in 50.9% of cases, with the occurrence of permanent deficits in 37.7% of cases (only 4% of them were severe motor deficits) (Magill et al. 2017). Our data showed how a complete resection was achieved in 85.3% of cases. However this happened mainly in lesions with well-defined borders or contrast enhancement, this was true also in the large majority of lesions with irregular borders (lower-grade) and in those with previous treatments (independently by tumour localization) (Table 3). Resections were associated with very low permanent morbidity (2%). All the permanent deficits occurred in HGG patients. Considering that in all cases a low subcortical motor threshold was reached in order to extend the resection until the functional boundary, a high incidence of mild deficits was observed immediately post-op (always recovered in few weeks). Correlations between imaging features, clinical conditions and mapping protocol adopted led to the following considerations:

- The standard approach, To5 with the monopoloar probe, was highly reliable in defining a cortical and subcortical map in patients with these features: well-controlled seizures, lesions with well-defined borders or contrast enhancement in most cases reaching the surface of M1.

- The standard approach was not reliable in the assessment of motor pathways when the following clinical conditions were encountered: patients with previous treatments, HGG or metastases. In this setting it's reasonable that the excitability of the motoneurons was altered. Given that, to evoke reliable motor responses, a higher charge was requested. To this aim, we decide to not increase the intensity of stimulation in order to avoid the risk of inducing stimulation-related seizures. Instead of this we increased the number of pulses of the short train, associated in some cases also with an increase in pulse duration. In all cases, at the end of the resection, reliable MEPs were evoked from the cortical grid with the standard To5 approach, suggesting that the excitability of M1 increased after the removal of the compression effect of the lesion. A transient paresis was observed in these patients.

- The standard approach failed in defining a motor map in another set of patients with the following features: long clinical history with poor controlled seizures, lesions with irregular borders or with no contrast enhancement (lower grade) mainly not reaching the cortical surface. The To5 approach failed here in resolution, evoking responses in several muscles not allowing the individuation of a safe entry site at cortical level and a functional boundary at subcortical level always at threshold parameters. Given that was not possible to reduce the intensity, we reduced the number of stimuli from 5 to 2. This strategy allowed to find negative motor sites (no MEPs) both at cortical and subcortical level guiding safely the resection. Subcortically, a motor threshold (sMT) always searched with both the To5 and the reduced approach (To2). At threshold parameters (2mA) the To5 paradigm elicited in all patient responses from several muscles, while application of the To2 in the same sites did not evoke MEPs. At this point, increasing the intensity with the reduced approach (8-10mA) allowed always to find reliable MEPs from fewer muscles compared to the To5 stimulations. This allowed to extend the resection with the To2 mapping decreasing continuously the intensity until finding an sMT of 2mA. Switching from the To5 (not focal) to the To2 has a key benefit respect to simply decreasing the current, i.e. to

extend the resection beyond the functional boundary detected with the To5 standard approach. A post-operative low rate of permanent morbidity confirms the efficacy of this strategy. However effective in the clinical practice, the neurophysiological mechanism underlying this phenomenon is still unclear. Investigation with micro-stimulation and anatomical tracers in monkeys demonstrated the existence of different sectors within M1 (a posterior area, called new-M1, with fast monosynaptic corticomotoneuronal connections, and an anterior area, the old-M1, connected to the spinal cord via interneurons or slower fibres) (Rathelot and Strick 2009; Witham et al. 2016). We also recently demonstrated in the awake neurosurgical setting (Viganò et al. 2019, see also Study 1) how the surface of the precentral gyrus in the hand-knob region could hosts different anatomo-functional regions, probably reflecting the heterogeneity of the monkey's M1 or a transitional zone between M1 and the most caudal sector of the dorsal premotor cortex. Results of our study showed that the posterior sector has a higher cortical excitability compared to the anterior region. This data is confirmed by neurophysiological mapping useful to guide resections of M1 tumours: the anterior regions is in fact usually selected as safety entry point (see Fig. 3-D). The To2 technique showed to be able to recognise this posterior to anterior pattern of cortical excitability when the To5 approach missed focality and was not able to describe a reliable motor map. By modifying the number of pulses, we speculate that it may be possible to target corticofugal fibres with different functional properties, allowing for an increase in spatial resolution when searching for the safe entry point and when tracking the margin of resection, extending tumour removal.

Conclusions and Limitations

This study confirms and extends knowledge about the feasibility and safety of resection of tumours within M1, providing new data about the high versatility of High Frequency stimulation in assessing motor pathways. In this regard, considering how is crucial the intraoperative evaluation of MEPs amplitude and threshold stimulation parameters, we suggest that resection of M1 tumours should be performed under general anaesthesia (asleep-asleep). This setting provides in fact a stable cortical and subcortical excitability, while in the awake setting the excitability easily changes. Main result of this retrospective analysis is that the best extent of resection and

functional post-operative motor outcome is reached when the neurophysiological mapping is tailored for each surgery considering the clinical needs (imaging tumour features and patients' clinical history). As final consideration, we have to highlight some limitations of the study. As all retrospective study is limited by selection bias. Moreover, the functional outcome reported in this study was evaluated with the MRC scale, not sensible as a neuropsychological motor battery. Finally, the use of HF requires an advance intraoperative setting for the mapping and monitoring phase, an experienced neurophysiologist and a neurophysiology-trained surgeon

REFERENCES

Aboian MS, Solomon DA, Felton E, Mabray MC, Villanueva-Meyer JE, Mueller S, Cha S. 2017. Imaging characteristics of pediatric diffuse midline gliomas with histone H3 K27M mutation. Am J Neuroradiol 38:795–800

Bello L, Gambini A, Castellano A, Carrabba G, Acerbi F, Fava E, Giussani C, Cadioli M, Blasi V, Casarotti A, Papagno C, Gupta AK, Gaini S, Scotti G, Falini A. 2008. Motor and language DTI Fiber Tracking combined with intraoperative subcortical mapping for surgical removal of gliomas. Neuroimage 39: 369-82

Bello L, Riva M, Fava E, Ferpozzi V, Castellano A, Raneri F, Pessina F, Bizzi A, Falini A, Cerri G. 2014. Tailoring neurophysiological strategies with clinical context enhances resection and safety and expands indications in gliomas involving motor pathways. Neuro Oncol. 16:1110-1128.

Buckner J, Giannini C, Eckel-Passow J, Lachance D, Parney I, Laack N, et al: Management of diffuse low-grade gliomas in adults - Use of molecular diagnostics. Nat Rev Neurol 13: 340-351, 2017

De Witt Hamer PC, Robles SG, Zwinderman AH, Duffau H, Berger MS. 2012. Impact of intra operative stimulation brain mapping on glioma surgery outcome: A meta-analysis. J ClinOncol 30: 2559-65

Duffau H, Mandonnet E. 2013. The "onco-functional balance" in surgery for diffuse low-grade glioma: Integrating the extent of resection with quality of life. Acta Neurochir (Wien) 155:951-7

Han SJ, Morshed RA, Troncon I, Jordan KM, Henry RG, Hervey-Jumper SL, Berger MS .2018. Subcortical stimulation mapping of descending motor pathways for perirolandic gliomas: assessment of morbidity and functional outcome in 702 cases. J Neurosurg 1: 1-8

Ius T, Angelini E, Thiebaut de Schotten M, Mandonnet E, Duffau H. 2011. Evidence for potentials and limitations of brain plasticity using an atlas of functional resectability of WHO grade II gliomas: Towards a "minimal common brain." Neuroimage 56: 992-1000

Lemon RN. 2008. Descending pathways in motor control. Annu Rev Neurosci. 31:195-218.

Magill ST, Han SJ, Li J, Berger MS. 2017. Resection of primary motor cortex tumors: feasibility and surgical outcomes. J Neurosurg 129:1–12

Obermueller T, Schaeffner M, Gerhardt J, Meyer B, Ringel F, Krieg SM. 2014. Risks of postoperative paresis in motor eloquently and non-eloquently located brain metastases. BMC Cancer 14: 21

Penfield W, Boldrey E. 1937. Somatic motor and sensory representation in the cerebral cortex of man as studied by electrical stimulation. Brain. 9:389-443.

Rathelot JA, Strick PL. 2008. Subdivisions of primary motor cortex based on cortico-motoneuronal cells. Proc Natl Acad Sci U S A. 106(3):918-23.

Rossi M, Sani S, Nibali MC, Fornia L, Bello L, Byrne R W. 2019. Mapping in Low-Grade Glioma. Neurosurg Clin N Am. 30(1):55-63.

Surgery: Low- and High-Frequency Stimulation. Neurosurg Clin N Am 30:55–63, 2019

Sanai N, Berger MS. 2008. Glioma extent of resection and its impact on patient outcome. Neurosurgery 62: 753-64

Seidel K, Beck J, Stieglitz L, Schucht P, Raabe A. 2012. Low-threshold monopolar motor mapping for resection of primary motor cortex tumors. Neurosurgery 71: 104-14

Schucht P, Seidel K, Beck J, Murek M, Jilch A, Wiest R, Fung C, Raabe A. 2014. Intraoperative monopolar mapping during 5-ALA–guided resections of glioblastomas adjacent to motor eloquent areas: evaluation of resection rates and neurological outcome. Neurosurg Focus 37: E16,

Seidel K, Beck J, Stieglitz L, Schucht P, Raabe A. 2012. Low-threshold monopolar motor mapping for resection of primary motor cortex tumors. Neurosurgery 71: 104

Smith JS, Chang EF, Lamborn KR, Chang SM, Prados MD, Cha S, Tihan T, Vandenberg S, McDermott MW, Berger MS. 2008. Role of extent of resection in the long-term outcome of low-grade hemispheric gliomas. J Clin Oncol 26: 1338-45, 2008

Szelényi A, Senft C, Jardan M, Forster MT, Franz K, Seifert V, Vatter H. 2011. Intra-operative subcortical electrical stimulation: A comparison of two methods. Clin Neurophysiol 122: 1470-5, 2011

Viganò L, Fornia L, Rossi M, Howells H, Leonetti A, Puglisi G, Conti Nibali M, Bellacicca A, Grimaldi M, Bello L, Cerri G. 2019. Anatomo-functional characterisation of the human "hand-knob": A direct electrophysiological study. Cortex. 113:239-254

Witham CL, Fisher KM, Edgley SA, Baker SN. 2016. Corticospinal inputs to primate motoneurons innervating the forelimb from two divisions of primary motor cortex and area 3a. J Neurosci. 36(9):2605-16.

STUDY 3: CONTRIBUTION OF FRONTAL LOBE AREAS IN CONTROL OF DEXTERITY: DISSOCIATING SUBCORTICAL TRACTS COMBININING DIRECT ELECTRICAL STIMULATION AND TRACTORGRAPHY IN AWAKE NEUROSURGERY

Paper:

Henrietta Howells & Luca Viganò, Marco Rossi, Guglielmo Puglisi, Antonella Leonetti, Marco Rabufetti, Luciano Simone, Andrea Bellacicca, Lorenzo Bello, Luca Fornia, Gabriella Cerri (under review): *Dissociable effects on hand motor control during direct electrical stimulation of premotor white matter tracts*.

INTRODUCTION

Stimulation applied to frontal lobe regions produces distinct effects on muscle activity. DES applied to the caudal convexity of the precentral gyrus near the primary motor cortex (M1) evokes overt muscle contractions both at rest and during movement (Penfield & Boldrey, 1937; Viganò et al. 2019). When applied in premotor cortical regions, DES has no effect on muscle activity when the hand is at rest, rather disruption occurs only when spontaneous ongoing movements are being performed by the awake neurosurgical patient (Lüders et al. 1995). A spectrum of interference with hand movements can occur, likely due to disruption of one of the many stages before a skilled action can reach execution. Our group has previously evaluated this on the cortical level during repetitive, haptically driven hand movements performed by patients during awake neurosurgery (Rossi et al. 2018; Vigano et al. 2019; Fornia et al. 2019). Using EMG, we showed that DES does not have a uniform effect on muscle activity across cortical regions: modulation of motor unit recruitment, and changes in movement regularity were recorded in different premotor sectors. This technique, akin to non-human primate studies, thus provides an opportunity to causally dissociate functional roles of different premotor regions in orchestrating hand movements.

Within the premotor cortex, a mosaic of brain regions involved in manual control have been well defined in non-human primates, clustered into clear ventral and dorsal sectors based on function as well as cytoarchitectonic boundaries and connectional

anatomy (Matelli & Luppino, 1985; Borra & Luppino, 2017). The ventral sector (vPM) is considered the core of the so-called lateral grasping network (Borra et al. 2017) and computes sensorimotor transformations required for flexible hand-object interaction in different conditions (Nelissen et al. 2011, 2017; Ehrsson et al. 2000, Binkofski et al. 1999). The dorsal sector (dPM) integrates components of the required action, online, to formulate appropriate motor programs (Thura & Cisek, 2014). Both regions are strongly interconnected with M1, receiving segregated but complementary inputs from posterior parietal regions (Hoshi & Tanji 2007). In humans, the mosaics making up premotor sectors are less clearly dichotomized due to differences in frontal anatomy (Genon et al. 2016; Croxson et al. 2017). Dorsal and ventral sectors are commonly defined across cortical areas surrounding the meeting of the precentral sulcus and the posterior borders of the superior and inferior frontal sulci, respectively. Transcranial magnetic stimulation and neuroimaging studies indicate that some aspects of these cortical areas share homologies with macaque motor sectors (Davare et al. 2006; Cavina-Pratesi et al. 2010, Brandi et al. 2014), however the connectional anatomy is still relatively underexplored.

DES delivered at subcortical level directly interrupts communication between brain regions via white matter pathways, causing a 'transient disconnection', therefore by combining this technique with diffusion imaging tractography we may provide a unique window to evaluate the role of specific frontal lobe tracts in hand movement. High angular resolution diffusion imaging approaches (HARDI) have recently been developed to model multiple fibre orientations within single voxels, making it possible to study tracts previously untraceable with early diffusion tensor methods. This is of particular relevance in studying motor control, as it enables tracing of parieto-frontal pathways collectively termed the superior longitudinal fasciculus, which are associated with hand movements in monkeys and humans (Luppino, 1999; Budisavljevic et al. 2016, Howells et al. 2018). Other premotor tracts linked to programming movement extend from the supplementary motor complex (SMA and pre-SMA), including the recently described frontal aslant tract and fronto-striatal tracts (Catani et al. 2012; Budisavljevic et al. 2017). Finally, local U-shaped tracts directly connecting the hand region of the precentral gyrus (the 'hand-knob') with adjacent gyri have been linked to impairments in manual ability (Yousry et al. 1991; Catani et

al. 2012; Thompson et al. 2017; Vigano et al. 2019). However, no causal approach has yet evaluated whether application of DES affects with specific features the motor control of the hand when inducing a transient lesion of these tracts on the subcortical level.

We studied the effect of DES applied to subcortical regions of the frontal lobe during an object manipulation task used for awake neurosurgical resection of brain tumours in thirty-six patients (17 left hemisphere, 19 right hemisphere). Using a quantitative approach detailed in a previous study (Fornia et al., 2019), we used behavioural and EMG analysis to evaluate the effect of stimulation of subcortical dorsal and ventral premotor sites on the manual ability needed to perform the hand-object manipulation task. We next assessed which white matter tracts were most likely to have been "transiently disconnected" by stimulation across all patients using Tractotron tools (Foulon et al., 2018). Using diffusion imaging tractography in a subset of fifteen patients, we investigated precisely which tracts were 'transiently disconnected' by DES in a subject-specific way. Finally, using a lesion-symptom mapping analysis, we correlated the post-operative motor disturbances with the resection of specific tracts. We confirmed this result in the subset of fifteen patients with diffusion tractography. By combining functional and structural approaches, we set out to causally identify the subcortical white matter tracts involved in different components of hand motor control for the first time in the human brain.

METHODS

1 Study design and patient cohort

We studied thirty-six patients, who underwent an awake neurosurgical resection for a left (n=17) or right (n=19) hemisphere brain tumour at Humanitas Research Hospital (Prof. Bello Neurosurgical Oncology Unit, University of Milan) between 2015 and 2018. Patients were included in the study using the following criteria: no preoperative motor or praxis deficit, no long-term history of epilepsy and use of the object manipulation tool during the intraoperative brain mapping procedure. Patients with a previous open biopsy were included. All patients were assessed for handedness using the Zappala Handedness Inventory and underwent a full pre-operative neurological and neuropsychological evaluation of cognitive ability. Demographic information is reported in Table 1. Tumour volume was calculated on a gadolinium-enhanced MRI for high grade glioma and FLAIR for low grade glioma using a semi-automated segmentation software (Smartbrush, Element Suite, BrainLab).

The following figure illustrates a flowchart of the analysis adopted in the study.

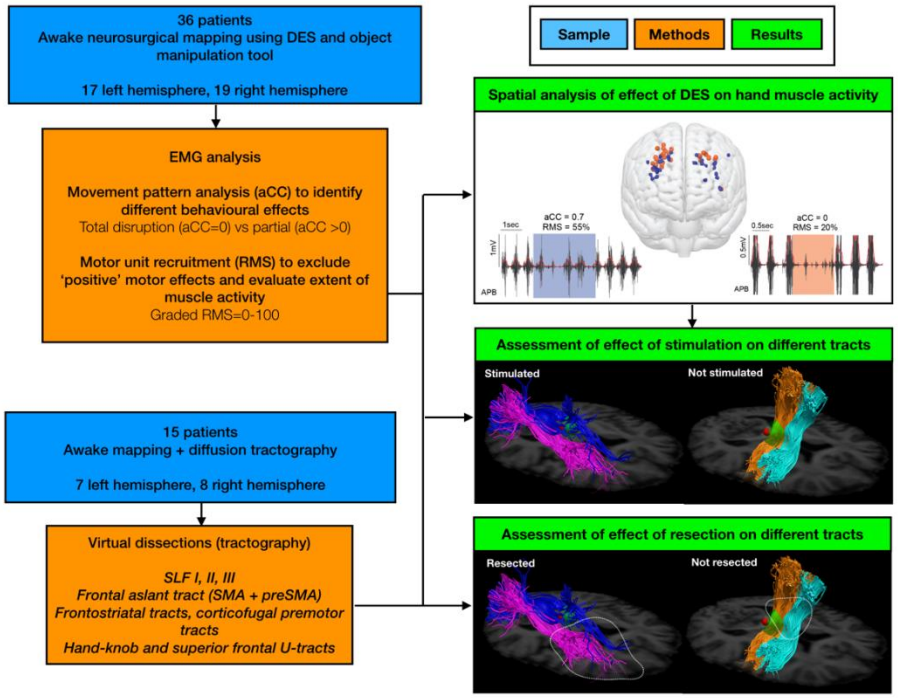

Fig. 1: Study flowchart. Reproduced from Howells & Viganò et al. (under review).

Table 1.

Pt	*Hemisphere*	*Age*	*Handedness*	*WHO grade*	*Diffusion tractography*	*5 days outcome*	*1 month outcome*
1	Right	50-55	R	OligoastrocytomaIII	X	Hemiplegia	--
2	Right	40-54	R	AstroII	X	Hemiplegia	--
3	Left	55-60	R	OligodendroII	X	Hyposthenia	--
4	Right	30-35	R	OligodendroII	X	--	--
5	Right	30-35	R	OligodendroII	X	--	--
6	Right	30-35	L	OligodendroII	X	--	--
7	Right	50-55	R	OligodendroII	X	--	--
8	Right	50-55	R	OligodendroII	X	--	--
9	Right	45-50	L	OligodendroII	X	--	--
10	Left	45-50	R	OligodendroII	X	--	--
11	Left	40-45	L	OligodendroII	X	--	--
12	Left	55-60	R	AstroIII	X	--	--
13	Left	35-40	L	GBMIV	X	--	--
14	Left	55-60	R	GBMIV	X	--	--
15	Left	40-45	R	AstroIII	X	--	--
16	Right	40-45	R	AstroIII		SMA syndrome	--
17	Right	55-60	R	AstroIII		--	--
18	Right	25-30	R	OligodendroII		--	--
19	Left	60-65	R	GBMIV		--	--
20	Left	40-45	R	OligodendroIII		--	--
21	Right	25-30	Mixed	AstrocytomaII		--	--
22	Left	40-45	R	OligodendroIII		--	--
23	Right	30-35	R	AstrocytomaII		--	--
24	Left	35-40	R	OligodendroII		--	--
25	Right	50-55	R	OligodendroIII		--	--
26	Left	50-55	R	GBMIV		Hemiplegia	--
27	Left	35-40	R	GBMIV		SMA syndrome	--
28	Left	60-65	R	AstroIII		--	--
29	Left	40-45	R	NeurocytomaII		Hemiplegia	--
30	Right	20-25	R	OligodendroII		Hemiplegia	--
31	Right	35-40	R	AstroIII		--	--
32	Left	35-40	R	OligodendroII		--	--
33	Right	35-40	R	GBMIV		SMA syndrome	--
34	Right	35-40	R	AstroIII		Hemiplegia	--
35	Right	20-25	R	OligodendroII		Hyposthenia	--
36	Right	30-35	R	OligodendroII		SMA syndrome	--

-- = no motor deficits

2 Subcortical mapping

During tumour resection, DES was applied continuously in order to identify and preserve functional boundaries. Motor ability was tested (Bello et al. 2014) and more complex praxis ability using the previously described tool (Rossi et al. 2018, General Material and Methods, Fig. 2b). The current intensity used was the same effective in

producing disruption to speech production during cortical mapping (mean intensity = 3.3mA, std = 0.9mA, range: 2mA-5mA). If stimulation disrupted task execution during progression of the resection, the site was verified by re-applying DES two non-consecutive times. These sites were then defined as 'effective'. Subcortical stimulation eliciting a hand movement behavioural disturbance were reported by the neuropsychologist, used as anatomical landmarks for establishing the functional boundaries of the resection and finally recorded using neuronavigation software (Curve, Brainlab AG, Munich, Germany). Task execution of each patient was videotaped for further analysis.

3 Data analysis

3.1 *Offline EMG analysis*

Each subcortical effective site identified during surgery was inspected offline using the synchronised EMG recording and a video-recording of the corresponding behavioural performance. The raw EMG data was extracted from the neurostimulator (ISIS IONM, Inomed Medizintechnik GmbH, Emmendingen, Germany) and analysed with a dedicated software (MatLab, Math Works 2016a). Quantitative analysis of EMG signal was performed on three out of 24 muscles recorded, specifically those involved in hand movement (i.e. APB, abductor pollicis brevis, FDI, first dorsal interosseous and EDC, extensor digitorum communis). In each patient we selected the EMG time window for which task execution was accurate, with no concurrent stimulation (the baseline), and time windows corresponding to the duration of the stimulus disrupting the task performance. The time window of stimulation was selected by using a stimulation-related artefact from an electrode routinely placed on the forehead (close to the orbicularis oculi muscle), which was recorded by one of the EMG-synchronized channels. The selected EMG was low pass filtered at 500 Hz and multiple notch filters from 60 to 480 Hz were applied to remove LF-DES artefacts and harmonics. This analysis is explained in greater detail in a recently published study (Fornia et al. 2019). Two main quantitative parameters were computed for each of the three muscles independently: the root mean square (RMS) and the autocorrelation coefficient (aCC). For each baseline and error site epoch, one RMS and one aCC value was computed for each muscle and each stimulation trial (n=2 for each site).

3.2 *Analysis of movement regularity*

The rhythmicity of phasic muscle contraction during the repetitive movement was calculated for the selected EMG time window using an autocorrelation coefficient (aCC) (Nelson-Wong et al. 2009). This provided a quantitative parameter by which to evaluate the extent of disruption to the overall regularity of the movement. Values range between 0 (no repetition) and 1 (sustained regularity of muscle contractions in time). One aCC value was assigned to each effective site, based on an average of the aCC values across the three muscles. Using this measurement, we classified two different patterns: complete movement arrest (aCC = 0) and 'clumsy' movement, referring to partial disruption of the phasic movement (aCC > 0).

3.3 *Analysis of motor unit recruitment*

We calculated motor unit recruitment during task execution in all conditions (baseline/stimulation), measuring amplitude of the signal as a function of time (Root Means Square; RMS). This provided a means of evaluating the amount of hand muscle activity during stimulation. RMS during effective stimulation was normalised for each patient relative to their baseline performance for each muscle. RMS across the three muscles was averaged to provide a single value for each effective site. Effective sites were defined as 'negative' when the RMS fell below the baseline.

3.4 *Diffusion tractography*

Spherical deconvolution modelling and whole brain deterministic tractography was performed with StarTrack software (www.mr-startrack.com). Diffusion data was first visually inspected for outliers, reordered and corrected for head motion and eddy current distortions using ExploreDTI (Leemans et al. 2009). Standard diffusion tensor imaging cannot show multiple fibre orientations within a voxel therefore we used spherical deconvolution to model the orientation distribution function, using a damped Richardson-Lucy algorithm (Dell'Acqua et al. 2010). An ALFA value of 1.7 was used with 300 iterations with an n of 0.001, a v of 8, and an absolute threshold of 0.001. Whole brain tractography was run using a step size of 1mm, with a constraint to display streamlines between 15 and 200mm in length. Euler interpolation was used to track streamlines using an angle threshold of 45 degrees. Spherical deconvolution modelling and whole brain deterministic tractography was performed with StarTrack software (Dell'Acqua et al. 2013. www.mr-startrack.com).

Tract dissections were performed using a region-of-interest (ROI) based approach, defining ROIs around regions of white matter reflecting the core of each tract (Catani & Thiebaut de Schotten, 2008; Rojkova et al. 2016). This allows for visualisation of all fibres of a single tract without constraining its cortical projections, which may vary from one subject to the other. Detailed description of the approach to tract dissection was performed as in previous studies (Howells et al. 2018; Catani et al. 2012). The premotor corticofugal tracts, three branches of the superior longitudinal fasciculus, the frontal aslant tract and fronto-striatal tracts were dissected. The U-shaped tracts connecting dorsal premotor hand regions (superior frontal gyrus (SFG), middle frontal gyrus (MFG) and precentral gyrus) were also mapped in both hemispheres in all patients, as their disruption by stimulation was hypothesised in a previous study using the same paradigm (Study 1; Vigano et al. 2019). For comparison the ventral U-shaped premotor tracts were dissected connecting the inferior frontal gyrus (IFG) and precentral gyrus (Catani et al. 2012). Tract density maps were exported in order to compare their overlap with stimulation sites, which count the number of streamlines traversing each voxel across the entire tract. The density map of the streamlines making up each tract in each patient was normalised using the robust range, to provide a standard index for comparison between tracts and patients using FSL tools.

3.5 *Estimating 'transient disconnection' of white matter tracts*

White matter atlas-based tools were used (Tractotron; Foulon et al. 2018) to identify likely white matter tracts to have been stimulated during the intraoperative procedure in all thirty-six patients. Following normalisation to a standard template, a 5mm sphere was centred on the coordinates of each effective site in all patients. This diameter was set in line with the proposed extent of stimulation of the bipolar probe (Haglund et al. 1993). This software provides an estimate of the probability that stimulation has 'disconnected' a certain tract, based on an atlas of white matter tracts generated from a healthy population of adults (Rojkova et al. 2016). The frequency that specific tracts were stimulated was assessed, as well as the likelihood that a given tract was stimulated in conjunction with others. Next, for the 15 patients in the tractography group, we compared each patient's stimulation site with the normalised tract density maps using the same Tractotron software (replacing its white matter atlas with each patient's normalised tract density maps). Streamlines are not a surrogate measure of

local axonal density (Jones et al. 2013), rather this provided an estimation of whether the stimulation had affected a core or peripheral portion of the tract (tract density is higher in the central portion of the tract). One sample t-tests were used to evaluate whether a tract was stimulated or not for each stimulation effect, using the normalised density measures. Independent t-tests were used to evaluate whether an effect was associated with one tract more than another.

3.6 Resection analysis

Patients motor ability was reported across all time points using clinical neurological examinations. Patients experiencing any immediate postoperative upper limb motor disturbance, ranging from hyposthenia to hemiplegia/SMA syndrome was classed as having a deficit. We compared the resections of this group with the rest of the sample using a region-of-interest based lesion symptom analysis to reduce dimensionality (Smith et al. 2013), limited to the right hemisphere using the AAL atlas, considering voxels resected in over 15% of patients (Puglisi et al. 2019). The results of this analysis showed, as a z-score, the statistical likelihood of resection of a given region predicting a decline in performance on a behavioural test. In the patients with tractography, the resection cavities were used as exclusion ROIs to calculate the percentage of streamlines remaining of each tract.

For detailed information on surgical procedure, MR and diffusion data acquisition and registration of intraoperative sites, see the General Material and Methods.

RESULTS

Patient demographics and characteristics are summarized in Table 1.

1 Effect of subcortical DES on ongoing hand movement

Across the whole sample, the right frontal lobe was mapped more than the left (priority is given to testing language in this hemisphere), with the highest common stimulated region (11 of 19 patients) within the deep white matter anterior to the precentral gyrus, extending along the precentral sulcus extending into more anterior frontal deep white matter, to incorporate both dorsal and ventral premotor regions (Fig. 2a). In the left hemisphere, the highest common overlap was in 5 of 16 patients and incorporated the same white matter region as the right hemisphere, but with lower sampling in ventral premotor regions sites (Fig. 2a).

Motor unit recruitment fell below the baseline epoch in all sites, which were distributed in subcortical white matter regions anterior to the precentral sulcus, running dorsomedial to ventrolateral in the right and left hemisphere (Fig. 2c). The mean RMS value of the three muscles across all stimulation sites (n=69) was normally distributed (Kolmogorov-Smirnov test: $d=0.1$, $p=0.20$), however changes to the movement pattern (mean aCC across sites) were not ($d=0.3$, $p<0.01$). Two main types of response were observed: complete hand arrest (aCC = 0; number of sites = 36; 52%), or 'clumsy movement' (aCC > 0; number of sites = 33; 48%) (Fig. 3a for EMG pattern examples and 3b for their distribution in a 3D MNI template). In the latter group, a linear correlation between RMS and aCC values was evident (Pearson $r=0.676$, $p=0.001$; Fig. 3c).

Comparing the anatomical distribution of the different sites based on the effect of DES on regularity of muscle activity using probability density estimation showed a correlation of these effects with different white matter sectors spatially distinct. Complete arrest-related sites were clustered within the dorsal white matter beneath the superior frontal sulcus and middle frontal gyrus, anterior to the precentral sulcus (Fig.

3d; LHem centre of mass: 66, 130, 115; RHem centre of mass: 116, 125, 115). while the clumsy-related sites clustered within more ventral white matter regions (LHem centre of mass: 61, 132, 99; RHem centre of mass: 121, 133, 105). In patients for which both effects could be recorded (n=14), arrest sites were always superior and medial to the clumsy effect.

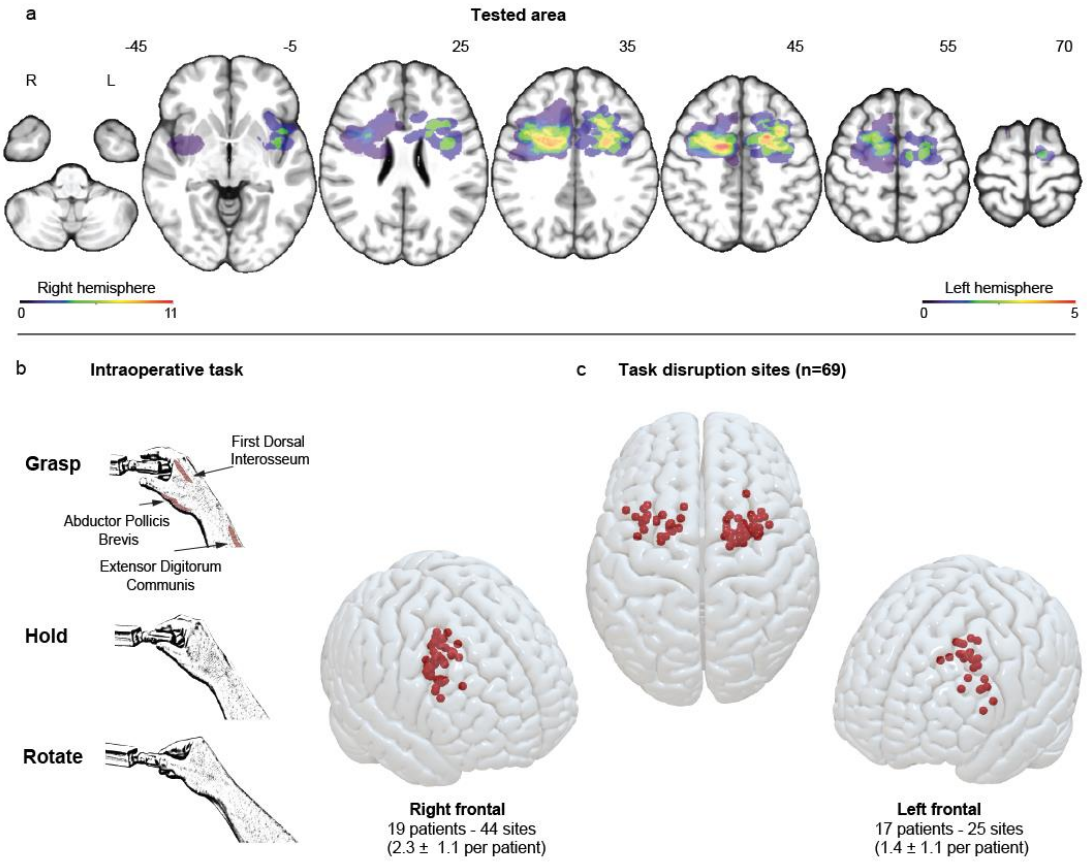

Fig. 2: Results of the intraoperative stimulation. (a) the common tested area in all patients in the frontal lobe, shown normalised to the MNI template on axial slices. The scales within the left and right hemisphere differ to better show the spatial distribution. (b) representation of the object manipulation tool used in the intraoperative setting. (c) the stimulation sites where motor unit recruitment (RMS) fell below the baseline during object manipulation. Reproduced from Howells & Viganò et al. (under review).

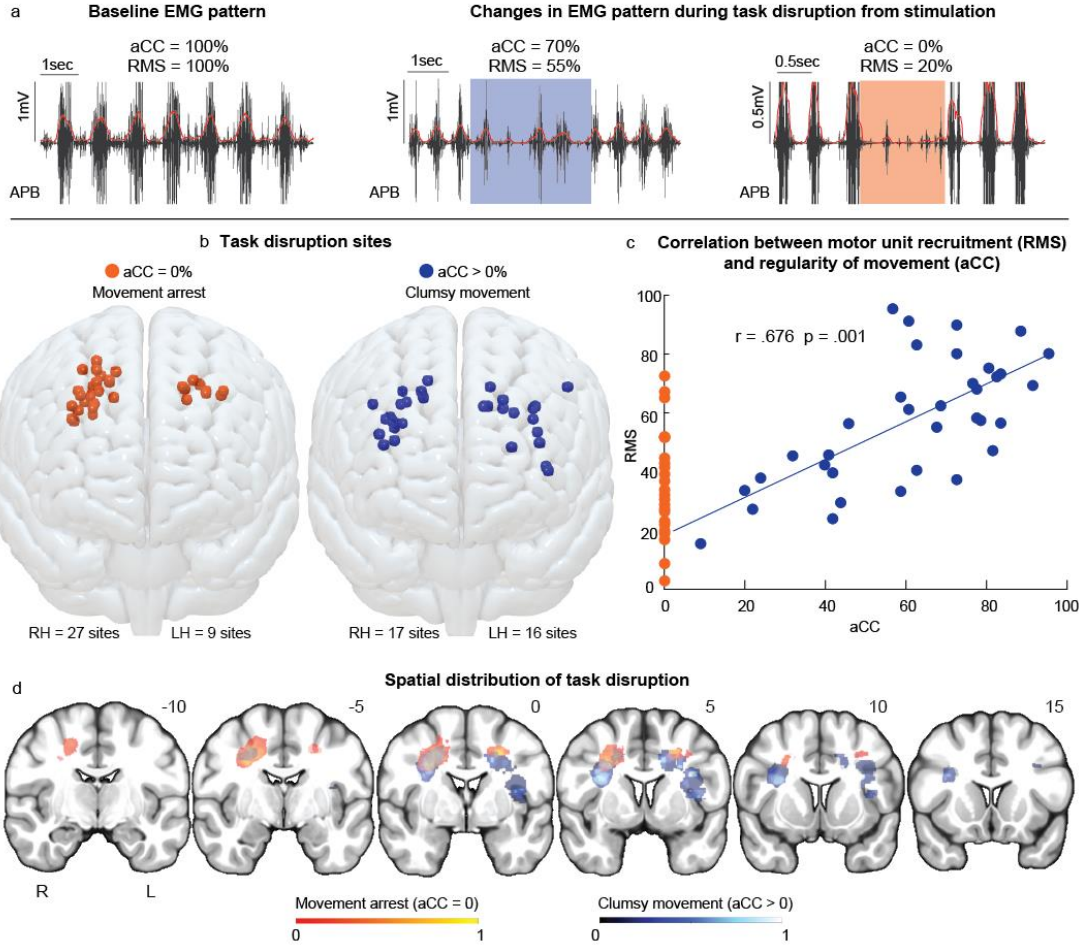

Fig. 3: Anatomical localisation of effect of DES on hand-object manipulation using EMG pattern analysis: (a) Abductor pollicis brevis activity (APB; raw signal in black, rectified signal in red) and corresponding RMS and aCC values of a baseline time period (left), and during two task disruption stimulations (middle and right panels show different EMG patterns reflecting task disruption). The normalized aCC reflect changes in movement regularity while the normalized RMS shows changes in motor unit recruitment in relation to the baseline (100 represents no change from baseline). (b) Distribution of negative sites based on aCC value (orange/blue) normalised to the MNI template.
(c) Scatterplot showing the association between aCC (x) and RMS (y). Sites were categorised either as movement arrest (aCC=0, orange) or 'clumsy' movement indicating a loss of regularity (aCC>0, blue).
(d) Probability map of likelihood of task disruption based on change in aCC value (orange/blue).
Reproduced from Howells & Viganò et al. (under review).

2 Stimulation of white matter tracts

A disconnectome analysis (Tractotron) was run using all sites in all patients to identify likely white matter tracts affected by stimulation to produce the two types of response (movement arrest vs clumsy movement). We considered only tracts for which there was over 50% probability that a stimulation site was within the trajectory of each white matter tract. These tracts included the three parieto-frontal branches of the superior longitudinal fasciculus, corticofugal fibres and fronto-striatal tracts, and the frontal aslant tract.

These connections were traced in the fifteen patients with diffusion tractography, in addition to local U-shaped connections. As the involvement of the corticospinal tract had been ruled out, only the corticofugal projections from the posterior superior frontal gyrus were traced. We compared these with the effective sites for these patients identified intraoperatively (1-4 effective sites per patient). Among the twenty-six sites recorded in this group, DES induced complete arrest (aCC=0) in 15 sites (4 left hemisphere, 11 right) and 'clumsy' movement (aCC>0) in 11 sites (5 left hemisphere, 6 right). Stimulation sites corresponded with one of the dissected tracts in all cases (Fig. 4). Notably in patients with more than one stimulation site, there was a dorsal-to-ventral distribution of sites showing lower to higher aCC values (Fig. 6). Due to the low sampling in the left hemisphere, and the similar functional effect in each hemisphere, we grouped both left and right hemisphere patients for this analysis.

We evaluated the frequency of stimulation of each tract to produce one of the two DES-induced movement outcomes (Fig. 4a). When considering stimulation of tracts extending from the superior frontal gyrus (including the SMA and pre-SMA), movement arrest sites were significantly associated with regions containing fibres of the corticofugal ($t(14)=3.6$, $p=0.003$), fronto-striatal ($t(14)=2.5$, $p=0.02$) and frontal aslant tracts ($t(14)=2.8$, $p=0.01$) in 60% or more patients. An independent t-test showed no significant difference in the type of effect observed for the frontal aslant tract which was also associated with stimulation sites where 'clumsy movements' were observed (60% of patients). There was a high degree of overlap of these tracts within stimulation sites (Fig. 4a).

We next considered parieto-frontal connections. Movement arrest was associated with stimulation of the superior (t(14)=2.6, p=0.02) and middle (t(14)=2.8, p=0.01) branches of the superior longitudinal fasciculus (SLF I and II) in over 60% of patients, but not with the clumsy movement effect. Clumsy movement was associated with stimulation of the inferior branch only, but not with movement arrest (SLF III; 80% of patients; (t(10)=3.9, p=0.003)). Stimulation sites corresponding with the SLF I were not associated simultaneously with the SLF II. Stimulation sites corresponding with the SLF III also commonly overlapped with ventral U-shaped fibres.

Stimulation of sites likely to affect the dorsal U-shaped tracts produced movement arrest only (90% of patients) but not clumsy movement (t(14)=8.3, p<0.0001). Ventral U-shaped tracts were not associated with stimulation sites producing either type of behavioural disruption. The dorsal U-shaped fibres were identified in sites with high probability to intersect the SLF I.

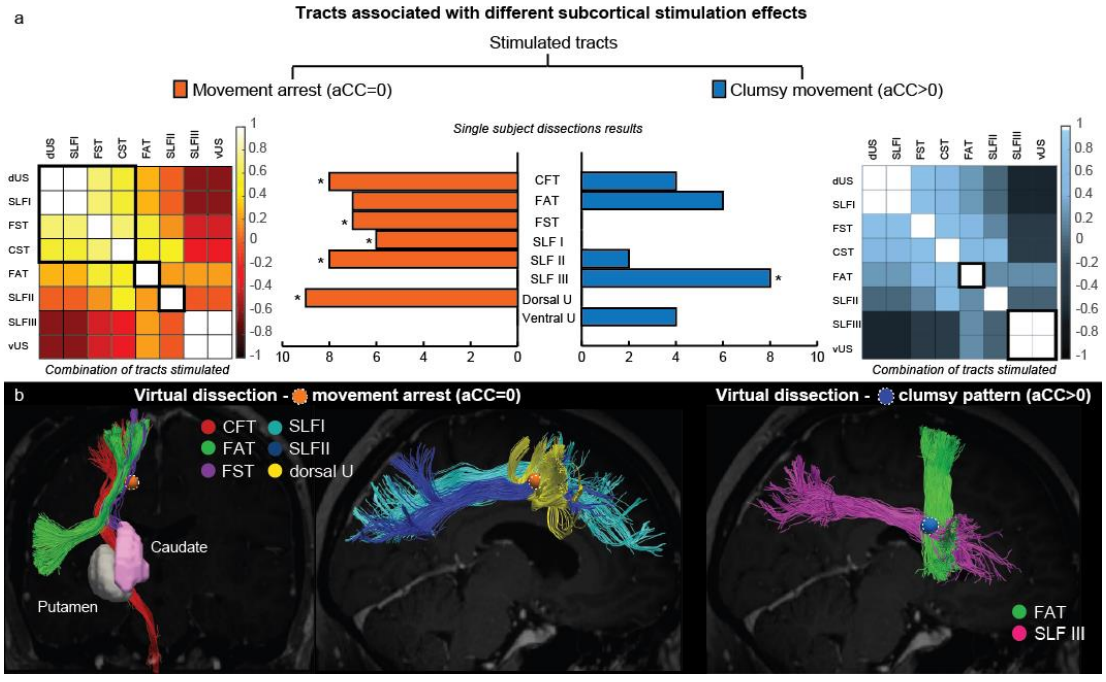

Fig. 4. The effect of stimulation on white matter: Using tractography dissections of eight tracts in 15 patients, we calculated (a) correlation matrices to show whether tracts were stimulated in common with others (scale indicates r^2 value) for the two types of movement pattern. The bar graphs indicate the number of patients for which a stimulation site corresponded with one of the eight tracts. The asterisks refer to the significance that a tract was associated with one movement pattern over another. Left and right hemisphere patients were grouped for this analysis. (b) Examples of stimulation sites for the different movement patterns. CFT: SMA-corticofugal projections; FAT: frontal aslant tract; FST: fronto-striatal tracts; SLF: superior longitudinal fasciculus; dorsal U: U-shaped fibres.

Reproduced from Howells & Viganò et al. (under review).

3 Impact of resection on hand motor ability

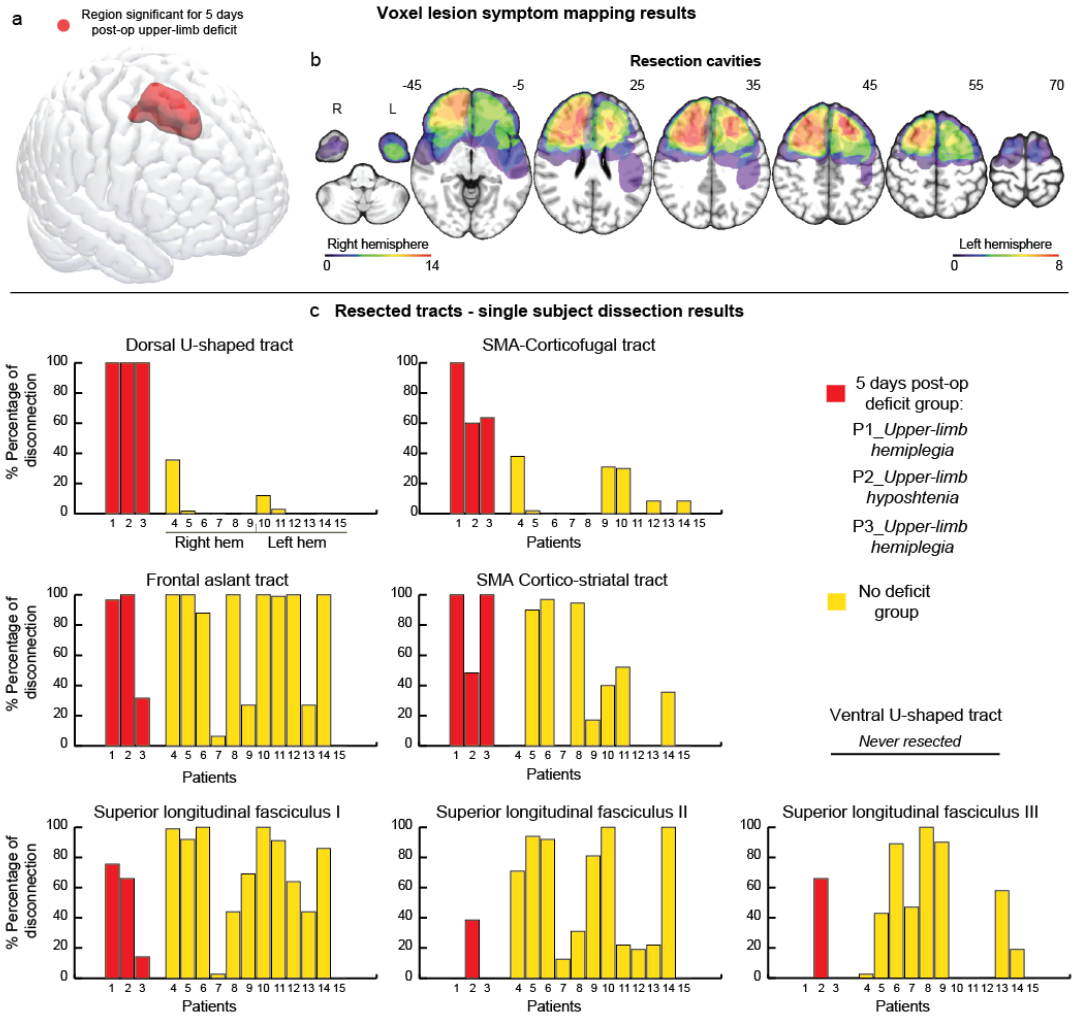

Fig. 5: (a) Lesion-symptom analysis in 35 patients showed that transient motor disturbance was associated with resection of the superior frontal gyrus, including the SMA. (b) the common resected area in all patients, shown on the MNI template on axial slices in the frontal lobe. (c) The percentage of streamlines disconnected by the neurosurgical procedure for each of the eight tracts in the 15 patients with tractography. Red shows the three patients with transient upper limb deficits (one with hyposthenia, two with hemiplegia). Reproduced from Howells & Viganò et al. (under review).

We evaluated the impact of resection of these tracts on postoperative motor ability in the entire sample (36 patients; Fig. 5). No patients experienced any permanent motor deficit following surgery. Twelve patients experienced transient motor disturbance reported at 5 days following the intervention which resolved by the one-month follow up (Table 1). ROI-based lesion symptom analysis showed these transient deficits were significantly associated with resection of the superior frontal gyrus only ($z=3.1$, $p<0.05$, 3000 permutations; Fig. 5a). We evaluated the impact of resection on the eight

studied tracts in the fifteen patients with tractography. In this group, three patients experienced transient motor disturbance, and in all these patients there was over 50% resection of fibres extending from the SMA, including those to the brainstem and basal ganglia, as well as the dorsal U-shaped fibres (Fig. 5c). Although we were underpowered for statistical analysis, our results indicated that the fronto-striatal, frontal aslant tract and branches of the superior longitudinal fasciculus were commonly resected without any motor disturbance (Fig. 5c and 6). The ventral U-shaped tracts were not resected in any patients.

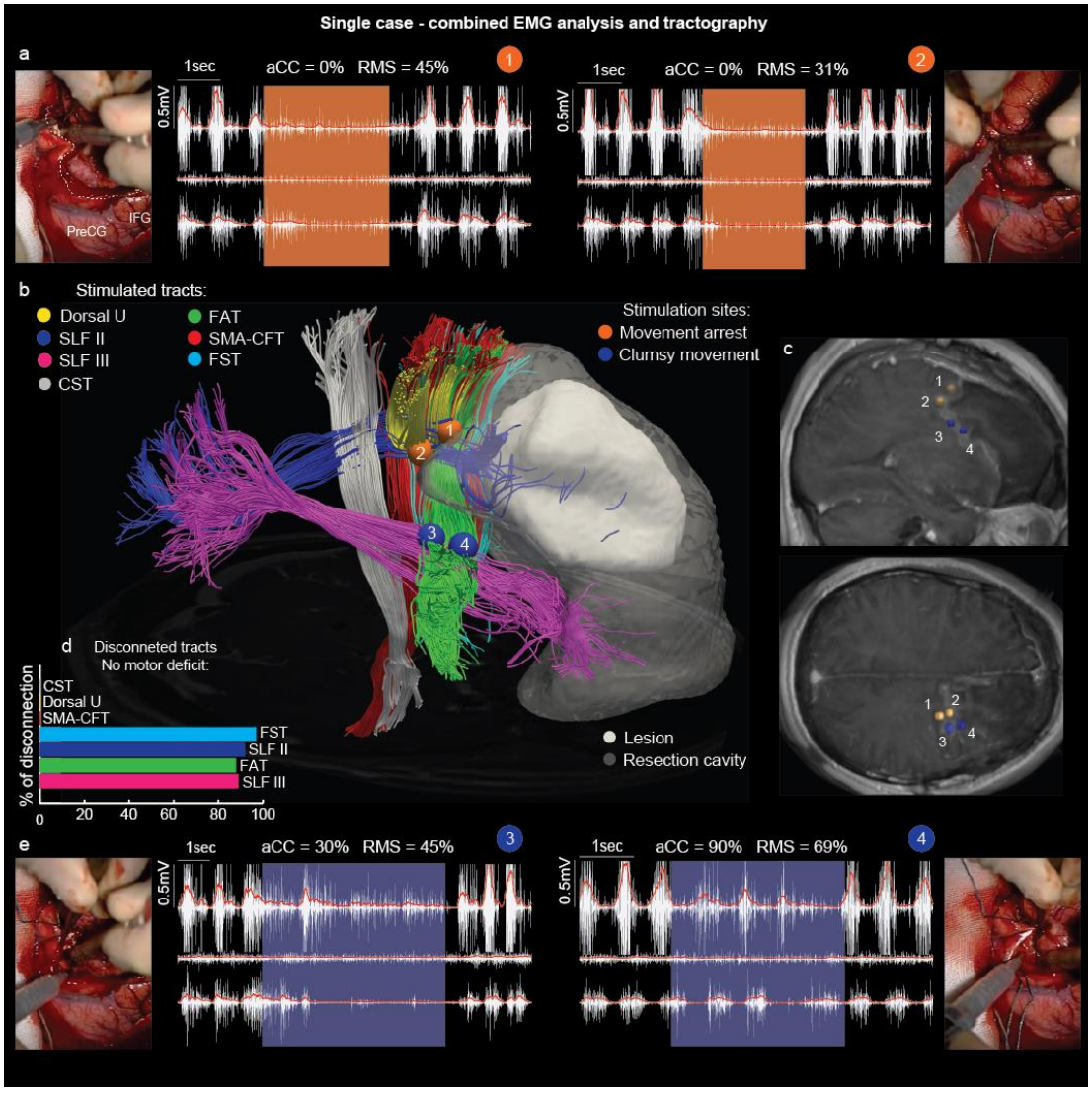

Fig. 6: Multiple effects on hand movement in a single patient who underwent surgery for a right temporo-insular anaplastic oligodendroglioma (grade III). (a,e) Screenshots from surgical video, taken during subcortical stimulation with bipolar probe. The corresponding EMG patterns are shown, with average muscle recruitment (RMS) and movement regularity (aCC) across the three muscles. These sites are shown relative to the (b) underlying white matter anatomy of the patient, traced using diffusion tractography. The resection cavity (c) is overlaid in (b), as well as a graph (d) showing which tracts were resected. Reproduced from Howells & Viganò et al. (under review).

DISCUSSION

The aim of this study was to investigate with a direct approach the role of different frontal white matter tracts in the motor control of hand movements for object manipulation. Subcortical white matter frontal regions were stimulated with DES during a repetitive 'screwing' action in the awake phase of neurosurgical procedures in thirty-six patients. Concurrent electromyographic recording of hand muscles enabled quantitative analysis of DES-induced changes in pattern of muscle activation. Disconnectome analysis and preoperative diffusion imaging tractography were used to evaluate white matter connections that were affected by DES. EMG analysis of movement patterns showed dissociable effects of DES that reflected stimulation along different white matter tracts. Hand movements were fully arrested when stimulating dorsomedial white matter at the crossroads of corticofugal, fronto-striatal, fronto-parietal and local U-shaped connections with the precentral gyrus, which may reflect direct motor loops involved in the final stages of motor programming. Resection of fibres in this region, especially the SMA-corticofugal tract and the dorsal U-shape connections as highlighted by single subject diffusion tractography results, also resulted in transient postoperative motor disturbance. Movement coordination was affected when the ventral fronto-parietal branch of the superior longitudinal fasciculus, connecting inferior frontal and parietal cortical regions, was stimulated. This provides support for the hypothesis that, akin to the macaque, sensorimotor transformation necessary for correct hand shaping is mediated by ventral fronto-parietal connections (Murata et al. 2000). Resection of these connections, however, was not correlated with post-operative motor disturbances. These results draw together anatomical, physiological and behavioural measures to causally identify white matter tracts involved in dissociable aspects of control of skilled hand movements for the first time in the human brain.

1 Dorsal premotor connections and movement control

One primary finding was that DES applied in dorsal premotor white matter beneath and anterior to the precentral sulcus caused movement arrest. Notably, stimulation in these sites did not increase muscle unit recruitment (a 'positive' motor effects) during task execution or when the hand was at rest, even when applying high frequency DES

and progressively increasing the current (until 15mA). This rules out the involvement of direct corticomotoneuronal fibres (Nossek et al. 2011; Raabe et al. 2014). The EMG pattern showed complete arrest of the phasic contractions across the three muscles required to perform the task. Our results showed DES caused this effect in subcortical regions of sets of connections extending from the superior frontal gyrus, which comprises the SMA complex (SMA and preSMA) as well as dorsal premotor cortex (BA6), areas associated with preparation of movement and action sequencing (Nachev 2008; Genon et al. 2018). In 15 patients out of 36, resection of these pathways caused transient 5 days post-operative deficit, ranging from hyposthenia to hemiplegia and SMA-syndrome (Table 1).

Diffusion tractography indicated that arrest occurred when stimulating the crossroads of dorsal long-range fibres, but also local U-shaped connections surrounding the superior frontal and precentral sulcus.

Connections between the superior frontal gyrus and brain stem via non-pyramidal corticospinal and other projection fibres seemed likely affected by DES (Wiesendanger, 1981; Dum & Strick, 1991; Porter & Lemon; 1993). Tractography is unfortunately unable to differentiate the terminations of streamlines within deep subcortical structures due to the convergence of fibres in the midbrain, however our results showed considerable corticofugal connectivity from the SMA region which was often disrupted by stimulation causing an abolishment of movement. In addition to non-pyramidal corticospinal fibres, stimulation of inhibitory corticoreticulospinal fibres running from premotor areas to the reticular formation may have disrupted motoneuronal activity at the level of the brain stem, causing arrest of ongoing movement, but some residual muscle activity (Rossi & Broadal, 1956; Kuypers, 1981). This system is involved in sensorimotor integration and movement preparation, and while usually associated with tone and position of proximal musculature (Buford & Davidson, 2004), has also been shown to influence distal muscles bilaterally (Lemon et al. 2008; Baker, 2011). Rubrospinal fibres are more commonly linked to control of fine movement in studies of macaques, however these are less prevalent in humans (Nathan & Smith, 1982). It is possible that these systems play an inhibitory role in hand motor control or play such a crucial role in computing features of movement that abrupt arrest of muscle coordination occurs when DES is applied. Future studies using

recording techniques at the level of the brain stem may be better able to evaluate the relative contributions of these different fibre populations.

Short-range U-shaped fibres connect the middle frontal gyrus (MFG) with SMA complex (SMA and preSMA) and hand-knob region of the precentral gyrus (Yousry, 1991). These superficial connections were first described using postmortem methods (Meynert, 1872; Rosett, 1933), but have more recently been indirectly visualised using diffusion tractography (Catani et al. 2012; Guevara et al. 2017; d'Albis et al. 2018). By providing direct communication between primary and secondary regions, these tracts are likely to be an essential component for the orchestration of hand movements (Mesulam, 1990). In Study 1, we showed that stimulation of precentral cortical terminations of these fibres produces arrest of movement using the same task, thus a comparable behavioural outcome occurs using both cortical and subcortical stimulation (Vigano et al. 2019). These fibres may reflect a final relay between movement programming and motor output conveyed by corticomotoneuronal fibres.

Our permanent disconnection results support the hypothesis that these two systems of connection (long range SMA-corticofugal fibres and short-range dorsal U-shaped fibres) play a crucial role in orchestrating the motor output. Resection of these tracts resulted in post-operative motor disturbance. Given their anatomical close correspondence, a future dedicated study with higher spatial resolution is requested to disentangle the functional role of these two projection systems.

The SMA complex forms also frontostriatal connections (FST), involved in the initiation and execution of movement, thus it is certainly plausible that arrest of movement caused by DES was correlated to the perturbation of this circuit (Hauber, 1998; Alexander & Crutcher, 1990). In the macaque, subcortical direct electrical stimulation of white matter superior to the dorsal striatum results in interruption of ongoing upper limb movement (Kitsikis, 1968). Dysfunction of basal ganglia structures can lead to a spectrum of motor syndromes in humans with either hypokinetic or hyperkinetic symptoms, both due to a disruption of appropriate modulation of movement (Delong, 1990). Previous intraoperative studies report 'negative' motor responses in response to DES in similar sites, grouping a spectrum

of disruption to ongoing upper limb movement, (Kinoshita et al. 2014; Schucht et al. 2013; Rech et al. 2017).

Finally, stimulation results indicated the Frontal Aslant Tract (FAT) as a candidate to cause, if stimulated, abrupt arrest of movement (in its dorsal portion) or clumsy movement (in its ventral portion) (e.g. Fig. 6). This tract was described recently using tractography (Oishi et al. 2008; Catani et al. 2012) and post-mortem dissection (Lawes et al. 2008; Vergani et al. 2014). It connects the superior and inferior frontal gyri and has been linked to movement kinematics (Catani et al. 2012; Budisavljevic et al. 2017). It is possible that when DES is applied subcortically, forward and backward propagation along the axon affects the cortical regions connected differently, producing distinct behavioural responses (Mandonnet et al. 2009). Alternatively, the different effects may rather reflect stimulation of other fibres in the same region, and the frontal aslant tract is not of relevance. Further studies are required to confirm this.

However, in our sample, resection results from the diffusion tractography group did not suggest a strict correlation with postoperative motor deficits and the disconnection of both the FST and the FAT.

2 Fronto-parietal tracts and motor control

Our results showed that when stimulating the white matter below the ventral premotor area, the phasic muscle contractions allowing a correct performance of the task decreased, without a full arrest of the movement. This 'clumsy' effect was identified in regions of white matter corresponding with the ventral branch of the superior longitudinal fasciculus (SLF III) and the frontal aslant tract. The SLFIII connects the supramarginal gyrus and intraparietal sulcus with inferior frontal regions (Makris et al. 2005) and is commonly regarded as the most likely homologue of the AIP-F5 circuit underlying grasp-related sensorimotor transformations in the macaque (Davare et al. 2006; Begliomini et al. 2007; Borra & Luppino, 2017). Although the precise cortical terminations of the homologous circuit in humans are still not clear due to differences in frontal lobe anatomy between human and monkey, an increase in functional connectivity has been reported between cortical regions connected by the SLF III when subjects grasped objects (Grol et al. 2007). Our results provide causal evidence for the

involvement of this tract in supporting complex hand configuration for object manipulation in humans. Total arrest of movement was never observed when stimulating this tract. In the macaque, inactivation of both AIP and F5 using muscimol results in similar disruption to hand shaping for grasping, while the execution of finger movements is preserved (Gallese et al. 1994; Fogassi et al. 2001). Disruption rather than arrest of movement during stimulation of this tract may suggest a transient disconnection of the sensorimotor transformation processes required for the appropriate hand configurations, as in the macaque (Rizzolatti et al. 2014). Notably, in a previous study using the same intraoperative technique we demonstrated that both an arrest and a clumsy pattern occurred when stimulating a sector of ventral premotor cortex just posterior to the subcortical area identified in this study (Fornia et al. 2019). The present results might suggest the cortical and subcortical responses to be related to the same SLFIII branches, however at different anatomical levels.

Considering the dorsal fronto-parietal pathways connecting the posterior parietal lobe and superior and middle frontal gyrus, stimulation results (Fig. 4) suggested the involvement of the superior and middle branches of the superior longitudinal fasciculus (SLF I and II) (Thiebaut de Schotten et al. 2012). These tracts are theorised to mediate visually guided online control of reaching and grasping movements (Goodale & Milner, 1992; Tarantino et al. 2014; Budisavljevic et al. 2016; Howells et al. 2018). In our stimulation sample, DES applied to SLFI and II resulted in arrest of movement.

However, our results also showed that while they may have been stimulated, all three branches of the SLF were commonly resected without any evident gross motor disturbance. We did not specifically test visually guided grasping in our cohort however we have previously demonstrated that resection of these tracts produces subtle changes in motor behaviour rather than any fine motor deficit per se (Howells et al., under review). This may be related to the bilateral role of these tracts in visually guided movement (Sainburg et al. 2002).

3 Limitations

Some limitations of our study warrant discussion. The intraoperative setting, while providing a unique opportunity for studying the role of tracts, cannot be perfectly controlled akin to those used to study mechanisms in non-human primates. Further, the volume of the tested white matter area is planned solely according to the clinical needs, and the other cognitive tests performed to preserve patient's integrity. Although we report similar results in both hemispheres, we are unable to comment on hemispheric differences, given that patients are tested in one hemisphere only and the left side was less tested (Fig. 2) because in that hemisphere predominant is the testing of language functions. However no hemispherical differences emerged from our results, the existence of specific pattern of neural activations for graping movements depending on handedness is suggested in literature (Begliomini et al. 2008). The task we used, resembling a 'grasping in the dark' and relying only on haptic feedback, is not suitable to explore the left and right hemisphere specializations, visually-guided and haptic-guided movements respectively (Stone et al. 2015). In order to provide a more accurate dissociation between white matter tracts relying on different DES-related hand movement disruption, a future dedicated task introducing a reaching phase and an online visual monitoring of the action is needed. This could allow to test the specialization of fronto-parietal circuits for visuomotor transformation for reaching and grasping, disentangling their role from different projectional systems. Finally, current understanding of the precise physiological mechanisms of DES is also still relatively limited (Borchers, 2012).

REFERENCES

Baker, S. N. (2011, December). The primate reticulospinal tract, hand function and functional recovery. Journal of Physiology, Vol. 589, pp. 5603–5612.

Begliomini, C., Nelini, C., Caria, A., Grodd, W., Castiello, U., 2008. Cortical activations in humans grasp-related areas depend on hand used and handedness. PLoS One 3, e3388.

Begliomini, C., De Sanctis, T., Marangon, M., Tarantino, V., Sartori, L., Miotto, D., Motta R, Stramare R, Castiello, U. (2014). An investigation of the neural circuits underlying reaching and reach-to-grasp movements: From planning to execution. Frontiers in Human Neuroscience, 8: 676.

Bello L, Riva M, Fava E, Ferpozzi V, Castellano A, Raneri F, Pessina F, Bizzi A, Falini A, Cerri G. 2014. Tailoring neurophysiological strategies with clinical context enhances resection and safety and expands indications in gliomas involving motor pathways. Neuro Oncol. 16:1110-1128.

Binkofski, F., Buccino, G., Stephan, K. M., Rizzolatti, G., Seitz, R. J., & Freund, H. J. (1999). A parieto-premotor network for object manipulation: evidence from neuroimaging. Experimental Brain Research, 128(1–2), 210–213.

Borchers, S., Himmelbach, M., Logothetis, N., & Karnath, H. O. (2012, January). Direct electrical stimulation of human cortex-the gold standard for mapping brain functions? Nature Reviews Neuroscience, Vol. 13, pp. 63–70.

Borra, E., Gerbella, M., Rozzi, S., & Luppino, G. (2017). The macaque lateral grasping network: A neural substrate for generating purposeful hand actions. Neuroscience and Biobehavioral Reviews, 75, 65–90.

Borra, E., & Luppino, G. (2017, December 1). Functional anatomy of the macaque temporo-parieto-frontal connectivity. Cortex, Vol. 97, pp. 306–326.

Brandi, M.-L., Wohlschläger, A., Sorg, C., & Hermsdörfer, J. (2014). The neural correlates of planning and executing actual tool use. The Journal of Neuroscience: The Official Journal of the Society for Neuroscience, 34(39), 13183–13194.

Budisavljevic, S., Dell'Acqua, F., Zanatto, D., Begliomini, C., Miotto, D., Motta, R., & Castiello, U. (2016). Asymmetry and Structure of the Fronto-Parietal Networks Underlie Visuomotor Processing in Humans. Cerebral Cortex (New York, N.Y. : 1991), 27(2), 1532–1544.

Budisavljevic S, Dell'Acqua F, Djordjilovic V, Miotto D, Motta R4, Castiello U. (2017). The role of the frontal aslant tract and premotor connections in visually guided hand movements. Neuroimage. 146:419-428.

Buford, J. A., & Davidson, A. G. (2004). Movement-related and preparatory activity in the reticulospinal system of the monkey. Experimental Brain Research, 159(3), 284–300.

Catani M, Dell'acqua F, Vergani F, Malik F, Hodge H, Roy P, Valabregue R, Thiebaut de Schotten M. 2012. Short frontal lobe connections of the human brain. Cortex. 48(2):273-91.

Catani, M., & Thiebaut de Schotten, M. (2012). Atlas of Human Brain Connections.

Cavina-Pratesi, C., Monaco, S., Fattori, P., Galletti, C., McAdam, T. D., Quinlan, D. J., Goodale MA, Culham JC. (2010). Functional magnetic resonance imaging reveals the neural substrates of arm

transport and grip formation in reach-to-grasp actions in humans. Journal of Neuroscience, 30(31), 10306–10323.

Croxson, P. L., Johansen-Berg, H., Behrens, T. E. J., Robson, M. D., Pinsk, M. A., Gross, C. G., Richter W, Richter MC, Kastner S, Rushworth MF. (2005). Quantitative investigation of connections of the prefrontal cortex in the human and macaque using probabilistic diffusion tractography. Journal of Neuroscience, 25(39), 8854–8866.

d'Albis, M.-A., Guevara, P., Guevara, M., Laidi, C., Boisgontier, J., Sarrazin, S., Duclap D, Delorme R, Bolognani F, Czech , Bouquet C9, Ly-Le Moal M, Holiga S, Amestoy A, Scheid I, Gaman A, Leboyer M, Poupon C, Mangin JF, Houenou J. (2018). Local structural connectivity is associated with social cognition in autism spectrum disorder. Brain : A Journal of Neurology, 141(12), 3472–3481. https://doi.org/10.1093/brain/awy275

Davare, M., Andres, M., Cosnard, G., Thonnard, J.-L., & Olivier, E. (2006). Dissociating the role of ventral and dorsal premotor cortex in precision grasping. The Journal of Neuroscience : The Official Journal of the Society for Neuroscience, 26(8), 2260–2268.

DeLong, M. R. (1990). Primate models of movement disorders of basal ganglia origin. Trends in Neurosciences, Vol. 13, pp. 281–285.

Dum, R. P., & Strick, P. L. (1991). The origin of corticospinal projections from the premotor areas in the frontal lobe. The Journal of Neuroscience : The Official Journal of the Society for Neuroscience, 11(3), 667–689.

Ehrsson, H. H., Fagergren, A., Jonsson, T., Westling, G., Johansson, R. S., & Forssberg, H. (2000). Cortical activity in precision- versus power-grip tasks: An fMRI study. Journal of Neurophysiology, 83(1), 528–536.

Fogassi L, Gallese V, Buccino G, Craighero L, Fadiga L, Rizzolatti G. 2001. Cortical mechanism for the visual guidance of hand grasping movements in the monkey: A reversible inactivation study. Brain. 124(Pt 3):571-86.

Fornia, L., Rossi, M., Rabuffetti, M., Leonetti, A., Puglisi, G., Viganò, L., Simone L, Howells H, Bellacicca A, Bello L, Cerri, G. (2019). Direct Electrical Stimulation of Premotor Areas: Different Effects on Hand Muscle Activity during Object Manipulation. Cerebral Cortex.

Foulon, C., Cerliani, L., Kinkingnéhun, S., Levy, R., Rosso, C., Urbanski, M., Volle E, de Schotten, M. T. (2018). Advanced lesion symptom mapping analyses and implementation as BCBtoolkit. GigaScience, Vol. 7, pp. 1–17.

Gallese, V., Murata, A., Kaseda, M., Niki, N., & Sakata, H. (1994). Deficit of hand preshaping after muscimol injection in monkey parietal cortex. NeuroReport, 5(12), 1525–1529.

Genon, S., Reid, A., Li, H., Fan, L., Müller, V. I., Cieslik, E. C., Hoffstaedter F, Langner R, Grefkes C, Laird A, Fox PT8, Jiang T, Amunts K, Eickhoff, S. B. (2018). The heterogeneity of the left dorsal premotor cortex evidenced by multimodal connectivity-based parcellation and functional characterization. NeuroImage, 170, 400–411.

Goodale, M. A., & Milner, A. D. (1992). Separate visual pathways for perception and action. Trends in Neurosciences, Vol. 15, pp. 20–25.

Grol, M. J., Majdandzić, J., Stephan, K. E., Verhagen, L., Dijkerman, H. C., Bekkering, H., Verstraten FA, Toni, I. (2007). Parieto-frontal connectivity during visually guided grasping. The Journal of Neuroscience : The Official Journal of the Society for Neuroscience, 27(44), 11877–11887.

Guevara, M., Román, C., Houenou, J., Duclap, D., Poupon, C., Mangin, J. F., & Guevara, P. (2017). Reproducibility of superficial white matter tracts using diffusion-weighted imaging tractography. NeuroImage, 147, 703–725.

Haglund, M. M., Ojemann, G. A., & Blasdel, G. G. (1993). Optical imaging of bipolar cortical stimulation. Journal of Neurosurgery, 78(5), 785–793.

Hauber, W. (1998, December). Involvement of basal ganglia transmitter systems in movement initiation. Progress in Neurobiology, Vol. 56, pp. 507–540.

Hoshi, E., & Tanji, J. (2007). Distinctions between dorsal and ventral premotor areas: anatomical connectivity and functional properties. Current Opinion in Neurobiology, 17(2), 234–242.

Howells H, Thiebaut de Schotten M, Dell'Acqua F, Beyh A, Zappalà G, Leslie A, Simmons A, Murphy DG, Catani M. 2018. Frontoparietal tracts linked to lateralized hand preference and manual specialization. Cereb Cortex. 28(7):2482-2494.

Ius, T., Angelini, E., Thiebaut de Schotten, M., Mandonnet, E., & Duffau, H. (2011). Evidence for potentials and limitations of brain plasticity using an atlas of functional resectability of WHO grade II gliomas: Towards a "minimal common brain." NeuroImage, 56(3), 992–1000.

Jones, D. K., Knösche, T. R., & Turner, R. (2013, June). White matter integrity, fiber count, and other fallacies: The do's and don'ts of diffusion MRI. NeuroImage, Vol. 73, pp. 239–254.

Kinoshita, M., de Champfleur, N. M., Deverdun, J., Moritz-Gasser, S., Herbet, G., & Duffau, H. (2015). Role of fronto-striatal tract and frontal aslant tract in movement and speech: an axonal mapping study. Brain Structure and Function, 220(6), 3399–3412.

Kitsikis, A. (1968). The suppression of arm movements in monkeys: threshold variations of caudate nucleus stimulation. Brain Research, 10(3), 460–462.

Kuypers, H. (1981) Anatomy of the descending pathways. In: Brooks, V., Ed., The Nervous System, Handbook of Physiology, Vol. 2, Williams and Wilkins, Baltimore, 597-666.

Lawes, I. N. C., Barrick, T. R., Murugam, V., Spierings, N., Evans, D. R., Song, M., & Clark, C. A. (2008). Atlas-based segmentation of white matter tracts of the human brain using diffusion tensor tractography and comparison with classical dissection. NeuroImage, 39(1), 62–79.

Lemon RN, 2008. Descending pathways in motor control. Annu Rev Neurosci. 31:195-218. doi: 10.1146/annurev.neuro.31.060407.125547.

Lüders, H. O., Dinner, D. S., Morris, H. H., Wyllie, E., & Comair, Y. G. (1995). Cortical electrical stimulation in humans. The negative motor areas. Advances in Neurology, Vol. 67, pp. 115–129.

Luppino, G., Murata, A., Govoni, P., & Matelli, M. (1999). Largely segregated parietofrontal connections linking rostral intraparietal cortex (areas AIP and VIP) and the ventral premotor cortex (areas F5 and F4). Experimental Brain Research, 128(1–2), 181–187.

Makris, N., Kennedy, D. N., McInerney, S., Sorensen, A. G., Wang, R., Caviness, V. S., & Pandya, D. N. (2005). Segmentation of subcomponents within the superior longitudinal fascicle in humans: a quantitative, in vivo, DT-MRI study. Cerebral Cortex (New York, N.Y. : 1991), 15(6), 854–869.

Meynert T, Putnam J (translated) (1872) The brain of mammals. In: Stricker S (ed) A Man. Histol. W. Wood & company, New York, pp 650–766

Murata, A., Gallese, V., Luppino, G., Kaseda, M., & Sakata, H. (2000). Selectivity for the shape, size, and orientation of objects for grasping in neurons of monkey parietal area AIP. Journal of Neurophysiology, 83(5), 2580–2601.

Nathan, P. W., & Smith, M. C. (1982). The rubrospinal and central tegmental tracts in man. Brain : A Journal of Neurology, 105(Pt 2), 223–269.

Nelissen, K., & Vanduffel, W. (2011). Grasping-related functional magnetic resonance imaging brain responses in the macaque monkey. The Journal of Neuroscience : The Official Journal of the Society for Neuroscience, 31(22), 8220–8229.

Nelson-Wong, E., Howarth, S., Winter, D. A., & Callaghan, J. P. (2009). Application of autocorrelation and cross-correlation analyses in human movement and rehabilitation research. The Journal of Orthopaedic and Sports Physical Therapy, 39(4), 287–295.

Nossek, E., Korn, A., Shahar, T., Kanner, A. A., Yaffe, H., Marcovici, D., Ben-Harosh C, Ben Ami H, Weinstein M, Shapira-Lichter I, Constantini S, Hendler T, Ram, Z. (2011). Intraoperative mapping and monitoring of the corticospinal tracts with neurophysiological assessment and 3-dimensional ultrasonography-based navigation. Clinical article. Journal of Neurosurgery, 114(3), 738–746.

Penfield, W., & Boldrey, E. (1937). Somatic motor and sensory representation in the cerebral cortex of man as studied by electrical stimulation. Brain, 60(4), 389–443.

Porter R, Lemon R. 1993. Corticospinal function and voluntary movement. Oxford, UK: Oxford Science.

Puglisi, G., Howells, H., Leonetti, A., Fornia, L., Bellacicca, A., Viganò, L., Simone L., Catani M, Cerri G, Bello L. (2019). Frontal pathways in cognitive control: direct evidence from intraoperative stimulation and diffusion tractography. Brain : A Journal of Neurology, 142(8), 2451–2465.

Raabe, A., Beck, J., Schucht, P., & Seidel, K. (2014). Continuous dynamic mapping of the corticospinal tract during surgery of motor eloquent brain tumors: evaluation of a new method. Journal of Neurosurgery, 120(5), 1015–1024.

Rizzolatti G, Cattaneo L, Fabbri-Destro M, Rozzi S. 2014. Cortical mechanisms underlying the organization of goal-directed actions and mirror neuron-based action understanding. Physiol Rev. 94(2):655-706.

Rech, F., Duffau, H., Pinelli, C., Masson, A., Roublot, P., Billy-Jacques, A., Brissart H, Civit, T. (2017). Intraoperative identification of the negative motor network during awake surgery to prevent deficit following brain resection in premotor regions. Neuro-Chirurgie, 63(3), 235–242.

Rojkova, K., Volle, E., Urbanski, M., Humbert, F., Dell'Acqua, F., & Thiebaut de Schotten, M. (2016). Atlasing the frontal lobe connections and their variability due to age and education: a spherical deconvolution tractography study. Brain Structure & Function, 221(3), 1751–1766.

Rosett J. 1933. Intercortical Systems of the Human Cerebrum. Columbia University Press, New York.

Rossi, G. F., & Brodal, A. (1956). Corticofugal fibres to the brain-stem reticular formation; an experimental study in the cat. Journal of Anatomy, 90(1), 42–62.

Rossi M, Fornia L, Puglisi G, Leonetti A, Zuccon G, Fava E, Milani D, Casarotti A, Riva M, Pessina F, Cerri G, Bello L. 2018. Assessment of the praxis circuit in glioma surgery to reduce the incidence of postoperative and long-term apraxia: a new intraoperative test. J Neurosurg. 23:1-11

Rossi, M., Sani, S., Nibali, M. C., Fornia, L., Bello, L., & Byrne, R. W. (2019, January 1). Mapping in Low-Grade Glioma Surgery: Low- and High-Frequency Stimulation. Neurosurgery Clinics of North America, Vol. 30, pp. 55–63.

Schucht, P., Moritz-Gasser, S., Herbet, G., Raabe, A., & Duffau, H. (2013). Subcortical electrostimulation to identify network subserving motor control. Human Brain Mapping, 34(11), 3023–3030.

Smith, D. V, Clithero, J. A., Rorden, C., & Karnath, H.-O. (2013). Decoding the anatomical network of spatial attention. Proceedings of the National Academy of Sciences of the United States of America, 110(4), 1518–1523.

Stone, K.D., Gonzalez, C.L.R., 2015. The contributions of vision and haptics to reaching and grasping. Front. Psychol. 6, 1–18.

Tarantino, V., De Sanctis, T., Straulino, E., Begliomini, C., & Castiello, U. (2014). Object size modulates fronto-parietal activity during reaching movements. The European Journal of Neuroscience, 39(9), 1528–1537.

Thiebaut de Schotten, M., Dell'Acqua, F., Valabregue, R., & Catani, M. (2012). Monkey to human comparative anatomy of the frontal lobe association tracts. Cortex, 48(1), 82–96.

Thompson A, Murphy D, Dell'Acqua F, Ecker C, McAlonan G, Howells H, Baron-Cohen S, Lai MC, Lombardo MV; MRC AIMS Consortium, and Marco Catani. 2017. Impaired communication between the motor and somatosensory homunculus is associated with poor manual dexterity in autism spectrum disorder. Biol Psychiatry. 81(3):211-219.

Thura, D., & Cisek, P. (2014). Deliberation and commitment in the premotor and primary motor cortex during dynamic decision making. Neuron, 81(6), 1401–1416.

Vergani, F., Lacerda, L., Martino, J., Attems, J., Morris, C., Mitchell, P., … Dell'Acqua, F. (2014). White matter connections of the supplementary motor area in humans. Journal of Neurology, Neurosurgery, and Psychiatry, 85(12), 1377–1385.

Viganò L, Fornia L, Rossi M, Howells H, Leonetti A, Puglisi G, Conti Nibali M, Bellacicca A, Grimaldi M, Bello L, Cerri G. 2019. Anatomo-functional characterisation of the human "hand-knob": A direct electrophysiological study. Cortex. 113:239-254

Wiesendanger, M. (2011). Organization of Secondary Motor Areas of Cerebral Cortex. In Comprehensive Physiology.

Yousry, T. A., Schmid, U. D., Alkadhi, H., Schmidt, D., Peraud, A., Buettner, A., & Winkler, P. (1997). Localization of the motor hand area to a knob on the precentral gyrus. A new landmark. Brain, 120(1), 141–157.

CONCLUSIONS

This PhD thesis has reported the results of three original studies conducted in the Neurosurgical Oncology Unit (Prof. Bello) and the MOtor, Cognition and Action Laboratory (MOCA lab, Prof. Cerri). The focus of the project was to combine neurophysiological, anatomical and lesion analysis to study the organisation of frontal networks shaping sensorimotor programming which allows skilled hand movements, not yet causally characterised in the human. We provided novel data to describe this connectional system, which, besides the direct clinical impact on glioma surgery involving motor pathways, where it is crucial to extend the resection beyond its boundaries while preserving patient's integrity, also has a critical translational impact within the context of EDEN2020 project. EDEN2020 is aimed at engineering a steerable catheter for diagnostics and treatment, in that the trajectory can be tailored and intra-operatively modified to preserve selected tissue. This requires an appropriate anatomo-functional frame of frontal eloquent structures for skilled hand movements, feeding the planned computations with this structural information, thus avoiding the possibility of post-operative deficits.

The first study presented has investigated, in 17 patients, the functional organization of the human hand-knob area in the rostro-caudal direction, using a direct electrophysiological approach. A gradient of cortical excitability along this axis emerged, with the caudal hand-knob being the most excitable sector, based on quantitative analysis of motor output elicited with high frequency stimulation. The analysis of this specific pattern of interference, caused by stimulating two sectors during an object manipulation task, further suggested a possible functional subdivision: while the caudal region may host muscle representations used for the transmission of the motor command to the spinal motoneurons, the rostral sector may represent a crucial area for shaping functional synergies for hand-object interaction. Finally, different patterns of local connectivity between the rostral and caudal sectors with adjacent areas were observed: U-shaped fibres originating from the caudal portion project to the primary somatosensory area in the post-central gyrus while sets of U-shape fibres connect the rostral sector with the caudal-most districts of the superior and middle frontal gyri. Overall, the anatomo-functional distinction suggested by our

results could reflect either the distinction between the new and the old M1, resembling the monkey architecture, or the existence of a transitional cortical area between M1 and caudal dorsal premotor cortex.

The second study, beyond proving the feasibility of resection in general anaesthesia of lesions harbouring within M1 and its descending fibres, demonstrated how essential it is to tailor neurophysiological mapping according to clinical conditions to obtain the best extent of resection without long-term post-operative motor deficits. Of the sample analysed (102 patients), it was possible to obtain a complete resection in 85.3% of cases, with only 2% experiencing permanent morbidity. High frequency stimulation was proved to be the most reliable and versatile mapping paradigm, allowing the identification of cortical and subcortical motor thresholds in all clinical conditions. The "reduced approach" results were relevant in the context of this PhD project: this paradigm consisted in reducing the number of pulses when stimulations with the train of 5 pulses (To5) were not focal. This did not allow the definition of a clear motor map and recognition of cortico-motoneuronal fibres, preventing an optimal extent for the resection and their preservation. The cortical and subcortical motor map observed when defining the motor thresholds with this paradigm confirmed the rostro-caudal gradient of excitability demonstrated on the hand-knob region in Study 1: lower motor thresholds were always found moving posterior, approaching the central sulcus, thus the rostral sector can be indeed considered a safe point of entry for surgery and for catheters.

Since the monkey literature had consistently proved that higher excitability correlated with a direct access to motoneurons in the spinal cord, we here speculate that cells located close to the human central sulcus and their projections may give rise to monosynaptic connection with motoneurons in the spinal cord and thus it would be mandatory to preserve them in surgical practice. To avoid permanent morbidity, catheter insertion and drug delivery along the corticospinal tract should consider the anatomo-functional rostro-caudal gradient demonstrated in Study 1 and 2.

In the last study presented in the project (Study 3) we analysed the EMG pattern of hand muscles during the application of DES on white matter frontal pathways during the intraoperative realization of the object manipulation task, and we correlated the

patterns of interferences with specific tracts by means of diffusion tractography. Stimulation of dorsal and ventral premotor regions resulted in dissociable effects: complete arrest of phasic muscle contractions and clumsy movement respectively. This finding could reflect a functional distinction between dorsal premotor white matter, possibly involved in the control of final stages of movement programming before sending output to corticomotoneuronal cells, and ventral white matter premotor pathways, more devoted to compute sensorimotor transformation useful for proper hand shaping. Coupling the stimulation data with the resection cavities analysis, which offers the possibility to evaluate the correlation between post-operative outcome and the permanent disconnection of tracts, we suggested that the SMA-corticofugal tract and the dorsal U-shaped connection between M1 and the superior frontal gyrus play a fundamental role in shaping motor outcome. Their stimulation during the object manipulation task resulted in a complete abolishment of movement and their disconnection resulted in transient 5-day postoperative upper-limb deficit. Resection of all the other studied tracts did not correlate with any postoperative motor disturbances.

The absence of visual-motonitoring of the hand and the object and the lack of a transport phase toward the target makes challenging to incorporate our results in the monkey and human neural correlate of grasping models which account for these aspects (Turella and Lignau 2014; Borra et al. 2017). The ‘prehension system’ was dychotomized in a dorso-dorsal pathway, connecting mainly the medial intraparietal sulcus (MIP) and area V6A with area F7 and F2 (dPM), and a ventro-dorsal stream connecting the anterior intraparietal ares (AIP and PFG) with F5 (vPM) (Rizzolatti and Matelli, 2003). While the first was traditionally associated with the visuo-motor control of reaching (i.e. the transport phase in the space to the target object), the latter one was thought to be specialized in the visuo-motor coding of grasping, computing the instrinc features of the object such as the size and the shape (Jeannerod et al. 1995; Caminiti et al. 1998; Culham et al. 2003; Brochier and Umiltà, 2006). The independent coding of reaching and grasping in separate anatomo-functional modules is challenged by growing evidences, reaveling how both components are represented in an extended fronto-parietal circuit (Fattori et al. 2010; Battaglie-Meyer et al. 2006; Nelissen et al. 2017; Takahashi et al. 2017; Cavina-Pratesi et al. 2018). In Study 1 and in a previous

paper of our group (Fornia et al. 2019) we demonstrated how grasping abilities are causally impaired when stimulation is applied on the rostral convexity of the hand-knob and the ventro-caudal sector of dPM, with a mixed effect of suppression and excitation of distal muscles. What we found seems coherent with the electrophysiological data showed by Raos et al. (2003; 2004): dPM (F2) is responsible for the coding of grasping-related informations and hosts distal muscle represention. Moreover, showing how grasping execution is compromised both stimulating dorsal and ventral premotor white matter pathways (Study 3), we support that grasping computations significantly rely also on the medial aspect of frontal premotor regions.

Finally we disclosed, for the first time in the human, anatomo-functional distinctions existing within the frontal white matter premotor pathways involved in the orchestration of hand skilled movements, and evaluated their effects on hand ability after resection. We thus provided a topographical frame crucial in establishing the functional borders of resections as well as the trajectory and the final positioning of steerable catheters.

REFERENCES

Battaglia-Mayer, A., Archambault, P. S., and Caminiti, R. (2006). The cortical network for eye-hand coordination and its relevance to understanding motor disorders of parietal patients. Neuropsychologia 44, 2607–2620.

Borra E, Gerbella M, Rozzi S, Luppino G. 2017. The macaque lateral grasping network: a neural substrate for generating purposeful hand actions. Neurosci Biobehav Rev. 75:65-90.

Brochier, T., and Umiltà, M. A. (2007). Cortical control of grasp in non-human primates. Curr. Opin. Neurobiol. 17, 637–643.

Caminiti, R., Ferraina, S., and Mayer, A. (1998). Visuomotor transformations: early cortical mechanisms of reaching. Curr. Opin. Neurobiol. 8, 753–761.

Cavina-Pratesi C, Connolly JD, Monaco S, Figley TD, Milner AD, Schenk T, Culham JC. 2018. Human neuroimaging reveals the subcomponents of grasping, reaching and pointing actions. Cortex. 98:128–148.

Fattori P, Raos V, Breviglieri R, Bosco A, Marzocchi N, Galletti C (2010) The dorsomedial pathway is not just for reaching: graping neurons in the medial parieto-occipital cortex of the macaque monkeys. J Neurosci 30:342–349.

Fornia, L., Rossi, M., Rabuffetti, M., Leonetti, A., Puglisi, G., Viganò, L., Simone L, Howells H, Bellacicca A, Bello L, Cerri, G. (2019). Direct Electrical Stimulation of Premotor Areas: Different Effects on Hand Muscle Activity during Object Manipulation. Cerebral Cortex.

Jeannerod, M., Arbib, M., Rizzolatti, G., and Sakata, H. (1995). Grasping objects: the cortical mechanisms of visuomotor transformation. Trends Neurosci. 18, 314–320.

Nelissen K, Fiave PA, Vanduffel W. 2017. Decoding grasping movements from the parieto-frontal reaching circuit in the nonhuman primate. Cereb Cortex. 1–15.

Raos V, Franchi G, Gallese V, Fogassi L. 2003. Somatotopic organization of the lateral part of area F2 (dorsal premotor cortex) of the macaque monkey. J Neurophysiol. 89(3):1503-18.

Raos V, Umiltá MA, Gallese V, Fogassi L. 2004. Functional properties of grasping-related neurons in the dorsal premotor area F2 of the macaque monkey. J Neurophysiol. 92(4):1990-2002.

Rizzolatti, G., and Matelli, M. (2003). Two different streams form the dorsal visual system: anatomy and functions. Exp. Brain Res. 153, 146–157.

Takahashi K, Best MD, Huh N, Brown KA, Tobaa AA, Hatsopoulos NG. 2017. Encoding of both reaching and grasping kinematics in dorsal and ventral premotor cortices. J Neurosci. 37(7):1733–1746.

Turella L, Lingnau A. 2014. 2014. Neural correlates of grasping. Front Hum Neurosci. 8:686.